Institute of Nuclear Sciences „Vinča”
Materials Science Laboratory
University of Belgrade

Annual Report (2009-2010)

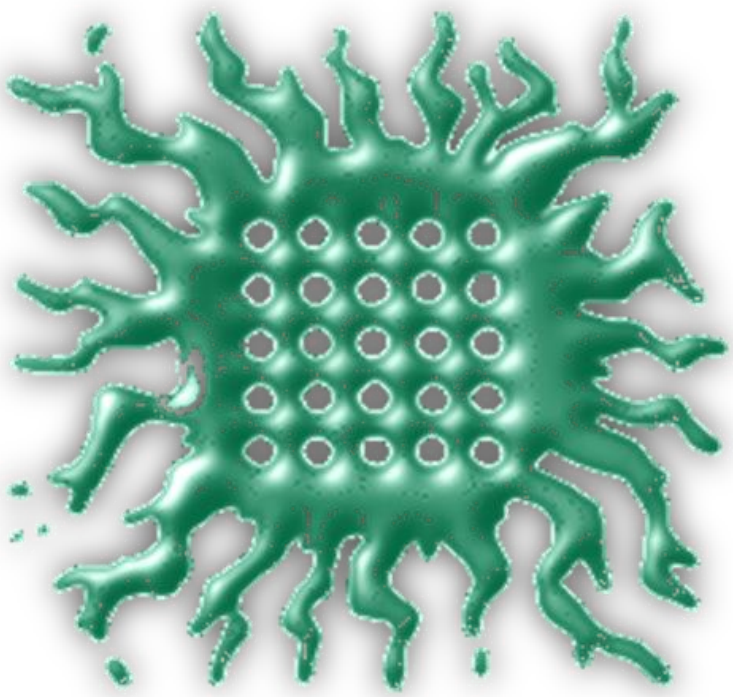

Belgrade, 2014.

Publication of the Materials Science Laboratory

Series: ANNUAL REPORT

Publisher
Institute of Nuclear Sciences „Vinča“
Materials Science Laboratory
University of Belgrade, P.O. Box 522, 11001 Belgrade, Serbia
Phone: (381-11) 3408-224

For the Publisher
Dr. Rer. Nat. Branko Matović, Director of the Laboratory

ISSN
Institute of Nuclear Sciences „Vinča“

Associate Editors
Scientific board

Editors
Dr. Vesna Maksimović
Dr. Branko Matović

Layout
Dipl.ing. Jelena Pantić

Printed by
Printing office of the Institute of Nuclear Sciences „Vinča“ in 20 copies
July 2014

Research topics

Metallic materials

Energy

Enviromental protection

Advanced ceramics

Functional ceramics

Biomaterials

Carbon materials

Ceramic composites

Raw materials and heritage

Doctoral dissertations

Table of Contents:

1. Metallic materials 1
2. Energy 26
3. Enviromental protection 39
4. Advanced ceramics 49
5. Functional ceramics 64
6. Biomaterials 74
7. Carbon materials 83
8. Ceramic composites 91
9. Raw materials and heritage 114
10. Doctoral dissertations 117
11. Domestic collaborations 121
12. International collaborations 125

Metallic materials

Microstructural evolution of Cu-TiB_2 composite powder particles obtained by high-energy milling

Višeslava Rajkovic[1], Dušan Božić[1], Smilja Marković[2], Milan T. Jovanović[1]

[1]Department of Material Science, INN Vinca, Serbia
[2]Institute of Technical Sciences of the SASA, Serbia

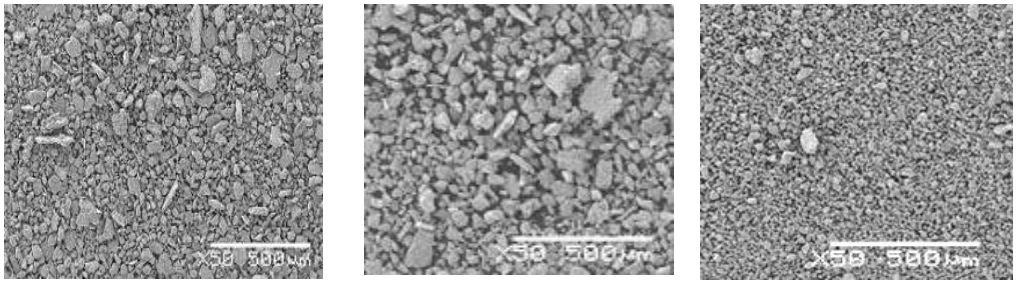

SEM micrograph. Morphology of Cu-4 wt.% TiB_2 particles after different milling time; (a) 5h, (b) 10h and (c) 20 h

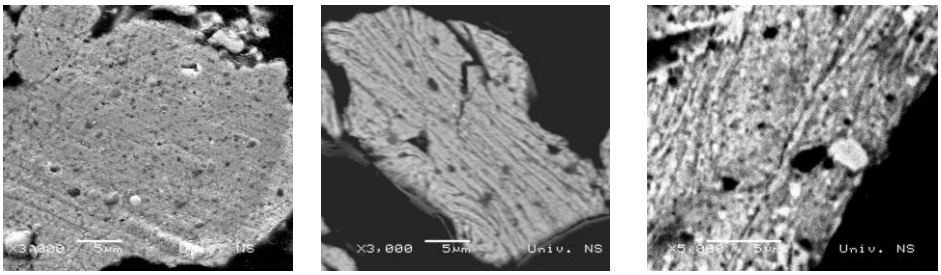

SEM micrograph. Microstructure of Cu-4 wt.% TiB_2 powder particles after different milling time; (a) 5h, (b) 10h and (c) 20 h

***4th Serbian Congress of Microscopy*, Belgrade, 11-12. October 2010. pp. 101-102.**

Strength and thermal stability of Cu-Al_2O_3 composite obtained by internal oxidation

V. Rajković, D. Božić, A. Devečerski, S. Bojanić, M. T. Jovanović

Institute of Nuclear Sciences, Vinča, University of Belgrade, 11001 Belgrade, Serbia

The objective of the work is to study the effects of the high-energy milling on strengthening, thermal stability and electrical conductivity of Cu-Al_2O_3 composite. The prealloyed copper powders, atomized in inert gas and containing 3 wt. % Al, were milled up to 20 h in the planetary ball mill to oxidize *in situ* aluminium with oxygen from the air. Composite compacts were obtained by hot-pressing in an argon atmosphere at 800 °C for 3 h under the pressure of 35MPa. The microstructural characterization was performed by the optical microscope, scanning electron microscope (SEM), transmission electron microscope (TEM) and X-ray diffraction analysis (XRD). The microhardness, electrical conductivity and density measurements were also carried out. The effect of internal oxidation and high-energy milling on strengthening of Cu-Al_2O_3 composite was significant, The increase of the microhardness of composite compacts (292 HV) is almost threefold comparing to compacts processed from the as-received Cu-3 wt.%Al powder (102 HV). The grain size of Cu-Al_2O_3 compacts processed from 5 and 20 h-milled powders was 75 and 45 nm, respectively. The small increase in the grain size and the small microhardness drop indicate the high thermal stability of Cu-Al_2O_3 composite during high-temperature exposure at 800 °C.

Keywords: powder processing; metal matrix composites; microstructural characterization; microhardness; high-temperature properties.

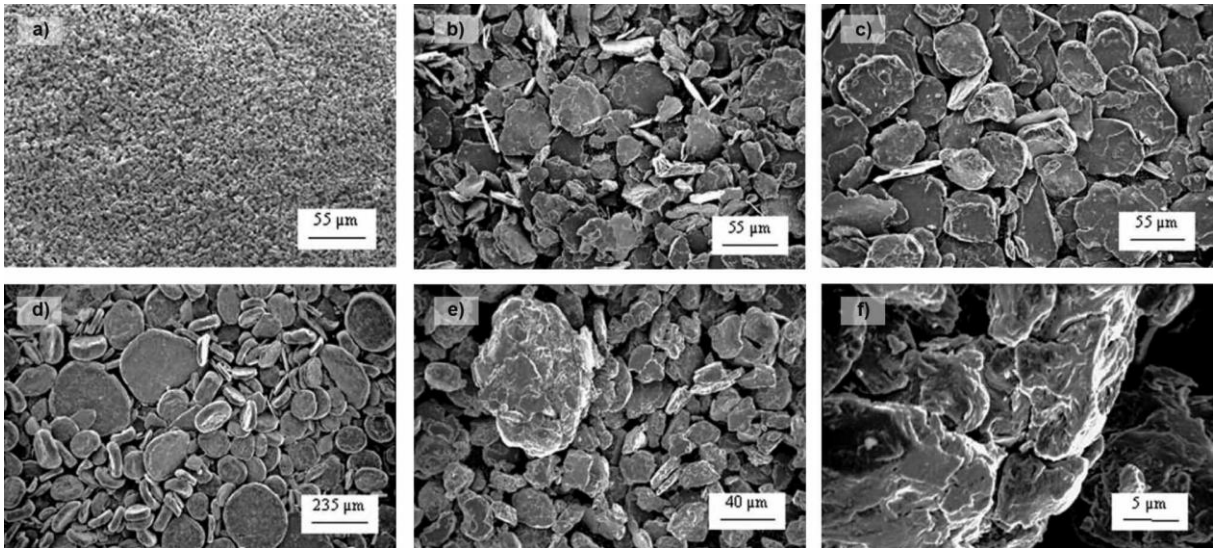

Figure:SEM.Morphology of as-received and milled Cu-3 wt.% Al particles: (a) as-received; (b) 3 h; (c) 5 h; (d) 10 h, (e) 20 h, (f) detail of figure (e).

***Revista De Metalurgia*, 46 (2010) 520-529.**

Influence of potential pulse conditions on the formation of honeycomb-like copper electrodes

Nebojša D. Nikolić[1], Goran Branković[2], Vesna M. Maksimović[3], Miomir G. Pavlović[1], Konstantin I. Popov[4]

[1]ICTM – Institute of Electrochemistry, University of Belgrade, Njegoševa 12, Belgrade, Serbia
[2]Institute for Multidisciplinary Research, Kneza Višeslava 1a, Belgrade, Serbia
[3]Vinča Institute of Nuclear Sciences, University of Belgrade, Belgrade, Serbia
[4]Faculty of Technology and Metallurgy, University of Belgrade, Karnegijeva 4, Belgrade, Serbia

Electrodeposition of copper by pulsating overpotential (PO) regime in the hydrogen co-deposition range was examined by the determination of the average current efficiency of hydrogen evolution and by microscopic analysis of the morphology of the formed deposits. The techniques of scanning electron microscopy (SEM) and optical microscopy were used for the structural analysis of the copper deposits. Honeycomb-like electrodes were formed with an amplitude overpotential of 1000 mV, a pause of 10 ms, and deposition pulses of 3, 5, 10 and 20 ms. Holes formed by attached hydrogen bubbles were surrounded by dendrites (for deposition pulses of 3 and 5 ms) or agglomerates of copper grains (for 10 and 20 ms). In an interval of deposition pulses between 3 and 10 ms, the length of deposition pulse did not affect the size, number and depth of holes. The change of morphology of copper formed around holes was discussed by the effect of quantity of evolved hydrogen on effectiveness of stirring of solution in the near-electrode layer. The application of square-wave PO with the shorter deposition pulses enabled energy savings in the production of such copper electrodes. For example, the applied deposition pulse of 3 ms enabled energy saving of about 15% in relation to the copper electrode obtained with a deposition pulse of 10 ms (for the unchanged number, size and depth of holes).

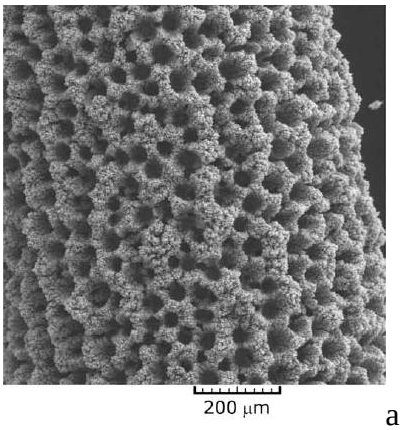

a

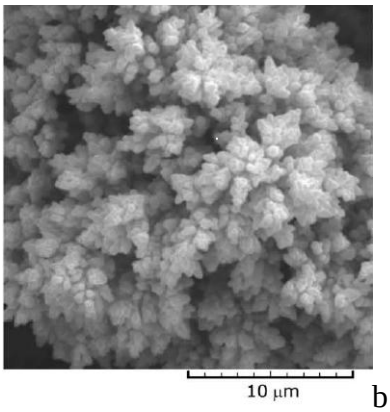

b

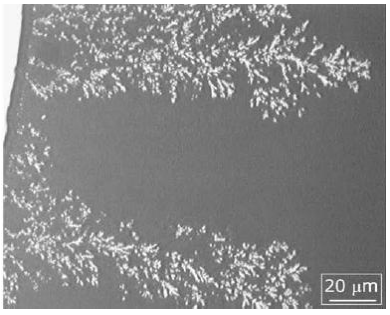

c

Figures: (a) The honeycomb-like copper structure; (b) agglomerate of copper grains obtained with a deposition pulse of 20 ms. Deposition time: 185 s; (c) Cross-section of the copper deposits obtained with deposition pulse of 20 ms.

***Journal of Electroanalytical Chemistry,* 635 (2009) 111-119.**

Cross-section analysis of morphology of electrodeposited copper obtained in hydrogen co-deposition range

N.D. Nikolić[1], V. Maksimović[2], M.G. Pavlović[1], K.I. Popov[3]

[1]ICTM – Institute of Electrochemistry, University of Belgrade, Njegoševa 12, P.O. Box 473, 11001 Belgrade,
[2]Vinča Institute of Nuclear Sciences, University of Belgrade, P.O. Box 522, 11001 Belgrade
[3]Faculty of Technology and Metallurgy, University of Belgrade, Karnegijeva 4, P.O. Box 3503, 11001 Belgrade, Serbia

Cross-section analysis of copper deposits electrodeposited in the hydrogen co-deposition range at a constant overpotential and in a pulsating overpotential (PO) regime was performed. It was shown that a complete structural analysis of these technologically very important electrodes is impossible without an analysis of their internal structure. An insight into the compactness (or porosity) of the deposits, as well as into the depth of the holes, can only be obtained by this type of analysis.

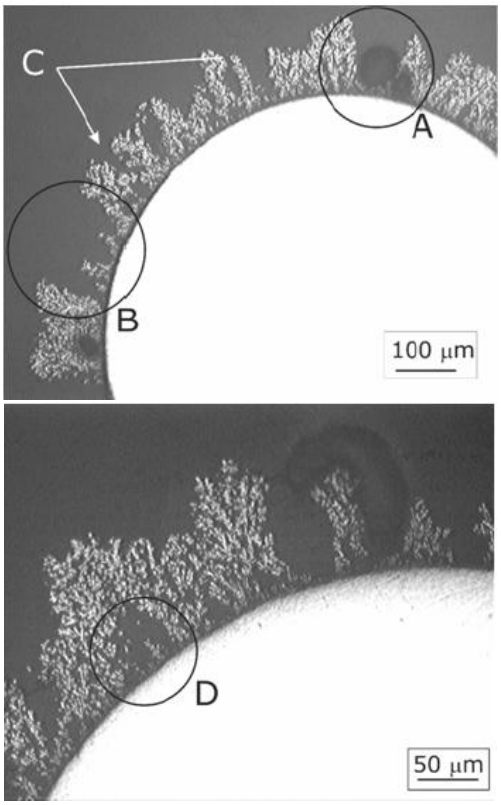

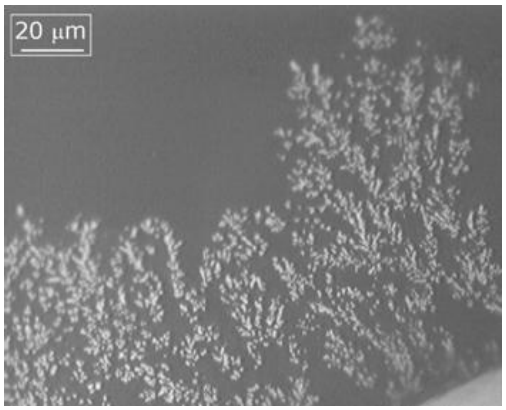

Figure: Cross-section of a copper deposit electrodeposited from 0.15 M $CuSO_4$ in 0.50 M H_2SO_4, at an overpotential of 1000 mV with a quantity of the electricity of 10 mA h cm^{-2}.

***Journal of the Serbian Chemical Society,* 74 (2009) 689-696.**

Characterization of copper powder particles obtained by electrodeposition as function of different current densities

V.M.Maksimović[1], M.G.Pavlović[2], Lj.J.Pavlović[2], M.Tomić[3]

[1]Vinča Institute of Nuclear Sciences, University of Belgrade, P.O. Box 522, 11001 Belgrade
[2]ICTM – Institute of Electrochemistry, University of Belgrade, Njegoševa 12, P.O. Box 473, 11001 Belgrade,
[3]Faculty of Technology Zvornik, University of Eastern Sarajevo, 75400 Zvornik, Republic of Srpska

Technological properties of powders depend on their granulometry and morphology. Very often one method is inadequate for characterization of powder particles. This article studied different methods intended for clear definition of the copper powder granulometric and morphological properties. Quantitative microstructural analysis, sieve analysis, and XRD analysis of copper powder as well as scanning electron microscopy analysis of the copper powder particles were performed. It was determined that selected stereological parameters, such as area, perimeter, and shape factor (roundness) show a linear decreasing dependence of current density, while the morphology was changed from massive to branched 3D dendrites. XRD analysis indicated that the crystallite size shows a linearly increasing dependence on current density. The shape factor could be a useful parameter for description of powder morphologies deposited by different regimes.

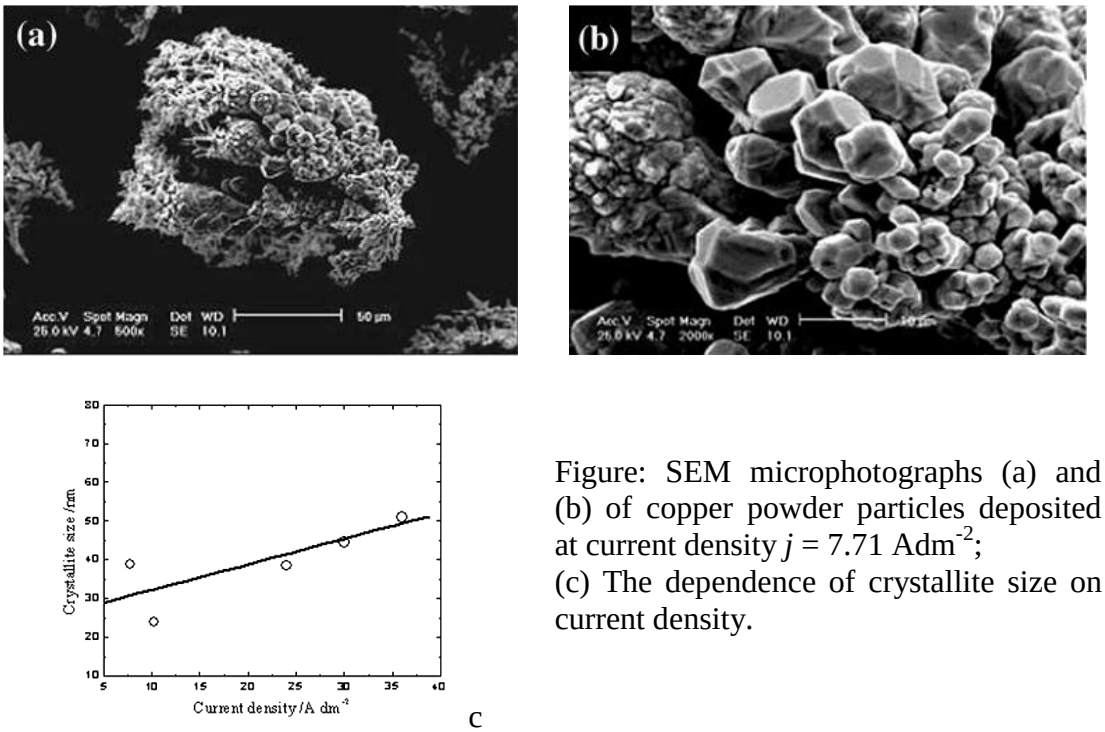

c

Figure: SEM microphotographs (a) and (b) of copper powder particles deposited at current density j = 7.71 Adm^{-2};
(c) The dependence of crystallite size on current density.

***Journal of Applied Electrochemistry*, 39 (2009) 2545-2552.**

Characterization of electrodeposited Fe-Ni alloys powders recrystallized in air at 600 ºC

U.Lačnjevac[1], B.M.Jović[1], V.M.Maksimović[2], M.G.Pavlović[3], V.D.Jović[1]

[1]Institute for Multidisciplinary Research, P.O. Box 33, 11030 Belgrade, Serbia
[2]Institute of Nuclear Sciences Vinča, P.O. Box 522, 11001 Belgrade, Serbia
[3]ICTM – Institute of Electrochemistry, University of Belgrade, Njegoševa 12, Belgrade, Serbia

The electrodeposition of Fe-Ni powders from citrate-sulphate supporting electrolytes containing Fe (III) salts of different Ni/Fe ions concentration ratios at pH 4.5, was investigated by polarization measurements. The morphology, chemical composition and phase composition of as-deposited and recrystalized powders were investigated using SEM, EDS and XRD analysis. The EDS analysis of ac-deposited alloy powders confirmed anomalous co-deposition of Fe and Ni from all investigated electrolytes. After annealing in air at 600 °C for 1 h all alloy powders completely oxidized forming NiO, $NiFe_2O_4$ and Fe_2O_3 phases in different proportions depending on the original powder composition.

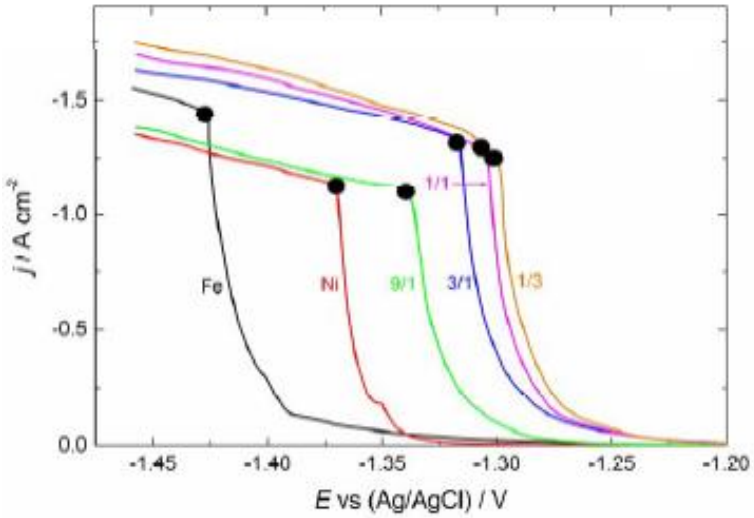

Figure: The polarization diagram for the Fe-Ni powders electrodeposition recorded at a sweep ratio of 1mV s^{-1} (after IR drop compensation) for different Ni/Fe ions concentration ratios (marked in the figure).

ΤΙΜΗΤΙΚΗ ΕΚΔΟΣΗ ΓΙΑ ΤΟΝ ΚΑΘΗΓΗΤΗ ΕΜΠ ΝΙΚΟΛΟ ΣΠΥΡΕΛΛΗ**, Book, Atina, (2009) p. 199-206.**

Phase composition of electrodeposited Fe-Ni powders before and after recrystallization in air

B.M.Jović[1], U.Lačnjevac[1], V.M.Maksimović[2], V.D.Jović[1]

[1]Institute for Multidisciplinary Research, P.O. Box 33, 11030 Belgrade, Serbia
[2]Institute of Nuclear Sciences, Vinča, P.O. Box 522, 11001 Belgrade, Serbia

The Fe-Ni powders were electrodeposited from citrate-sulfate containing electrolytes for different Ni/Fe ions concentration ratios at pH 4.5. The chemical and phase compositions of the powders were investigated using EDS (SEM) and XRD analysis. EDS analysis of as-deposited alloy powders confirmed anomalous co-deposition of Fe and Ni. The phase composition analysis of the powders was performed using XRD. In the case of ac-deposited powders intensity of recorded shape peaks was very small, as can be seen in Figure. The only two peaks that could for certain be ascribed to some phases are peaks marked with the triangle (▲) and they correspond to the ά-Fe phase. As can be seen they are well defined in the powder containing 95 at. % Fe. A small peak at 2θ = 44º (pointed with the arrow and marked as $FeNi_3$?) for the powder electrodeposited from the solution with Ni/Fe = 9/1 and Ni/Fe = 3/1 could be ascribed to the (111) reflection of the $FeNi_3$ phase.
After annealing in air at 600 ºC for 1h all alloy powders completely oxidized forming NiO, $NiFe_2O_4$ and Fe_2O_3 phases in different proportions depending on the original powder composition. The appearance of needle-like crystals on powder particles surface is the main characteristic of the morphology of recrystallized powders. These crystals become more pronounced with increase of Fe content in the alloy powder. In order tp find out what could be these crystals EDS analysis was performed on the positions were needle-like crystals were mainly formed, i.e. in the cone-shaped cavities. Only Fe and O were detected at these positions, indicating that these crystals could be ascribed to the Fe_2O_3 phase. On the other investigated positions of the powder particles Ni was detected together with the Fe and O indicating that $NiFe_2O_4$ phase might be present. The common characteristic of all investigated powders is presence of 65 – 70 at. % of oxygen due to additional oxidation of all powder particles during the annealing procedure.

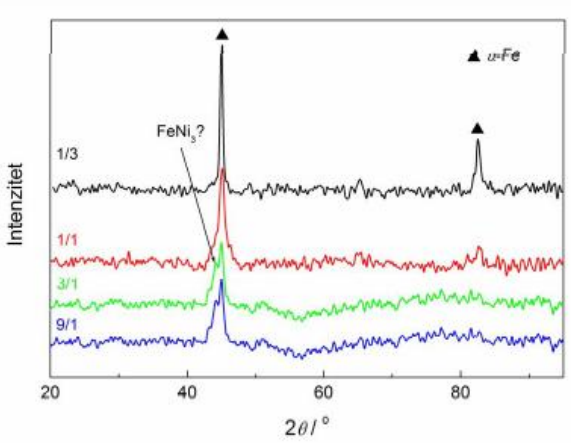

Figure: The diffractograms for the powders electrodeposited at different Ni/Fe ions ratios (marked in the figure).

***2nd Internacional Symposium on Surface Imaging/Spectroscopy at the Solid/Liquid Interface*, May 31st-June 3rd, 2009, Cracow, Poland, pp. 62.**

Morphology and composition of electrodeposited Fe-Ni powders

U.Lačnjevac[1], B.M.Jović[1], V.M.Maksimović[2], V.D.Jović[1]

[1]Institute for Multidisciplinary Research, P.O. Box 33, 11030 Belgrade, Serbia
[2]Institute of Nuclear Sciences, Vinča, P.O. Box 522, 11001 Belgrade, Serbia

The electrodeposition of the Fe-Ni powder from citrate-sulfate containing electrolytes for different Ni/Fe ions concentration ratios at pH 4.5 was investigated by polarization measurements. Typical polarization curves for alloy powder electrodeposition were obtained. Powders were deposited at a current density corresponding to the diffusion control of alloy powder deposition. The morphology and chemical composition of electrodeposited powders were investigated using SEM and EDS analysis. The EDS analysis of ac-deposited alloy powders confirmed anomalous co-deposition of Fe and Ni. The morphology of ac-deposited powders was found to depend on the Ni/Fe ions concentration ratio. A common characteristic for all as-deposited powders samples was the presence of cone shaped cavities and nodules. The nodules surface was either flat or covered with crystals of different shapes. More or less flat surface of nodules was detected for samples electrodeposited from the solution with Ni/Fe ions concentration ratio 9/1, 3/1 and 1/1 and their number decreased with the decrease of Ni/Fe (with the increase of Fe content in the powder). Well defined crystals were detected on the nodules of all powder. For the Ni/Fe = 9/1 pagoda-like crystals were only detected, indicating the presence of $FeNi_3$ phase in the powder. For the Ni/Fe ratios 3/1, typical were "Chrismas tree-like" crystals shown in Fig. a. Crystals of the shape of triangles (Fig. b) and of the shape of rectangle were detected for the powders containing more than 62 at.% of Fe.

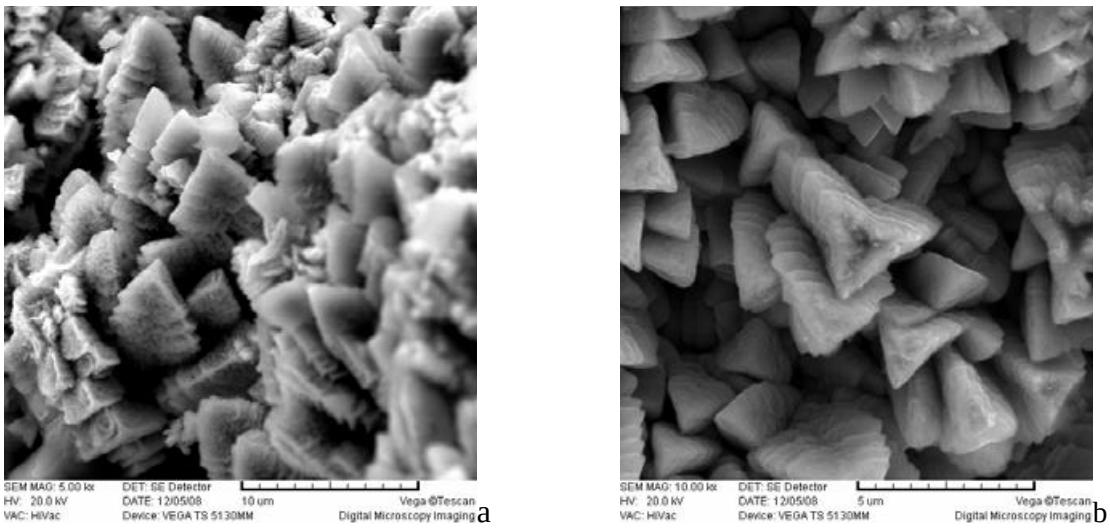

Figure: (a) Christmas tree-like crystals; (b) crystals of the shape of triangles.

***2nd Internacional Symposium on Surface Imaging/Spectroscopy at the Solid/Liquid Interface*, May 31st-June 3rd, 2009, Cracow, Poland, pp. 67.**

Influence of the shape of square-wave pulsating overpotencional (PO) on formation of copper electrodes suitable for fuel cells

N.D.Nikolić[1], V.M.Maksimović[2], G.Branković[3], M.G.Pavlović[1], K.I.Popov[4]

[1]ICTM – Institute of Electrochemistry, University of Belgrade, Njegoševa 12, Belgrade, Serbia
[2]Institute of Nuclear Sciences, Vinča, P.O. Box 522, 11001 Belgrade, Serbia
[3]Institute for Multidisciplinary Research, P.O. Box 33, 11030 Belgrade, Serbia
[4]Faculty of Technology and Metallurgy, University of Belgrade, Karnegijeva 4, Belgrade, Serbia

Electrodeposition is very valuable way of obtaining open porous structure of copper with an extremely high surface area, because such structurea are ideally suited for electrodes in many electrochemical devices, such as fuel cells, batteries and chemical sensors. Such copper structures, denoted as both 3D foam and honeycomb-like one, are obtained at high current densities and overpotentials, where parallel to copper electrodeposition, the hydrogen evolution reaction occur. The basic characteristics of these electrodes are: holes and pores formed due to attached hydrogen bubbles with agglomerates of copper grains among them. The walls of the holes are aslo very porous and they are composed of disperes agglomerates of copper grains or of dendricic particles. In constant regimes of electrolysis, the number, distribution and pore size can be easily controlled by the choise of appropriate electrolysis parametars. The increase of the specific surface area of the porous electrodes manifested through the decrease of the size of the pores, as well as branches in the foam or agglomerates of copper grains in the honeycomb-like structures can be achieved by addition of specific substances, known as additives, to the plating solution, or by the application of pulsating overpotential (PO) regime with the constant deposition pulse and different pause duration.
In this paper, the effect of the length of deposition pulse on electrodeposition of copper by square-wave PO regime in hydrogen co-deposition range was examined by determination of the average current efficiency of hydrogen evolution and by the scanning electron microscopic (SEM) analysis of the morphology of the formed deposits. The following parameters of the a squere-wave PO were employed: an amplitude overpotential of 1000 mV, a pause of 10 ms, and deposition pulses of 1, 3, 5, 10 and 20 ms. The pyramid-like precursors of dendrites were formed with a deposition pulse of 1 ms and pause of 10 ms. Honeycomb-like electrodes were formed with deposition pulses of 3, 5, 10 and 20 ms. Holes formed by attached hydrogen bubbles were surrounded by dendrites (for deposition pulses of 3 and 5 ms) or agglomerates of copper grains (for 10 and 20 ms). In an interval of deposition pulses between 3 and 10 ms, the length of deposition pulse did not affect the size, number and depth of holes. The change of morphology of copper formed around holes was discussed by the effect of quantity of evolved hydrogen on effectiveness of stirring of solution in the near-electrode layer. The application of square-wave with the shorter deposition pulses enabled energetic savings in the production of these copper electrodes. For example, the applied deposition pulse of 3 ms enabled energetic savings of about 15 % in relation to the copper electrode obtained with a deposition pulse of 10 ms (for the unchanged number, size and depth of holes).

***2nd Internacional Symposium on Surface Imaging/Spectroscopy at the Solid/Liquid Interface*, May 31st-June 3rd, 2009, Cracow, Poland, pp. 80.**

Characterization of Electrodeposited Ni-Co Alloy Powders

V.M.Maksimović[1], B.M. Jović[2], U.Č. Lačnjevac[2], M.G. Pavlović[3], V.D. Jović[3]

[1]Institute of Nuclear Sciences, Vinča, P.O. Box 522, 11001 Belgrade, Serbia
[2]Institute for Multidisciplinary Research, P.O. Box 33, 11030 Belgrade, Serbia
[3]ICTM – Institute of Electrochemistry, University of Belgrade, Njegoševa 12, Belgrade, Serbia

Almost all materials can be made into powder, but the method selected for production of powder depends on the specific material properties. The electrolytic powder production method usually yields products of high purity, which can be well pressed and sintered. Only a few papers concerning Ni-Co powder electrodeposition exist in the literature. The morphology, phase and chemical composition of Ni-Co alloy powders electrodeposited from ammonium sulfate-boric acid containing electrolyte with different ratio of Ni^{2+}/Co^{2+} ions were investigated. Ni-Co powders were electrodeposited at constant current density of approximately 70 $mAcm^{-2}$ from electrolytes containing 0.4M H_2BO_3, 0.2M Na_2SO_4 and Ni and Co sulfate salts. The ratios of Ni^{2+}/Co^{2+} ions were 1.00, 0.50 and 0.33. The morphology of the Ni-Co alloy powders is sensitive to the Ni^{2+}/Co^{2+} ions ratio in the electrolyte. At the highest investigated ratio Ni^{2+}/Co^{2+} ions typical 2D fern-like dendritic particles were obtained (Fig.a). With the decrease of Ni^{2+}/Co^{2+} ions ratio among 2D fern-like dendrites, compact agglomerates were detected (Fig.b). Further decrease of the ions ratio (Ni^{2+}/Co^{2+} = 0.33) also dictates the appearance of densely packed 3D dendritic particles (Fig.c). According to the results of the chemical analysis of electrodeposited powders, the ratio of Ni^{2+}/Co^{2+} ions, i.e. electrolyte composition, significantly influenced the composition of electrodeposited powders. It should be noted that both elements, Ni and Co were analyzed independently and that for all samples their sum was not 100%, but about 90%. The results of the EDS analysis denote that the third element was oxygen. According to Brenner's classification, the behavior indicates anomalous type of powder co-deposition. The characteristic of anomalous co-deposition is that it occurs only under certain condition of concentration and operating variables for a given plating bath. It has already been shown that from simple salt containing electrolytes co-deposition of Ni-Co powder possesses irregular or anomalous character, depending on the electrolyte composition.

From the presented results it can be concluded that the composition of the electrolyte, i.e. the ratio of Ni^{2+}/Co^{2+} ions concentration, influences on morphology, phase and chemical composition of Ni-Co alloy powders.

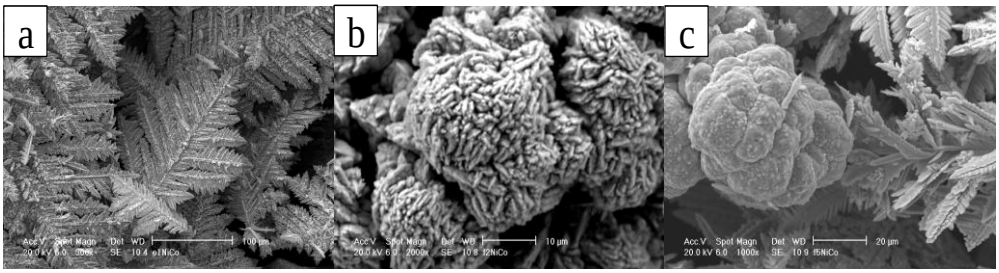

Figure: Morphology of Ni-Co powders electrodeposited from electrolytes containing: (a) Ni^{2+}/Co^{2+} = 1.00; (b) Ni^{2+}/Co^{2+} = 0.50; (c) Ni^{2+}/Co^{2+} = 0.33.

***MC 2009, Microscopy Conference,* 30 August – 4 September 2009, Vol. 3 Materials Science, pp. 229.**

Elektrohemijsko dobijanje i morfologija čestica bakarnog praha dobijenog pri različitim režimima elektrolize

M.G.Pavlović[1], M.V.Tomić[2], Lj.Pavlović[1], V.Maksimović[3], N.D.Nikolić[1]

[1]ICTM – Institute of Electrochemistry, University of Belgrade, Njegoševa 12, Belgrade, Serbia
[2]Faculty of Technology Zvornik, University of Eastern Sarajevo, 75400 Zvornik, Republic of Srpska
[3]Institute of Nuclear Sciences Vinča, P.O. Box 522, 11001 Belgrade, Serbia

Ispitivan je uticaj različitih režima elektrolize (konstantna i reversna struja) na morfologiju bakarnog praha. Morfologija istaloženog bakarnog praha je proučavana pomoću skening elektronskog mikroskopa (SEM). Diskutovan je efekat katodne i anodne amplitudne gustine struje, odnos katodnog i anodnog vremena kao i vremena katodnog taloženja i anodnog rastvaranja. Pokazano je da parametri koji određuju oblik talasa reversne struje određuju i mikromorfologiju čestica istaloženog bakarnog praha.

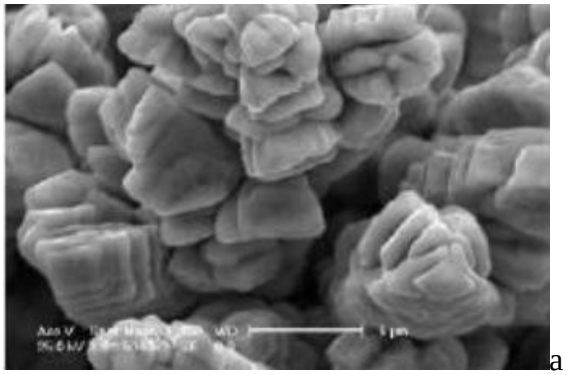
a

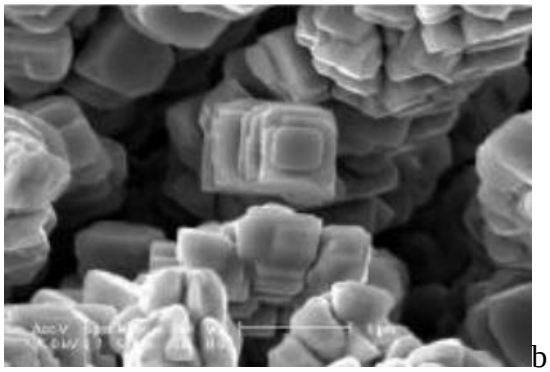
b

Slika: SEM mikrofotografije čestica bakarnog praha dobijenih reversnim režimom elektrolize. Odnos katodnog i anodnog vremena 2.5. Vreme katodnog taloženja 1s. Vreme anodnog rastvaranja 0.4s. Katodne (anodne) amplitudne gustine struje i srednje gustine struje: a) $j_k=j_a$= 24 A/dm^2, j_{sr}=10.28 A/dm^2; b) $j_k=j_a$= 30 A/dm^2, jsr=12.85 A/dm^2.

***Journal of Engineering & Processing Management,* 1 (2009) 46-53.**

Morfologija prahova Ni-Fe legura elektrohemijski istaloženih iz citratno-sulfatnih rastvora

U. Lačnjevac[1], V.D. Jović[1], B.M. Jović[1], Z. Baščarević[1], V.M. Maksimović[2], M.G. Pavlović[3]

[1]Institut za Multidisciplinarna istraživanja, 11030 Beogra, Kneza Višeslava 1, Srbija
[2]Institut za nuklearne nauke, Vinča, 11001 Beograd, Srbija
[3]Institut za elektrihemiju IHTM, 1000 Beograd, Njegoševa 12, Srbija

Elektrohemijsko taloženje prahova Fe-Ni legura ispitano je snimanjem polarizacionih dijagrama u citratno-sulfatnim rastvorima pri različitom odnosu koncentracija Ni/Fe jona na pH 4.5. Sve polarizacione krive imaju sličan oblik i okarakterisane su prisustvom dve prevojne tačke na dijagramu. Prva prevojna tačka odgovara početku taloženja Fe-Ni legure, dok druga predstavlja momenat kada ukupna elektrohemijska reakcija postaje kontrolisana brzinom formiranja mehurova vodonika. Potencijali taloženja Fe-Ni legura pri svim ispitivanim odnosima Ni/Fe pozitivniji su od potencijala taloženja čistih metala, pri čemu se sa smanjenjem odnosa Ni/Fe polarizacione jrive pomeraju ka malo pozitivnijim vrednostima potencijala. Morfologija čestica prahova ispitivana je korišćenjem skenirajuće elektronske mikroskopije (SEM). Zajednička karakteristika svih prahova Fe-Ni legura je prisustvo šupljina konusnog oblika. Čestice praha istaloženog pri odnosu Ni/Fe =9/1 uglavnom su sastavljene od čvorića, glatke ili neravne površine, kod kojih se na pojedinim mestima mogu uočiti dobro definisani kristali. Sa smanjenjem odnosa Ni/Fe, prisustvo kristala na površini čvorića postaje sve izraženije, dok su kod prahova sa najvećim sadržajem Fe (Ni/Fe = 1/3) na celoj površini čestica prisutni kristali različitog oblika.

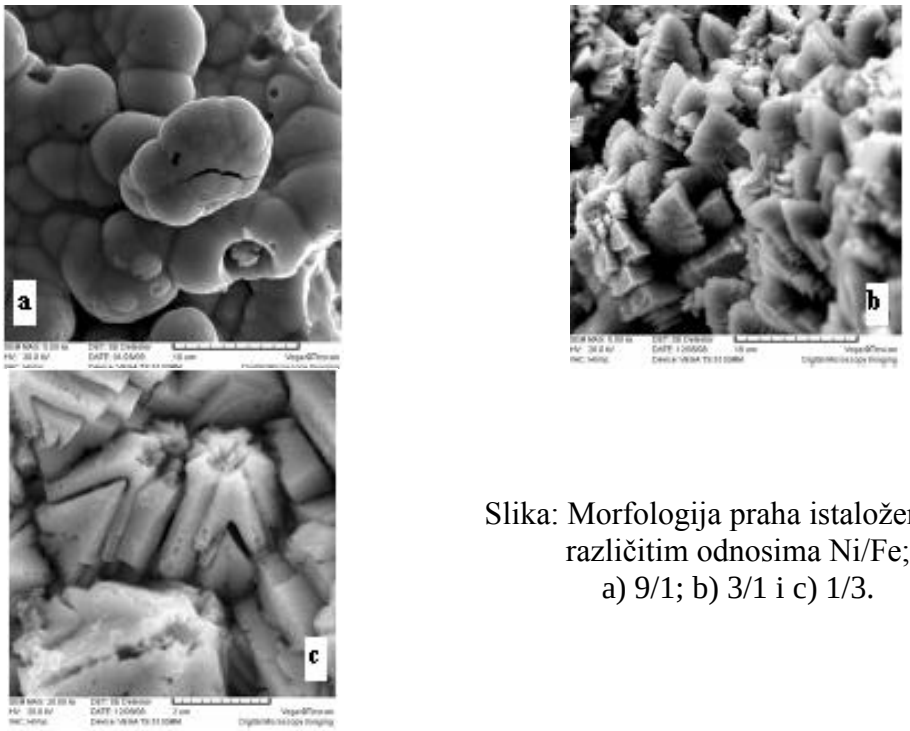

Slika: Morfologija praha istaloženih pri različitim odnosima Ni/Fe;
a) 9/1; b) 3/1 i c) 1/3.

***XI YUCORR*, 17.05.-20.05.2009. Tara, Serbia, 2009, Proceedings, p. 330-336.**

Characterization and Morphology of Copper Powder Particles as a Function of Different Electrolytic Regimes

M.G. Pavlović[1], Lj.J. Pavlović[1], V.M. Maksimović[2], N. D. Nikolić[1], K.I. Popov[3]

[1]ICTM – Institute of Electrochemistry, University of Belgrade, Njegoševa 12, P.O. Box 473, 11001 Belgrade,
[2]Institute of Nuclear Sciences Vinča, University of Belgrade, P.O. Box 522, 11001 Belgrade, Serbia
[3]Faculty of Technology and Metallurgy, University of Belgrade, Karnegijeva 4, Belgrade, Serbia

The effect different deposition regimes (constant and reversing currents), on the powdered copper electrodeposits morphology were investigated. The results obtained in constant regimes were compared with those obtained in reversing regimes. The morphology of electrodeposited copper powder was investigated using a scanning electron microscope (SEM). The effect of the current amplitude, cathodic-to-anodic time ratio and period of the current wave are discussed. It is shown that the parameters determining the reversing current wave determine the micromorphology of the copper powder particles deposited. On the other side, technological properties of powders depend on their granulometry and particle morphology. Very often one method is inadequate for characterization of the morphology of powder particles. This paper also studied different methods for clear describing of the copper powder granulometry and morphology.

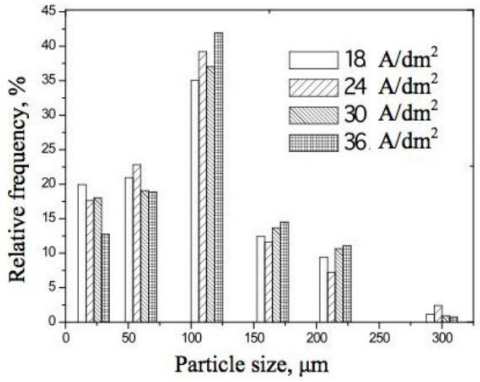

a

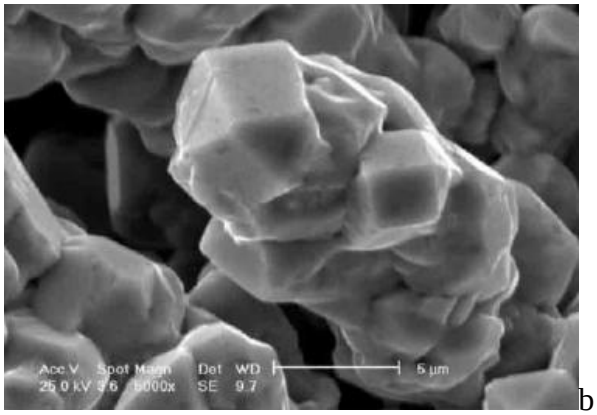

b

Figure: (a) Particle size distribution of copper powder particles obtained by reversing currents (sieve analysis); (b) SEM photomicrograph of copper powder particles obtained by reversing currents. Cathodic-to-anodic time ratio 2.5. Cathodic pulse duration 1s. Anodic pulse duration 0.4s. Cathodic (anodic) amplitude current density and average current density $j_c=j_a=$ 36 A/dm^2, j_{av}=15.42 A/dm$^{2.}$

***International Journal of Electrochemical Science,* 5 (2010) 1862 – 1878.**

Application of pulsating overpotential regime on the formation of copper deposits in the range of hydrogen co-deposition

N. D. Nikolić[1], G. Branković[2], V. M. Maksimović[3], M. G. Pavlović[1], K. I. Popov[4]

[1]ICTM – Institute of Electrochemistry, University of Belgrade, Njegoševa 12, P.O. Box 473, 11001 Belgrade,
[2]Institute for Multidisciplinary Research, P.O. Box 33, 11030 Belgrade, Serbia,
[3]Institute of Nuclear Sciences, Vinča, University of Belgrade, P.O. Box 522, 11001 Belgrade, Serbia
[4]Faculty of Technology and Metallurgy, University of Belgrade, Karnegijeva 4, Belgrade, Serbia

Electrodeposition of copper by pulsating overpotential (PO) regime in the range of hydrogen co-deposition was examined by scanning electron microscopy. It was found that the increase of the pause-to-pulse ratio produced a strong effect on the morphology of electrodeposited copper. Honeycomb-like copper structures were formed with the pause-to-pulse ratios up to 5. Up to this value of the pause-to- pulse ratio, the diameter of the holes formed by attached hydrogen bubbles was decreasing, while their number was increasing by the application of PO regime. The compactness of the formed honeycomb-like structures was also increasing with the increasing pause duration. The increase of the pause-to-pulse ratio suppressed a coalescence of neighboring hydrogen bubbles. Copper dendrites in the interior of the holes and at their shoulders were formed with the higher pause-to-pulse ratios. The size of the formed dendrites, as well as their number, increased with the increasing pause duration. Depth of holes was decreasing with the increasing pause duration. The increased compactness of the obtained structures was explained by the use of a set of equations describing the effect of square-wave PO on electrodeposition process.

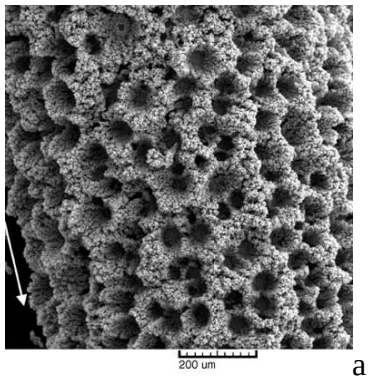

a

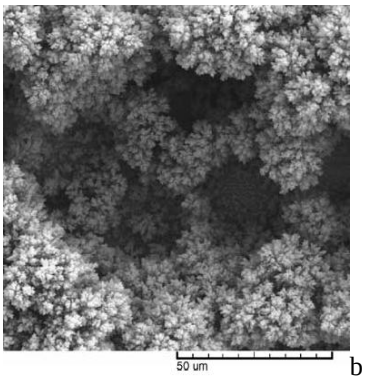

b

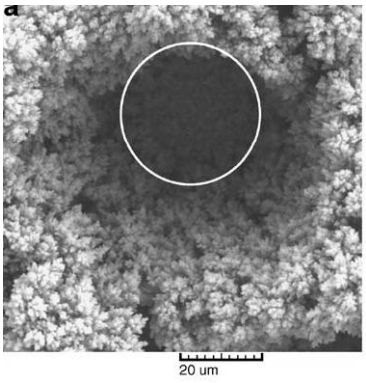

c

Figure: (a) Copper deposit obtained at an overpotential of 1,000 mV; (b) the coalesced hole and (c) non-coalesced hole obtained by PO regime of electrolysis with a pause duration of 5 ms.

***Journal of Solid State Electrochemistry*, 14 (2010) 331-338.**

Velocity and texture of a plasma jet created in a plasma torch with fixed minimal arc length

M. Vilotijević[1], B. Dačić[2] and D. Božić[3]

[1]Plasma Jet Co, Braničevska 29, 11000 Belgrade, Serbia
[2]Plasma Jet Co, 8/14 Willcott St, 1025 Auckland, New Zealand
[3]Institute of Nuclear Sciences, Vinča, University of Belgrade, 11001 Belgrade, Serbia

A new plasma jet (PJ-100) plasma spraying torch with a fixed minimal arc length was tested and the basic working parameters were measured and evaluated. The velocity of the plasma exiting both the cylindrical and the conical anode nozzles was assessed by measuring the thrust generated by the plasma jet and by photographing the translation of plasma clouds (parts with different brightnesses) in the last third of the length of the plasma plume. The basic characteristics of the argon/hydrogen plasma jets (enthalpy, mean temperature, mean plasma velocity and effective exhaust thrust velocity) were determined for different working regimes, for both the cylindrical and the conical nozzles. The thermal efficiency of the new plasma torch is between 70% and 74% for the plasma generation power up to 90 kW. The plasma plume generated in the cylindrical nozzle has a homogeneous radial temperature (and velocity) distribution with a full laminar flow.

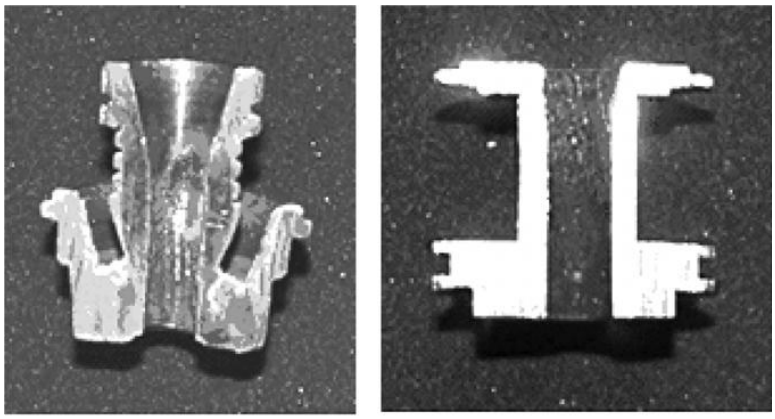

Figure: Photographs of the erosion paths at cut anodes: (a) Metco7 MB, 25–35 kW (courtesy of Inst. Nuclear Science, Vinca) and (b) PJ-100, 80–100 kW.

Plasma Sources Science & Technology, **18 [1] (2009) 015016 (8pp)**

An attempt to produce $NiFe_2O_4$ powder from electrodeposited Fe–Ni alloy powders by subsequent recrystallization in air

U. Lačnjevac[1], B.M. Jović[1], V.M. Maksimović[2], V.D. Jović[1]

[1]Institute for Multidisciplinary Research, University of Belgrade, P.O. Box 33, 11030 Belgrade, Serbia
[2]Institute of Nuclear Sciences, Vinča, University of Belgrade, P.O. Box 522, 11001 Belgrade, Serbia

The electrodeposition of the Fe–Ni powders from citrate-ammonium chloride containing electrolytes for different Ni/Fe ions concentration ratios at pH 4.0 was investigated by the polarization measurements. The morphology, chemical composition, and phase composition of the obtained powders were investigated using SEM, EDS, and XRD analysis. EDS analysis of as-deposited alloy powders confirmed anomalous co-deposition of Fe and Ni. A common characteristic for all as-deposited powder samples was the presence of cone-shaped cavities and nodules on the big agglomerates of the order of 200–400 μm. After annealing in air at 400, 600, and 700 °C for 3 h, all alloy powders oxidized forming NiO, $NiFe_2O_4$, and Fe_2O_3 phases in different proportions depending on the original powder composition. The $NiFe_2O_4$ phase was found to be dominant in the sample with the highest percentage of Fe after annealing at 600 °C.

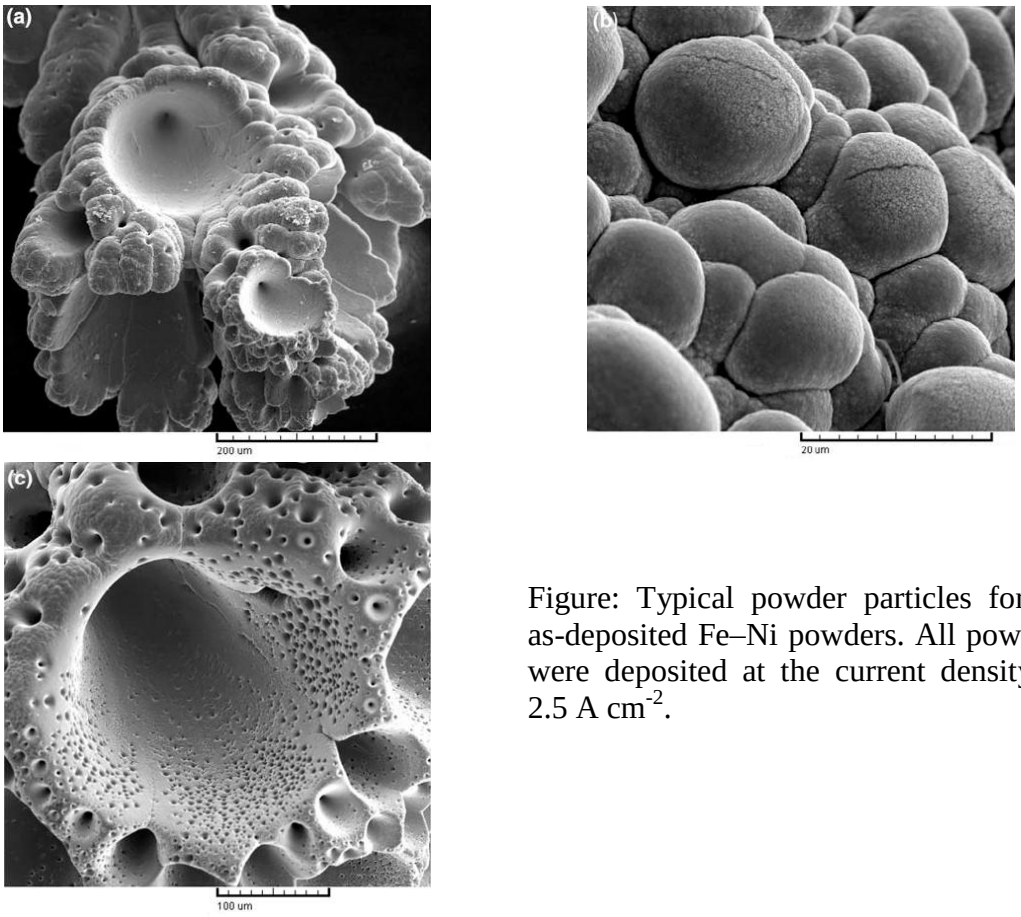

Figure: Typical powder particles for all as-deposited Fe–Ni powders. All powders were deposited at the current density of 2.5 A cm^{-2}.

***Journal of Applied Electrochemistry*, 40 (2010) 701-708.**

Electrodeposition of Cobalt Powders with Novel Three-Dimenstional Structure

V.M.Maksimović[1], U.Č.Lačnjevac[2], V.D.Jović[2], B.M.Jović[2], M.G.Pavlović[3]

[1]Institute of Nuclear Sciences, Vinča, University of Belgrade, P.O. Box 522, 11001 Belgrade, Serbia
[2]Institute for Multidisciplinary Research, University of Belgrade, P.O. Box 33, 11030 Belgrade, Serbia
[3]ICTM – Institute of Electrochemistry, University of Belgrade, Njegoševa 12, P.O. Box 473, 11001 Belgrade

Novel three-dimensional cobalt powder structures were successfully prepared by electrodeposition. Electrodeposited cobalt powder were characterized by scanning electron microscopy (SEM) and light microscopy. It was possible to control the morphology and structure of cobalt particles by adjusting process parameters of electrodeposition such as current density and type of working electrode. The morphology and structure of cobalt powders were investigated and the formation mechanism of agglomerate was also discussed.
In general, the type of electrodes used does not substantially affect the morphology of cobalt powder particles electrodeposited at diffusion limiting current density. It is known that surface where the metal precipitates may affect the formation of the first few layers of deposit in two ways: (a) providing a strong force of attraction that allowing strong a adhesion between the metal which is deposited and the substrate, (b) providing its own regulated grid that defines the layout and structure of the newly formed crystals. Cobalt with hcp lattice wants to keep crystal structure of nickel substrate with fcc crystal structure, creating an error in the order of several layers. Cobalt deposition on nickel electrode suppresses the appearance of agglomeration and needle dendrites. This phenomenon is not conditioned by the different properties of the electrolyte-electrode, but the primary distribution of current, speed and method of transport of adatoms to the electrode surface must also be considered.

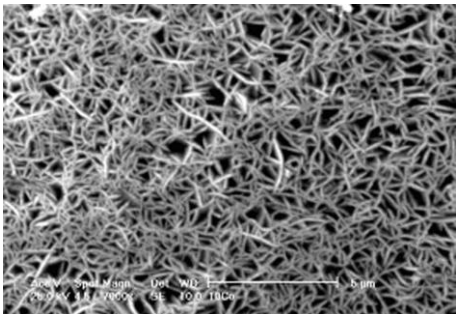

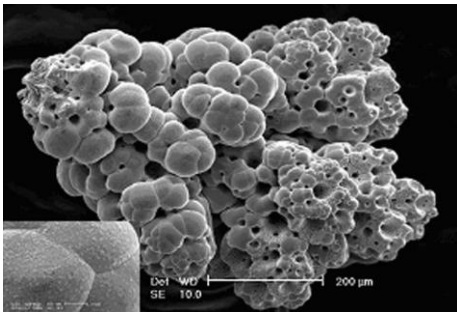

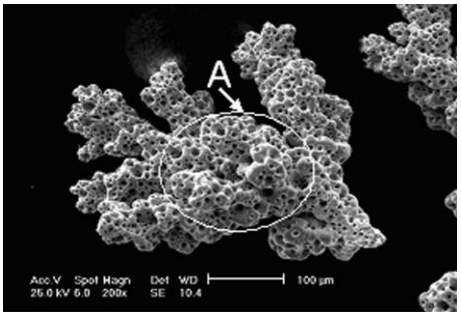

Figure: SEM photographs of morphology of cobalt powder particles deposeted onto (a) glassy carbon; (b) cobalt and (c) nickel electrode.

***4th Internacional Conferecne Processing and Structure of Materials*, May 27-29, 2010. Palić, Serbia, Proceedings, pp.195-200**

Hardening mechanisms in Cu-Ti-TiB_2 composites

Dušan Božić, Jelena Stašić, Biljana Dimčić, Visešlava Rajković

Institute of Nuclear Sciences, Vinča, University of Belgrade, 11001 Belgrade, Serbia

The multiple hardening mechanisms of a copper matrix have been presented anddiscussed. The gas atomized Cu-0.6 wt.%Ti-2.5 wt.%TiB_2 (Cu-Ti-TiB_2) powders have been used as starting materials. Dispersoid particles TiB_2 were formed *in situ* in the copper matrix during gas atomization. The powders have been consolidated by hotisostaticpressing (HIP). Optical microscopy, transmission electron microscopy (TEM), and X-ray diffraction (XRD) analysis were performed for microstructural characterization of powders and composite compacts. High strenthening of Cu-Ti-TiB_2composite achieved by aging is a consequence of the simultaneous influence of the following factors: the development of modulated structure with metastable $Cu_4Ti_{(m)}$particles and *in situ* formed TiB_2dispersoid particles.

Keywords: Cu-Ti-TiB_2, dispersoid hardening, precipitation and spinodal hardening, structure, microhardness.

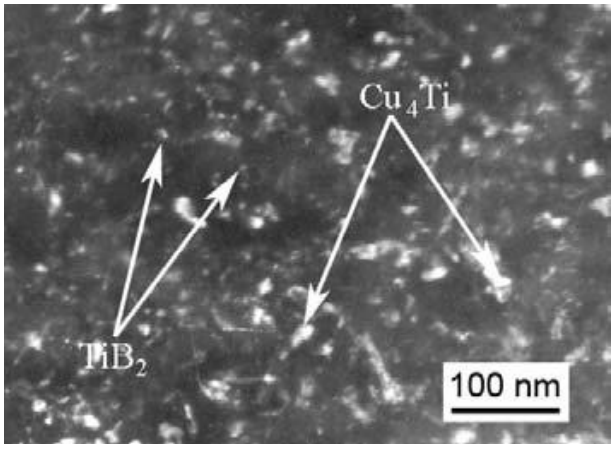

Figure: TEM. TiB_2 particles and Cu_4Ti equilibrium precipitates in the copper matrix.

***Metallurgical & Materials Engineering*, 15 (2009) 159-168.**

Sinterovane legure titana
Sintered titanium alloys

D. Božić, J. Stašić, V. Rajković

Institute of Nuclear sciences, Vinča, University of Belgrade, 11001 Belgrade, Serbia

Razvoj avio i automobilske industrije, pomorske i kosmičke tehnike, kao i hemijske industrije, doveo je primenu titana i legura titana u prvi plan. Legure titana imaju visok odnos čvrstoća/gustina, dobre mehaničke karakteristike na povišenim temperaturama i odlične korozione osobine. Međutim, kako izrada legura zahteva specijalne uslove topljenja i posebne načine prerade, a procesi recikliranja osnovnog metala nisu jednostavni, ove legure su skupe u odnosu na druge materijale. Na visoku cenu ovih materijala, osim skupih sirovina, utiče i odgovarajuća mašinska obrada. Ovaj problem danas može da se umanji primenom novih tehnologija i izradom kompozitnih materijala na osnovi titana. Tehnologija koja je značajno proširila primenu titana i njegovih legura je metalurgija praha, čijim tehnikama je omogućeno dobijanje kvalitetnih sinterovanih i kompozitnih proizvoda.
U monografiji je prikazano stanje u istraživanjima poslednjih nekoliko decenija sinterovanih legura titana, pri čemu je u fokusu najpoznatija, komercijalna legura Ti6Al4V.

Development of aerplane and automotive industry, naval and space engineering, as well as chemical industry, has brought the application of titanium and its alloys to the first plan. Titanium alloys have high strength/density ratio, good mechanical characteristics at elevated temperatures and excellent corosive properties. However, since the manufacturing of alloys requires special melting conditions and particular processing methods, and recycling of the basic metal is not simple, these alloys are expensive comparing to other materials. Apart from costly raw material, high price of these materials is also affected by the appropriate machining. This problem can be moderated by the use of new technologies and production of titanium based composite materials. Technology that has significantly broadened the application of titanium and its alloys is powder metallurgy, whose techniques enabled the obtaining of high quality sintered and composite products.
This monograph shows state in the researches of sintered titanium alloys over the last few decades, with the emphasis on the best known, commercial Ti6Al4V alloy.

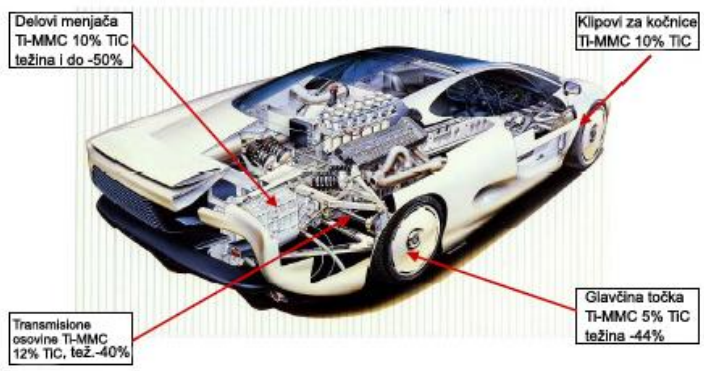

Slika: Potencijalna primena kompozita na osnovi titana kod šasije automobila.
Figure: Potential application of titanium-MMC alloys for chassis components.

***Monografija nacionalnog značaja*, ISBN-10(13): 978-86-7306-103-0, izdavač: Institut za nuklearne nauke "Vinča", Beograd, 2010.**

Nickel-based super-alloy Inconel 600 morphological modifications by high repetition rate femtosecond Ti: sapphire laser

J. Stašić[1], B. Gaković[1], A. Krmpot[2], V. Pavlović[3], M. Trtica[1], B. Jelenković[2]

[1]Institute of Nuclear Sciences, Vinča, University of Belgrade, 11001 Belgrade, Serbia
[2]Institute of Physics, Belgrade, Serbia
[3]Faculty of Agriculture, Department of Mathematics and Physics, Belgrade, Serbia

The interaction of Ti: sapphire laser, operating at high repetition rate of 75 MHz, with nickel-based super-alloy Inconel 600was studied. The laser was emitting at 800 nm and ultrashort pulse duration was 160 fs. Nickel-based super-alloy surface modification was studied in a low laser energy/fluence regime of maximum 20 nJ–15 mJ/cm^2, for short (10 s) and long irradiation times (range of minutes). Surface damage threshold of this material was estimated to be 1.46 nJ, i.e., 0.001 J/cm^2 in air. The radiation absorbed from Ti: sapphire laser beam under these conditions generates at the surface a series of effects, such as direct material vaporization, plasma creation, formation of nano-structures and their larger aggregates, damage accumulation, etc. Laser induced surface morphological changes observed on Inconel 600 were: (1) intensive removal of surface material with crater like features; (2) material deposition at near and farther periphery and creation of nano-aggregates/nano-structures; (3) sporadic micro-cracking of the inner and outer damage area. Generally, features created on nickel-based super-alloy surface by high repetition rate femtosecond pulses are characterized by low inner/outer damage diameter of less than 11 mm/30 mm and relatively large depth on the order of 150 mm, in both low (10 s) and high (minutes) irradiation time regimes.

Keywords: Femtosecond; Laser-matter interaction; Nickel-based super-alloy Inconel 600; Ti:sapphire laser.

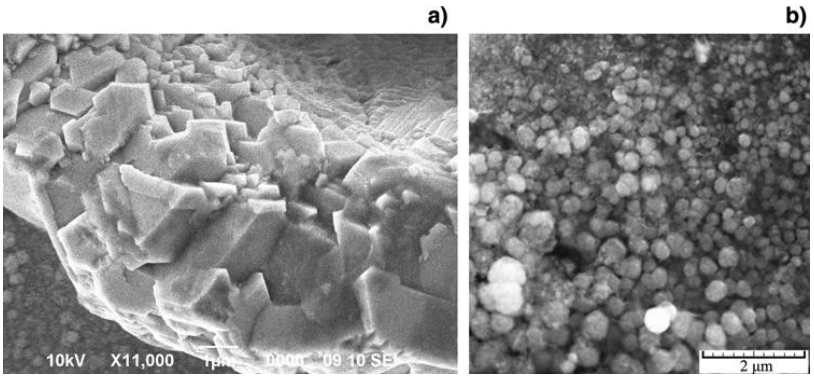

Figure: The view of a crater rim (a) and periphery (b) of irradiated surface on the super-alloy Inconel 600 (160 fs laser pulse, laser energy 19 nJ, irradiation time 7 min, pulse repetition rate 75 MHz, SEM analysis).

Laser and Particle Beams, 27 (2009) 699-707.

High electrical conductivity Cu-based alloys, Part 1

M T. Jovanović, V. Rajković

Institute of Nuclear Sciences „Vinča“, 11001 Belgrade, Serbia

Effect of thermomechanical heat treatment (TMHT), i.e. prior plastic deformation, time and temperature of aging on microstructure, hardness, electrical conductivity and thermal stability of Cu-0.4%Cr-0.08%Zr and Cu-0.4%Cr-0.08%Zr-0.05%Mg (in wt.%) alloys has been investigated. Both alloys behave in the similar manner under TMHT. The maximum value of hardness was within the range of 1520 to 1630 MPa after cold rolling for 50 and 80% followed by aging at 425 ^{o}C for 2h. The maximum of electrical conductivity which is between 89 and 92% IACS appears at 480 ^{o}C. These properties together with high thermal stability of both alloys (around 520 ^{o}C) are quite satisfactory compared to properties of commercial Cu-based alloys. Considering practical application Cu-0.4%Cr-0.08%Zr-0.05%Mg alloy might be regarded as very interesting because the TMHT avoids high temperature solution annealing and quenching, without reducing the hardness and electrical conductivity.

Key words: thermal stability, recrystallization, hardness, electrical conductivity, spot welding electrodes.

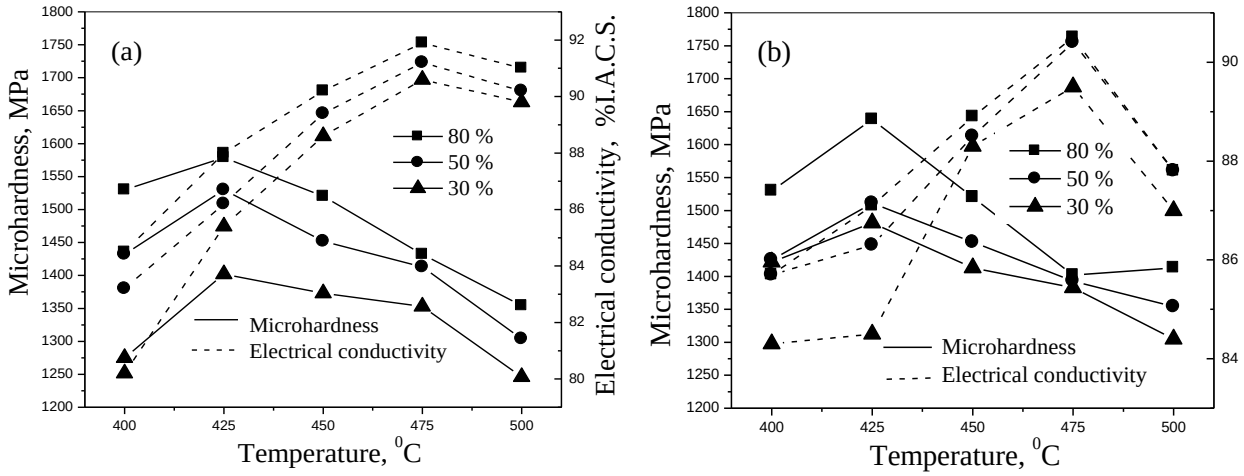

Figure: Effect of prior cold deformation and aging temperature on hardness and electrical conductivity; (a) Cu-Cr-Zr; (b) Cu-Cr-Zr-Mg. Aging time-2h.

***Metalurgija, Journal of Metallurgy (MJoM),* 15 [2] 2009, 125-133.**

Metallic materials-application of TEM, EPMA and SEM in science and engineering practice

M.T. Jovanović, N. Ilić, I. Bobić, I. Cvijović-Alagić, V. Rajković, Z. Mišković

Institute of Nuclear Sciences, Vinča, University of Belgrade, P.O. Box 522, 11001 Belgrade, Serbia

Examples of application of transmission electron microscope (TEM), electron probe X-ray microanalyzer (EPMA) and scanning electron microscope (SEM) in microstructural investigation of metallic materials are described. All investigations have been carried out at the Department of Materials Science, Institute of Nuclear Sciences, Vinča, Serbia.

Keywords: metallic materials, TEM, EPMA, SEM, microstructure, science, practice

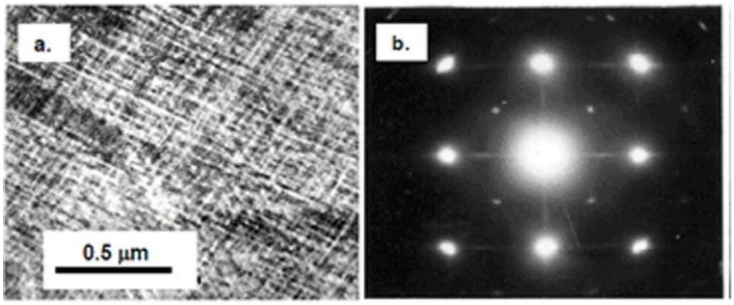

Figure: TEM micrograph of Cu-2Be after aging at 250 ^{o}C for 120 h. (a) "Tweedlike" microstructure; (b) SADP showing continuous streaks in (001) direction. Thin foil.

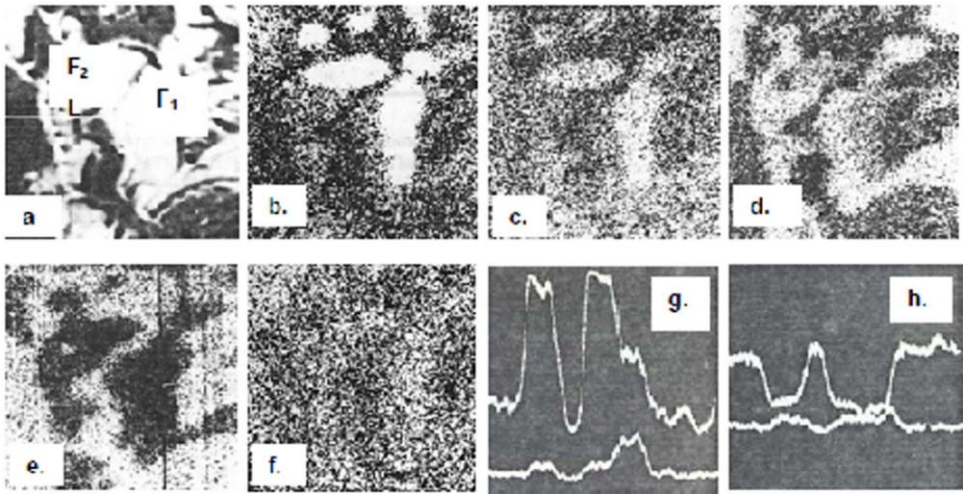

Figure: EPMA micrograph of Ag-11Au-20Pd-2Pt-13.5Cu-1.5Zn alloy. (a) Electron image; (b) Zn distribution; (c) Pd distribution; (d) Cu distribution; (e) Ag distribution; (f) Pt distribution; (g) Cu+Pd distribution along line L; (h) Ag+Pt distribution along line L.

***Metalurgija – Journal of Metallurgy (MJoM)*, 15 [4] (2009) 257-266.**

Determination of processing window for adi materials alloyed with copper

Olivera Erić[1], Tanja Brdarić[1], Nikola Stojsavljević[1], Milan Tonić[1], Nebojša Grahovac[2], Rade Đuričić[3]

[1]Kirilo Savić Institute, Vojvode Stepe 51, 11000 Belgrade, Serbia,
[2]The Institute of Nuclear Sciences, Vinča, 11000 Belgrade, Serbia
[3]The Institut of Mining, Zemun, Serbia

Austempered ductile iron (ADI) materials belong to the group of new materials which are processed by isothermal transformation of nodular cast iron when the unique microstructure – ausferrite is obtained. The aim of the paper was to investigate the effect of austempering parameters (time and temperature) on the microstructure and mechanical properties of ADI alloyed with 0.45% Cu in order to establish the optimal processing window. Light microscopy (LM) and X-ray diffraction (XRD) analysis were performed for microstructural characterization, whereas hardness, tensile and impact tests were determined after different austempering temperatures. It was shown that strength, elongation and impact energy strongly depend on amounts of ausferritic ferrite and stable, high carbon enriched retained, reacted austenite. Processing window was established according to the results of kinetics of isothermal transformation. The processing window is open from 300 to 400 ^{o}C and above this temperature is closed.

Key words: austempered ductile iron, processing window, ausferritic ferrite

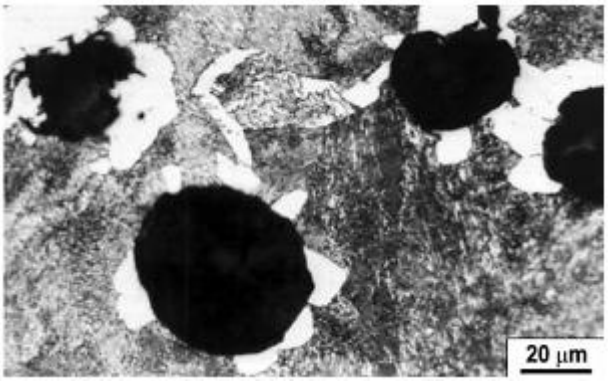

Figure: LM. Microstructure of as-cast ADI specimen.

Laser damage in thin films and bulk materials

M. Srećković [1], A. Kovačević [2], V. Rajković [3], Ž. Tomić[4], M. Dukić[5]
S. Bugarinović[6], P. Jovanić[7]

[1]Faculty of Electrical Engineering, University of Belgrade, Belgrade, Serbia,
[2]Institute of Physics, Serbia,
[3]Department of material science, INN Vinca, Belgrade, Serbia,
[4]IRITEL AD, Belgrade, Serbia,
[5]North Carolina Central University, Durham, USA,
[6]Telecom of Serbian Republic, Bijeljina, Serbian Republic,
[7]Institute for Multidisciplinary Research, Belgrade, Serbia

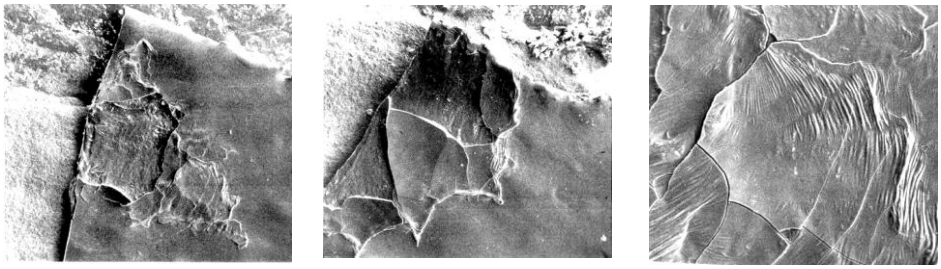

(a) **(b)** **(c)**

Figure: Amorphous material,70%Ti-30%Fe: (a)-Damage view, SEM 50x (b); detail from (a), SEM 500x; (c) detail from (a), 198x.

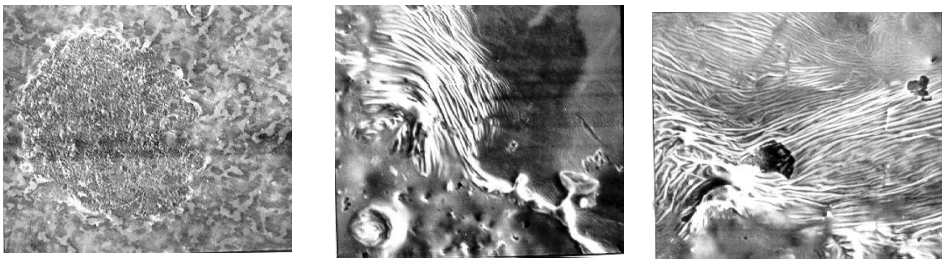

(a) **(b)** **(c)**

Figure: Tin plate: (a) Damage view, 28x; (b) bottom of the damage and nondamaged material, 500x (c); wall and the bottom of the crater, 660x.

***4th Serbian Congress of Microscopy*, Belgrade, 11-12, October 2010.** pp. 101-102.

Energy

Ab initio calculations of MgH_2, MgH_2: Ti and MgH_2: Co compounds

N.Novaković[1], Lj. Matović[2], J. Grbović Novaković[2], I.Radisavljević[1], M. Manasijević[1], N. Ivanović[1]

[1]Laboratory for Nuclear and Plasma Physics, Vinča Institute of Nuclear Sciences, PO Box 522, 11001 Belgrade, Serbia
[2]Laboratory of Material Science, Vinča Institute of Nuclear Sciences, PO Box 522, 11001 Belgrade, Serbia

The understanding of hydrogen bonding in magnesium and magnesium based alloys is an important step toward its prospective use. In the present study, a density functional theory (DFT) based, full-potential augmented plane waves method of calculation, extended with local orbitals (FP-APWþlo), was used to investigate the stability of MgH_2:TM (TM ¼ Ti and Co) 10 wt % alloys and the influence of this alloying on hydrogen storage properties of MgH_2 compound. Effects of a possible spin polarisation induced in the system by transition metal (TM) ions were considered too. It has been found that TM-H bonding is stronger than the Mg–H bond, but at the same time it weakens other bonds in the second and third coordination around a TM atom, which leads to overall destabilization of the MgH_2 compound. Due to a higher number of d-electrons, this effect is more pronounced for Co alloying, where in addition, the spin polarisation has a noticeable and stabilizing influence on the compound structure.

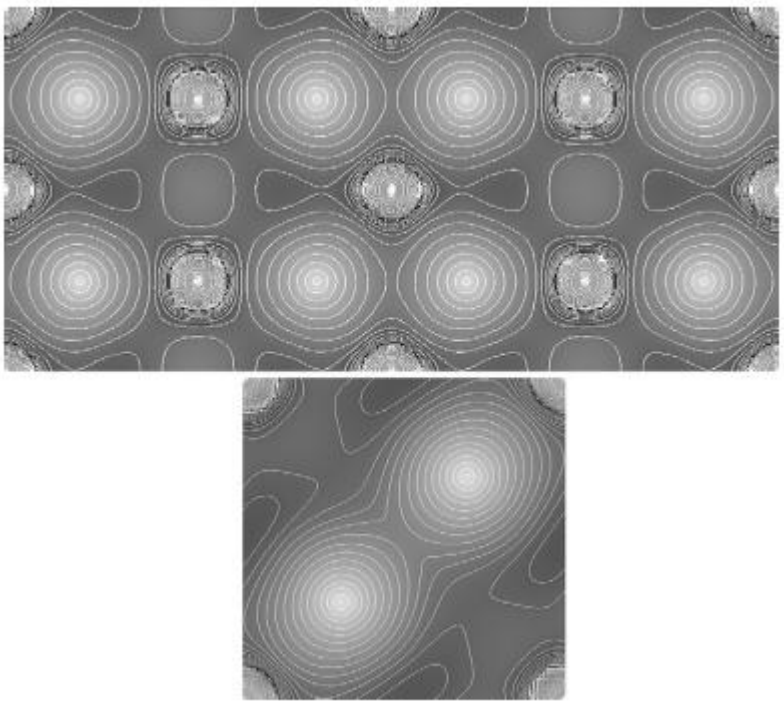

Figure: Valence electron charge densities in [110] (upper) and [100] (lower) crystal planes of the MgH_2 unit cell.

***Internacion Journal of Hydrogen Energy*, 35 (2010) 598-608**

Ispitivanje promena desorpcionih osobina MgH_2 nastalih bombardovanjem jonskim snopovima

Sandra V. Kurko, Ljiljana Lj. Matović, Nikola B. Novaković, Snežana S. Nenadović, Zoran M. Jovanović, Nenad B. Ivanović, Jasmina D. Grbović Novaković

Institut za nuklearne nauke Vinča

U ovom radu su ispitivane promene u strukturi MgH_2 izazvane bombardovanjem jonskim snopovima B^{3+}(45 keV) i Ar^{8+} (120 keV) fluence 10^{15} jona/cm^2 i njihov uticaj na desorpcione osobine jedinjenja. Interakcija upadnih jona i mete procenjenja je Monte Karlo numeričkom simulacijom korišcenjem SRIM (The Stoping and Range of Ions in Matter) programskog paketa. Za karakterizaciju indukovanih strukturnih promena korišcene su rendgenostrukturna analiza i analiza veličine čestica, a njihov uticaj na desorpcione osobine praćen je temperaturski programiranom desorpcijom (TPD). Promene na TPD spektrima pri promeni uslova bombardovanja ukazuju na to da proces desorpcije zavisi od koncentracije površinskih defekata, njihove interakcije i uredenja. Rezultati takode pokazuju da sistematskom kontrolom koncentracije defekata možemo uticati na termodinamicke parametare sistema.

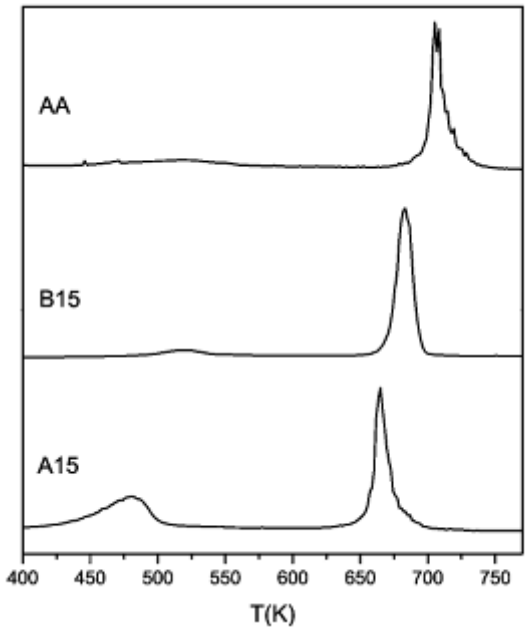

Figure: Rezultati TPD merenja, dobijenih pri konstantnoj brzini zagrevanja od 5 K/min, u temperaturskom opsegu od sobne temperature do 973 K, komercijalnog uzorka MgH_2 (AA) i uzoraka MgH_2 bombardovanih jonima B^{3+} energije 45 keV (B15) i Ar^{8+} energije 120 keV (A15), fluence 10^{15}jona/cm.

***Hemijska industrija*, 64 [3] (2010) 227-232.**

Impact of some meteorological parameters on SO_2 concentrations in the city of Obrenovac, Serbia

S. Milovanović, Lj. Matović, M. Milanović, S. Janićević, J. Grbović Novaković, M. Lješević

Institute of Nuclear Sciences, Vinča

In this paper, the impats of some meteorological parameters on the SO_2 concentrations in the City of Obrenovac are presented. The City of Obrenovac is located in the north-westpart of Serbiaon the banks of the River Sava. The observed source of emission, the power plants TENT A and B are situated on the bank of the Sava River in the vicinity of Obrenovac. During the period from January to November 2006, the concentrations of sulfur dioxide in the air at 4 monitoring sites in Obrenovac were measured. It was noticed that the maximal measured daily concentrations of sulfur dioxide ranged from 1 μgm^{-3} (16th November, 2006) to 98 μgm^{-3} (29th January 2006) and lie under the maximal allowed concentration value according to the Serbian Law on Environmental Protection. The measured sulfur dioxide concentrations mostly showed characteristic usual for a daily acidification sulfur dioxide cycle, excluding the specificities influenced by the measuring site itself. Sulfur dioxide transport was recorded at increased wind speeds, primarily from the southeast direction. Based on the impact of meteorological parameters on the sulfur dioxide concentration, a validation of the monitoring sites was also performed from the aspect of their representivity.

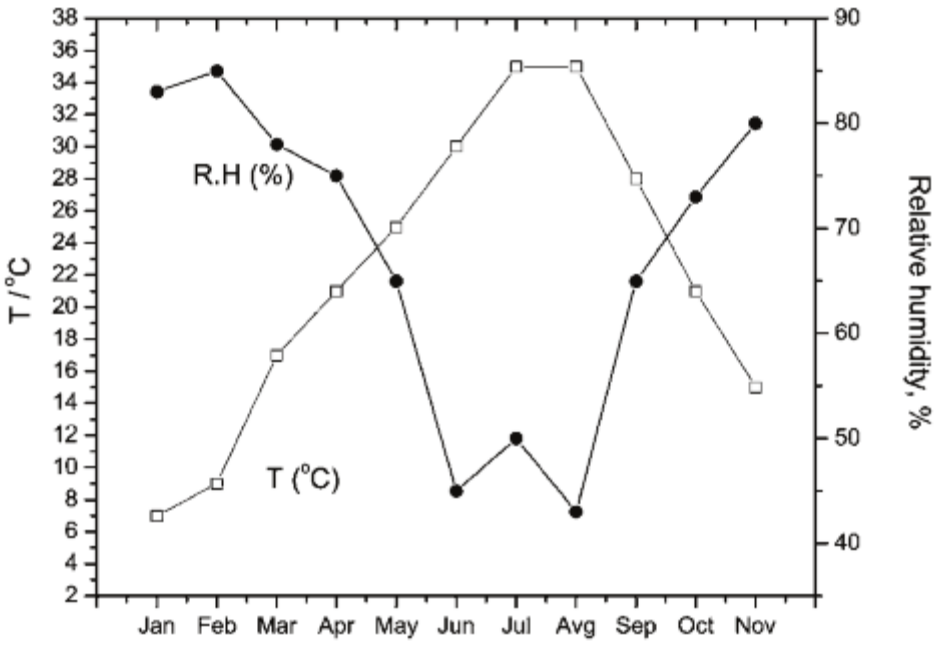

Figure: Meteorological parameters in the City of Obrenovac during 2006.

***Journal of Serbian Chemical Society,* 75 (5) (2010) 703–715.**

Improvement of Hydrogen Storage Properties of MgH_2-SiC

Lj. Matović[a], S. Kurko[a], Z.Rašković[a], Z.Baščarević[b], N.Novaković[a], J. Grbović Novaković[a]

[a]Laboratory of Material Science, Vinča Institute of Nuclear Sciences, Belgrade, Serbia
[b]IMSI University of Belgrade, Belgrade, Serbia

To understand the influence of various crystallographic phases on hydrogen storage properties, ball milling of MgH_2 with hexagonal (a) and cubic (b) SiC have been performed.Structural characterization of all samples has been done by X-ray diffraction (XRD) analysis, particle size analysis and scanning electron microscopy (SEM). Investigation of hydrogen desorption properties of prepared nanocomposites has been done using temperature programmed desorption (TPD) technique. Despite the results of structural and morphological characterization of obtained nanocomposites are very similar, TPD spectra show significant differences regarding existence of intermediate temperature peak. In the sample milled with hexagonal SiC this peak originates both from H_2 and H_2O, while in the sample milled with cubic phase it only comes from H2O. Both samples exhibit low temperature H_2 peak at 385 K.

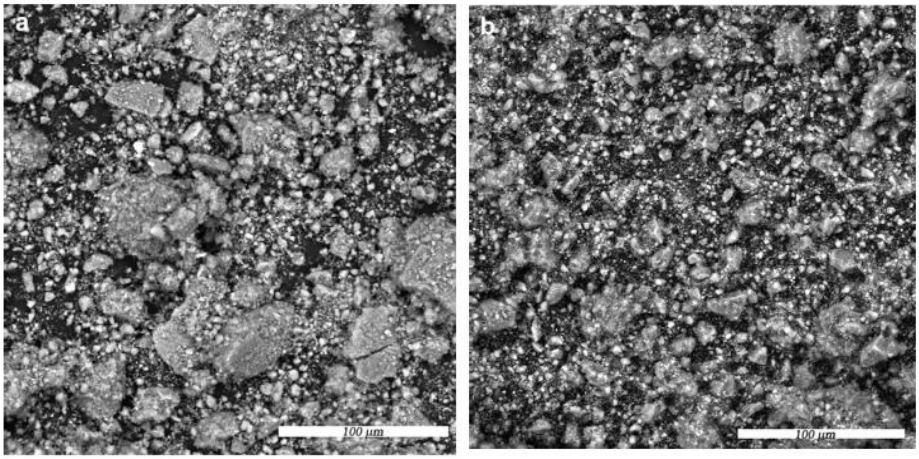

Figure: (a) SEM BSE micrographs of MgH_2/a-SiC composites. (b) SEM BSE micrographs of MgH_2/b-SiC composites.

***International conference of microscopy IMC 17*, Rio de Jenairo, Brasil, september 19-24, 2010.**

Hydrogen desorption from MgH_2-VO_2 composite

Sanja Milošević[a], Željka Rašković[a], Sandra Kurko[a], Ljiljana Matović[a], Nikola Cvjetićanin[b], Jasmina Grbović Novaković[a]

[a]Laboratory for Material Sciences, Vinča Institute of Nuclear Sciences
[b]Faculty of Physical Chemistry, University of Belgrade

The hydrogen desorption properties and kinetics of MgH_2–VO_2 composite prepared by mechanical milling of MgH_2 have been investigated. Structural characterization of produced nanocomposite was done by X-ray powder diffraction (XRD), particle size analysis and scanning electron microscopy (SEM). The structure and morphology of the composite have been correlated with hydrogen desorption properties investigated by differential thermal analysis (DTA). It has been shown that short mechanical milling of nanostructured VO_2 and MgH_2 leads to decrease of hydrogen desorption temperature of MgH_2 by 80 K. The mechanism of desorption has been changed from phase boundary reaction, spherical symmetry for untreated MgH_2 to phase boundary reaction, cylindrical symmetry for the composite material. The activation energy for desorption has been reduced by adding VO_2 ceramics as a catalyst.

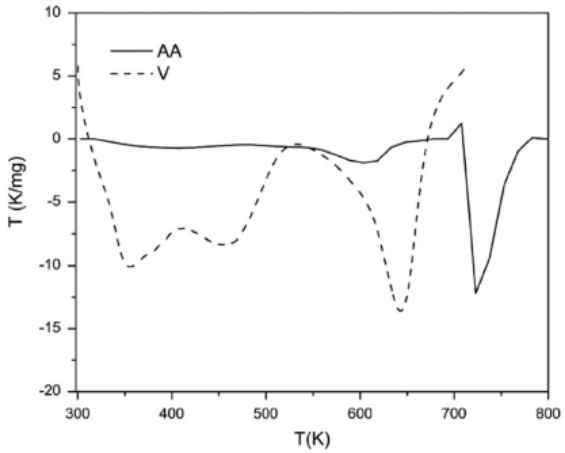

Figure: DTA curves of a commercial MgH_2 powder (AA) and MgH_2–VO_2(B) composite (V). Catalyzed system shows three maxima positioned at 642 K (HT), 456 K (IT) and 354 K (LT).

Ninth Young Researchers Conference Materials Sciences and Engineering **December 20-22, 2010, Belgrade, Serbia, pp. 33.**

Hydrogen storage properties of MgH_2-CeO_2 composites

Željka Rašković, Sandra Kurko, Radojka Vujasin, Jelena Gulicovski, Sanja Milošević, Ljiljana Matović, Jasmina Grbović Novaković

Laboratory for Materials Science, Vinča Institute of Nuclear Sciences

The hydrogen desorption (HD) properties of MgH_2-CeO_2 composite prepared by mechanically milling of MgH_2 and cubic CeO_2 have been examined. Morphology and microstructure of composites have been studied by X-ray powder diffraction (XRD), scanning electron microscopy (SEM), laser scattering analysis and correlated with desorption properties obtained by means of temperature programmed desorption (TPD). It has been shown that decrease of crystallite and particle size of the samples lead to significant lowering of desorption temperature. Further, the activation energy for desorption DE has been calculated using Kissinger equation. Obtained value of 60 kJ/mol indicates that the activation energy of hydrogen desorption is sufficiently decreased by the catalytic effect of vacant CeO2 structure. Consequently the surface activation of sample plays a major role in HD reaction.

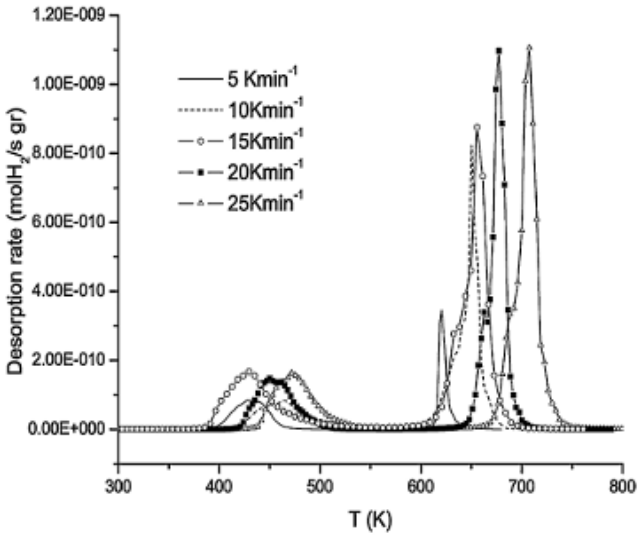

Figure: H-desorption rate curves for MgH_2–CeO_2 at different heating rates. 5 K/min (solid line) 10 K/min (dash line), 15 K/min (empty circle), 20 K/min (filled square), 25 K/min (empty triangle).

Ninth Young Researchers Conference Materials Sciences and Engineering **December 20-22, 2010, Belgrade, Serbia, pp. 33**

Improvement of Hydrogen Storage Properties of MgH_2 by Formation of MgH_2-SiC Nanocomposite

Lj.Matović, S.Kurko, Ž.Rašković, N.Novaković, Z. Jovanović, J.Grbović Novaković

Vinča Institute of Nuclear Sciences, University of Belgrade, Serbia

To understand the influence of various crystallographic phases on hydrogen storage properties, ball milling of MgH_2 with hexagonal (a) and cubic (b) SiC have been performed.Structural characterization of all samples has been done by X-ray diffraction (XRD) analysis, particle size analysis and scanning electron microscopy (SEM). Investigation of hydrogen desorption properties of prepared nanocomposites has been done using temperature programmed desorption (TPD) technique. Despite the results of structural and morphological characterization of obtained nanocomposites are very similar, TPD spectra show significant differences regarding existence of intermediate temperature peak. In the sample milled with hexagonal SiC this peak originates both from H_2 and H_2O, while in the sample milled with cubic phase it only comes from H_2O. Both samples exhibit low temperature H_2 peak at 385 K.

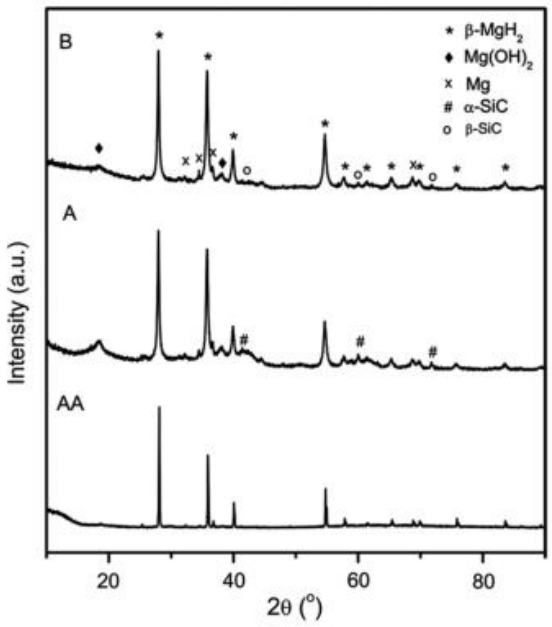

Figure: XRD patterns of commercial MgH_2 powder (AA) and MgH_2 milled with 5 wt % of different SiC phases: α-SiC (A) and β-SiC (B).

***11th Eurasia Conference on Chemical Sciences,* Amman, Jordan, 6-11.October 2010 pp. 132.**

The Influence of Boron Doping Concentration on MgH_2 Electronic Structure

S. Kurko, B. Paskaš Mamula, Lj. Matović, J. Grbović Novaković, N. Novaković

Vinča Institute of nuclear sciences, University of Belgrade, Serbia

We have performed ab initio electronic structure calculations of $Mg_{1-x}B_xH_2$compounds with different boron concentrations, ranging from x =0.0625 to 0.5. Full structural relaxation was performed in order to properly describe influence of dopant on host matrix. Results showed that there is a strong influence of boron concentration on structural and thermodynamic stability of compound. B-H bond length is substantially shorter then in Mg-H coordination polyhedron. Boron significantly contributes to density of states at Fermi level within energy gap. The width of boron electronic states heavily depends on boron concentration, causing reduction of energy gap of host MgH_2 and leading to metallic nature of compound with highest boron concentration. The predicted thermodynamic instability of compounds with higher boron concentration is in agreement with experimental findings that under similar stoichiometry, boron with magnesium forms only complex hydride, $Mg(BH_4)_2$ is also shown that existence of stable hydrides with MgH_2 rutile structure and small concentration of boron is possible in principle and that boron can be used to further destabilize MgH_2 in order to enhance its hydrogen sorption-desorption kinetics.

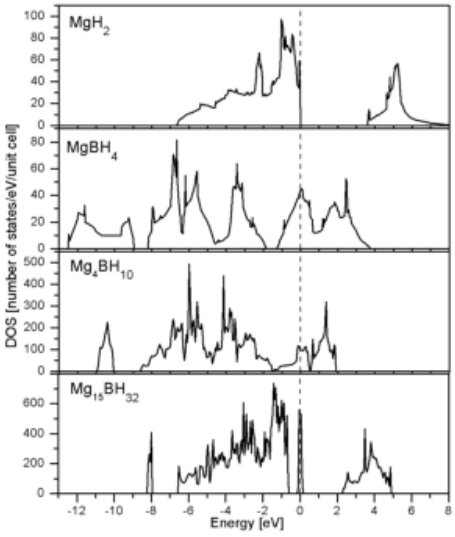

Figure: Total densities of states for all four investigated systems. Fermi level is marked with vertical dashed line.

12th Annual Conference YUCOMAT 2010 **Hotel "Plaža", Herceg Novi, Montenegro, September 6–10, 2010 Programme and The Book of Abstracts pp. 120.**

Improvement of Hydrogen Storage Properties of MgH_2 by α and β-SiC

Lj. Matovic[a], S. Kurko[a], Z.Raskovic[a], B. Paskaš Mamula[a] Z.Bascarevic[b], N.Novakovic[a], J. Grbovic Novakovic[a]

[a]Laboratory of Material Science, Vinča Institute of Nuclear Sciences, Belgrade, Serbia
[b]IMSI University of Belgrade, Belgrade, Serbia

The influence of various crystallographic phases of SiC on hydrogen storage properties of MgH_2, was followed. Structural characterization of all samples has been done by X-ray diffraction (XRD) analysis, particle size analysis and scanning electron microscopy (SEM). Investigation of hydrogen desorption properties of prepared nanocomposites has been done using temperature programmed desorption (TPD) technique. Despite the results of structural and morphological characterization of obtained nanocomposites are very similar, TPD spectra show significant differences regarding existence of intermediate temperature peak. In the sample milled with hexagonal SiC this peak originates both from H_2 and H_2O, while in the sample milled with cubic phase it only comes from H_2O. Both samples exhibit low temperature H_2 peak at 385 K.

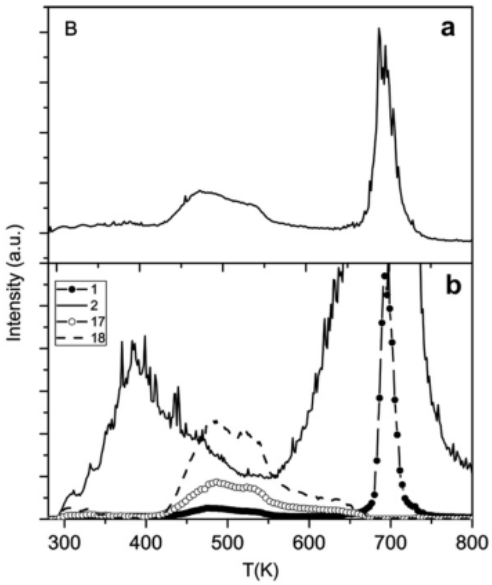

Figure: Results of TPD measurements, obtained at constant heating rate of 5 K/min, in the temperature range from RT to 973 K, of MgH_2/β-SiC powder (B): a) total signal of all desorption products, b) separate signals of desorption products: 1(H^+), 2 (H_2),17(OH^-) and 18 (H_2O).

12th Annual Conference YUCOMAT 2010 **Hotel "Plaža", Herceg Novi, Montenegro, September 6–10, 2010, Programme and The Book of Abstracts pp. 114.**

MgH_2: B Nanocomposite for hydrogen storage: Ab Initio Calculations and Experiment

S.Kurko, N. Novaković, Lj. Matović, Z.Rašković, Z.Jovanović, B.Matović, J.Grbović Novaković

Vinča Institute of Nuclear Sciences

An ab initio electronic structure calculations of $Mg_{1-x}B_xH_2$compounds with different boron concentrations, ranging from x =0.0625 to 0.5. Full structural relaxation was performed in order to properly describe influence of dopant on host matrix. Results showed that there is a strong influence of boron concentration on structural and thermodynamic stability of compound. B-H bond length is substantially shorter then in Mg-H coordination polyhedron. Boron significantly contributes to density of states at Fermi level within energy gap. The width of boron electronic states heavily depends on boron concentration, causing reduction of energy gap of host MgH_2 and leading to metallic nature of compound with highest boron concentration. The predicted thermodynamic instability of compounds with higher boron concentration is in agreement with experimental findings that under similar stoichiometry, boron with magnesium forms only complex hydride, $Mg(BH_4)_2$ is also shown that existence of stable hydrides with MgH_2 rutile structure and small concentration of boron is possible in principle and that boron can be used to further destabilize MgH_2 in order to enhance its hydrogen sorption-desorption kinetics.

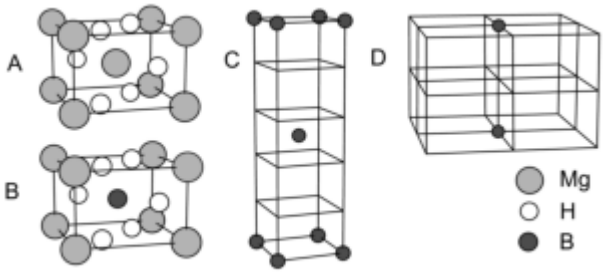

Figure: Unit cells of investigated compounds a) pureMgH_2, b) $MgBH_4$, c) Mg_4BH_{10} and d) $Mg_{15}BH_{32}$. For c) and d) only unit cells' stacking is shown, with positions of boron atoms.

International Symposium " Metal-Hydrogen Systems. Fundamentals and Application",
Moscow, Russia, July 19-23, 2010, The Book of abstract pp. 366.

Structural destabilisation of MgH_2 obtained by heavy ion irradiation

Lj. Matović[a], N.Novaković[b], S. Kurko[a], M. Šiljegović[c], B. Matović[a], N. Romčević[e], Z. Kacarević-Popović[d], N. Ivanović[b], J. Grbović Novaković[a]

[a]Laboratory for Material Sciences, Vinča Institute of Nuclear Sciences, P.O Box 522, 11000 Belgrade, Serbia
[b]Laboratory for Nuclear and Plasma Physics, Vinča Institute of Nuclear Sciences, P.O Box 522, 11000 Belgrade, Serbia
[c]Laboratory of Physics, Vinča Institute of Nuclear Sciences, P.O Box 522, 11000 Belgrade, Serbia
[d]Laboratory for Radiation Chemistry and Physics, Vinča Institute of Nuclear Sciences, P.O Box 522, 11000 Belgrade, Serbia
[e]Institute of Physics, P.O. Box 68, 11080 Belgrade, Serbia

MgH_2 powder samples have been irradiated with 120 keV Ar^{8+} ions with different ion fluencies ranging from $10^{12}$to 10^{16} ions/cm^2. Irradiation effects are estimated by SRIM calculations, and investigated experimentally using Raman spectroscopy and X-ray diffraction (XRD) analysis. The observed changes of structure and vibrational spectra are elaborated, their consequences on hydrogen bonding in MgH2 discussed, and influence onH-desorption properties investigated by Temperature Programmed Desorption (TPD) and Differential Scanning Calorimetry (DSC) techniques. It has been established that nearsurface defects have a predominant influence on decreasing the H-desorption temperature. Variations of Raman, TPD and DSC spectra with irradiation conditions suggest that here are several mechanisms of dehydriding, and that they depend on defect concentration, interaction and ordering.

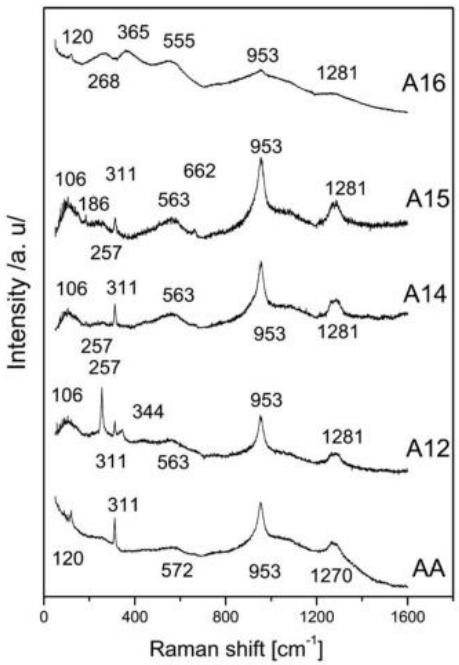

Figure: Raman shift of a commercial (AA) MgH_2 powder, and samples irradiated using 120 keV A^{r8+} ions, with ion fluencies of 10^{16}ions/cm^2(A16), 10^{15} ions/cm^2 (A15), 10^{14}ions/cm^2 (A14) 10^{12}ions/cm^2 (A12).

***Internacional Journal of Hydrogen Energy*, 34 (2009) 7275 -7282.**

Changes of Hydrogen Storage Properties of MgH_2 Induced by Boron Ion Irradiation

S. Kurko[a], Lj. Matović[a], N. Novaković[b], M. Šiljegović[c], Z. Jovanović[c], Z. Kačarević-Popović[d], J. Grbović Novaković[a]

[a]Laboratory of Material Science, Vinča Institute of Nuclear Sciences, PO Box 522, 11001 Belgrade, Serbia
[b]Laboratory for Nuclear and Plasma Physics, Vinča Institute of Nuclear Sciences, PO Box 522, 11001 Belgrade, Serbia
[c]Laboratory of Physics, Vinča Institute of Nuclear Sciences, PO Box 522, 11001 Belgrade, Serbia
[d b]Laboratory Gamma, Vinča Institute of Nuclear Sciences, PO Box 522, 11001 Belgrade, Serbia

MgH_2 powder samples have been irradiated with 45 keV B^{3+} ions with different ion fluencies ranging from 10^{12} to 10^{16} ions/cm^2. Irradiation effects have been estimated by SRIM calculations. To characterize induced modifications and its influence on the hydrogen desorption behavior of MgH_2, X-ray diffraction (XRD) analysis, particle size analysis and temperature programmed desorption (TPD) have been used. Changes of TPD spectra with irradiation conditions suggest that there are several mechanisms involved in desorption process which depend on defect concentration and their interaction and ordering. It has been demonstrated that the changes in near-surface area play the crucial role in hydrogen desorption kinetics. The result also confirm that there is possibility to control the thermodynamic parameters by controlling vacancies concentration in the systems.

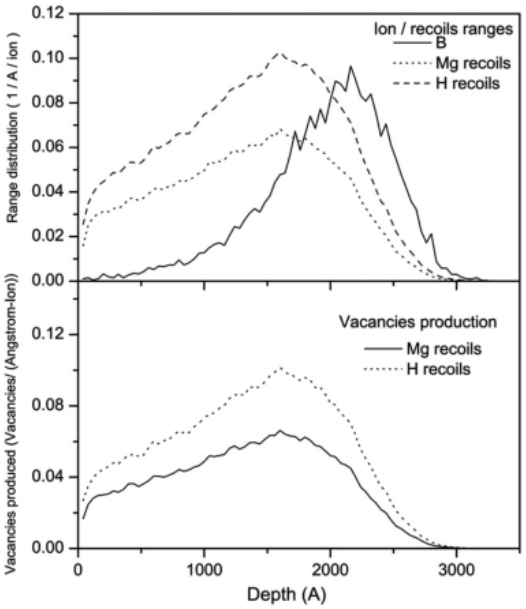

Figure: Results of Monte Carlo simulations of 45 keV B ions irradiation of MgH_2 obtained by SRIM 2003 package. (Top): depth distribution of incident ions and recoiled atoms, (Bottom): vacancies production as a function of depth.

Proceedings of Hydrogen Materials Science and Chemistry of Carbon nanonmaterials
ICHMS 2009, Yalta –Crimea, 25-31.08.2009, Ukraine pp. 210-211.

Enviromental protection

Preparation of Nanosized Non-Oxide Powders Using Diatomaceous Earth

A. Šaponjić, B. Babić, A. Devečerski, B. Matović

Vinča Institute of Nuclear Sciences, Materials Science Lab, P.O. Box 522, 11001, Belgrade, Serbia

In this paper the nanosized non-oxide powders were prepared by carbothermal reduction and subsequent nitridation of diatomaceous earth which is a waste product from coal exploitation. Our scope was to investigate the potential use of diatomaceous earth as a main precursor for low-cost nanosized non-oxide powder preparation as well as to solve an environmental problem. The influence of carbon materials (carbonized sucrose, carbon cryogel and carbon black) as a reducing agent on synthesis and properties of low-cost nanosized nonoxide powders was also studied. The powders were characterized by specific surface area, X-ray and SEM investigations. It was found that by using diatomaceous earth it is was possible to produce either a mixture of non-oxide powders (Si3N4/SiC) or pure SiC powders depending on temperature.

Keywords: Gas-solid reactions; Microstructure; X-ray diffraction; Scanning electron microscopy

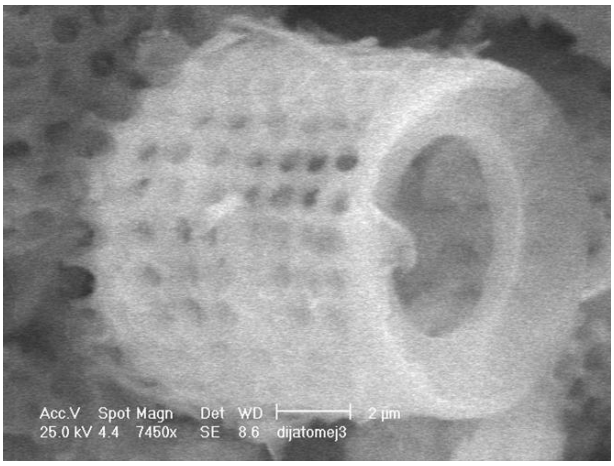

Figure: SEM image of a single frustule of as-received diatomaceous earth.

***Science of Sintering,* 41 (2009) 151-159.**

Ocenivanje usaglašenosti proizvoda – razvoj infrastrukture

P. Popović, R. Mitrović (urednici);
Broj koautora: 20;
Tip: nacionalna monografija

Monografija „Ocenjivanje usaglašenosti – razvoj infrastrukture“ je nastala kao rezultat napora većeg broja instituta i fakulteta na unapređenju infrastrukture za ocenjivanje usaglašenosti u Srbiji, što omogućuje domaćim proizvođačima da u zemlji sprovedu potrebna ocenjivanja usaglašenosti proizvoda, čime se skraćuje vreme razvoja proizvoda i smanjuju troškovi. Osvojene metode i tehnike ocenjivanja usaglašenosti proizvoda, obuhvaćene harmonizovanim standardima, izabrane su na osnovu potreba proizvođača i korisnika ovih proizvoda, uz aktivno učešće particpanata. S obzirom na izuzetno veliki broj harmonizovanih standarda jasno je da je proces harmonizacije tehničkog zakonodavstva dugotrajan i obiman posao koji zahteva uključivanje svih zainteresovanih strana i aktiviranje svih raspoloživih kapaciteta.

Monografija je koncipirana tako da na pregledan način predstavi principe tehničkog zakonodavstva EU, značaj i ulogu direktiva i harmonizovanih standarda, kao i praktične posledice njihove primene. Prikazano je:

- stanje tehničke regulative u oblasti ocenjivanja usaglašenosti u Srbiji
- koncept Novog i Globalnog pristupa EU sa posebnim osvrtom na ocenjivanje usaglašenosti proizvoda
- bitni zahtevi šest izabranih direktiva zasnovanih na Novom i Globalnom pristupu Evropske Unije, koje treba da ispune preduzeća i druga pravna lica kada svoje proizvode stavljaju u promet ili upotrebu na tržište EU. Monografija obrađuje ocenjivanje usaglašenosti proizvoda obuhvaćenih sledećim direktivama Novog pristupa:

i) ATEX 94/9/EC - Oprema i zaštitni sistemi koji se koriste u potencijalno eksplozivnoj atmosferi
ii) LVD 2006/95/EC - Niskonaponska električna oprema
iii) MD 2006/42/EC - Mašine
iv) PED 97/23/EC - Oprema pod pritiskom
v) PPE 89/686/EEC - Sredstva lične zaštite
vi) Direktiva 94/62/ES - Ambalaža i ambalažni otpad

- rezultati na unapređenju i poboljšanju sistema ispitivanja, kontrolisanja i sertifikacije proizvoda ostvareni u našim naučno-istraživačkim organizacijama. Posebno su istaknute i realne mogućnosti naših naučno-istraživačkih organizacija u ovladavanju i primeni novih metoda i tehnika ispitivanja, kontrolisanja i sertifikacije proizvoda prema harmonizovanim standardima odgovarajućih direktiva.

Izdavač: Institut za nuklearne nauke VINČA, Recenzenti: Dr Dragutin Stanivuković i Dr Gradimir Ivanović, Broj strana: 432, Rad: orginalni, ISBN: 978-86-7306-098-9; Beograd, februar 2009.

Managing packaging and packaging waste in the republic of Serbia according to new legislation

M. Kokunešoski, P. Popović

Institute of Nuclear Sciences Vinča, P. O. Box 522, 11000 Belgrade, Serbia

One of the conditions for our country to be included in contemporary European trends is harmonization of local legislation with that of the EU in the area of packaging and packaging waste. Harmonized technical legislation opens the possibilities for our economy to place its products without limitation on the big EU market and at the same time prevents the entry of poor quality goods and services onto the Serbian market. By adopting the Law on packaging and packaging waste in May 2009 transposition of the EU Directive 94/62/EC – Packaging and packaging waste into the national legislation was completed as well as harmonization of national measures in the area of packaging and packaging waste with the European law. In 2009 seven Rule books were adopted which more closely determine the requirements related to the conditions which packaging must fulfill in order to be placed on the market as well as management of packaging and packaging waste and reporting. Their application should begin in mid-2010.

Keywords: EU Directive 94/62/EC, Law on packaging and packaging waste, Rule books in the area of management of packaging and packaging waste

***International Journal Total Quality Management and Excellence,* 38 (2010) 305-310.**

Packaging as an energy source from the standpoint of the european and national legislation

M. Kokunešoski, P. Popović

Institute of Nuclear Sciences, Vinča, P. O. Box 522, 11000 Belgrade, Serbia

Getting the energy by using of usable packaging is one of the possible ways to reuse packaging when it can not be used for the same purpose, or it can not be recycled. Ways to getting energy from packaging depend on how the packaging waste being treated, the technology of the factories, and from the gains of total or partial combustion. The Law on Packaging and Packaging Waste refers to specification of minimum heating value and from the method of determining the gain of energy. The methodology and procedure for application of this standards has been established by Serbian harmonized standards.

Keywords: Legislation, Packaging waste, Energy from the packaging

***International Journal Total Quality Management and Excellence,* 38 (2010) 17-20.**

Results of conformity control of packaging from the local market with the EU Directive 94/62/EC

M. Kokunešoski, M. Pavlović, P. Popović

Institute of Nuclear Sciences Vinča, P. O. Box 522, 11000 Belgrade, Serbia

Packaging was invented thanks to the man's need to make delivery and sale of products easier and to improve handling, transport and storage of products as well as the way they are displayed in shops. Packaging is most often made of paper, metal, wood, glass and plastic. Determining the presence and measuring the content of four heavy metals, cadmium, chromium, lead and mercury in the packaging and components of packaging and control of their disposal in the environment has great environmental effects. It influences the quality of packaging and packaged goods, and health of the consumers. Considering the Republic of Serbia does most of it trade exchange with EU countries, it is necessary to fulfill the required conditions and to harmonize with EU regulations in the area of packaging and packaged waste. Requirements which are related to production and composition of packaging are defined by the EU Directive 94/62/EC. According to that Directive, after June 30 2001, the total content of the above mentioned heavy metals in the packaging must not exceed 100 ppm.

Keywords: Packaging, Heavy metals, EU Directive 94/62/EC

***International Journal Total Quality Management and Excellence,* 37 (2009) 403-408.**

Strategy of Treatment of Packaged Industrial Waste in the Republic of Serbia in Accordance with the EU Practice and Principles

M. Kokunešoski[1], M Pavlović[1], D. Kićević[2], P. Popović[1]

[1]Institute of Nuclear Sciences Vinča, P. O. Box 522, 11000 Belgrade, Serbia
[2]Nuclear Facilities of Serbia, 12-14 Mike Petrovića Alasa, Belgrade 11000

Industrialization significantly contributes to increase in the quantity of waste. In many factories industrial waste including packaging waste as its integral part is not treated in accordance with the current environmental regulations of the Republic of Serbia. Quantity of waste worldwide has been increasing year after year. It is the quantity of the packaging waste which has shown the biggest increase. An important goal of the EU Directive 94/62/EC, on packaging and packaging waste is harmonization of national measures in the area of packaging and packaging waste management. That means that the packaging may be sold only if it is in accordance with the harmonized EN standards, i.e. with their corresponding national standards from SPRS EN 13427:2005 to SPRS EN 13432:2005, in the area of packaging and packaging waste. By applying these standards the first step in reduction of toxicity of packaging waste would be done and that is the prevention of use of heavy metals and other hazardous substances in production of packaging.

Keywords: Industrial packaging waste, EU Directive 94/62/EC, Harmonized EN standards in the area of packaging and packaging waste

***2nd UIO/IWM II*, September, 14th – 17th 2009, Tara, Serbia, Proceedings, p. 23-32.**

Review of conformity assessment of packaging according to national standards and regulations

M. Kokunešoski, M. Pavlović, P. Popović

Institute of Nuclear Sciences, Vinča, P. O. Box 522, 11000 Belgrade, Serbia

Complex procedure of integration of our country with the EU implies the harmonization of the area of management of packaging and packaging waste in line with the EU Directive 94/62/EC. By adoption of the Law on packaging and packaging waste this Directive was introduced into the national legislation, which was one of its requirements and the purpose is to have the national measures harmonized in the area of management of packaging and packaging waste. The adopted harmonized standards in this area have gained the status of national standards, have been translated into Serbian and are identical with the original harmonized EU standards. Articles 8 to 14 of the Law on packaging and packaging waste refer to those. Upon adoption of the Law on technical requirements for products and evaluation of conformity all legal preconditions were achieved for evaluation of products from the local market in line with the EU requirements considering this law is an umbrella law in the area of evalaution of confirmity with the directives.

Keywords: Packaging and packaging waste, Harmonized standards, Legislation

***International Journal Total Quality Management and Excellence,* 37 (2009) 171-177.**

Eco-technological process of glass-ceramic production from galvanic sludge and aluminium slag

M. Stanisavljević[1], I. Krstić[1], S. Zec[2]

[1]Faculty of Occupational Safety, University of Nis, 18000 Nis, Serbia
[2]Vinča Institute of Nuclear Sciences, University of Belgrade, 11001 Beograd, Serbia

Methods of purification of waste water which are most commonly used in the Republic of Serbia belong to the type of conventional systems for purification such as chemical oxidation and reduction, neutralization, sedimentation, coagulation, and flocculation. Consequently, these methods generate waste sludge which, unless adequately stabilized, represents hazardous matter. The aluminium slag generated by melting or diecasting aluminium and its alloys is also hazardous matter. In this sense, this paper establishes ecological risk of galvanic waste sludge and aluminium slag and then describes the process of stabilization of these waste materials by means of transformation into a glass-ceramic structure through sintering. The obtained product was analyzed with Fourier Transform Infrared Spectroscopy (FT-IR) and X-ray diffraction (XRD). The object of the paper is the eco-technological process of producing glass-ceramics from galvanic sludge and aluminium slag. The aim of the paper is to incorporate toxic metals from galvanic sludge and aluminium slag into the glass-ceramic product, in the form of solid solutions.

Keywords: galvanic sludge, aluminium slag, glass-ceramics, ecological risk.

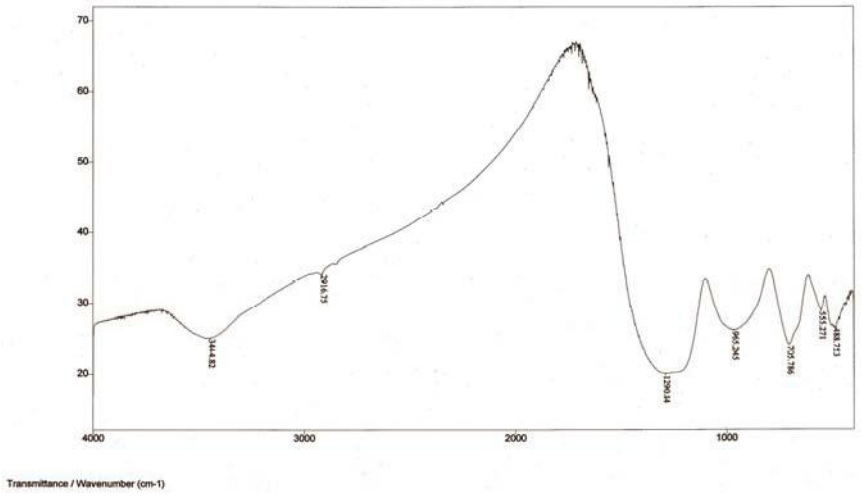

Figure: IR spectrum of glass ceramics.

***Science of Sintering,* 42 (2010) 125-130.**

Influence of diatomite microstructure on its adsorption capacity for Pb(II)

S.Kumrić, S. Nenadović, M. Nenadović, R.Kovačević, Lj. Matović, B.Matović, Jasmina Grbović Novaković

Vinča Institute of nuclear sciences

Adsorption of Pb(II) ions from wastewater on untreated diatomite was studied. Diatomite samples were mechanicaly milled and the effect of microstructure on adsorption properties were investigated.The microstructure of samples has been characterized by X-ray diffraction (XRD), scanning electron microscopy (SEM) and atomic force microscopy (AFM) while the degree of metal adsorption was evaluated analyzing the Pb(II) contaminated samples by Inductively Coupled Plasma Atomic Emission Spectrometry (ICP AES). The results show that metal sorption capacity of diatomite is considerably improved after mechanical modification caused by ball milling and it can be attributed to amorphysation of material. Our results show that immobilization efficiency increase from 22% for untreated samples to 81% to treated sample for 5h at BPR 4 giving rise to possible use of mechanically modified diatomite as possible material for wastewater remediation

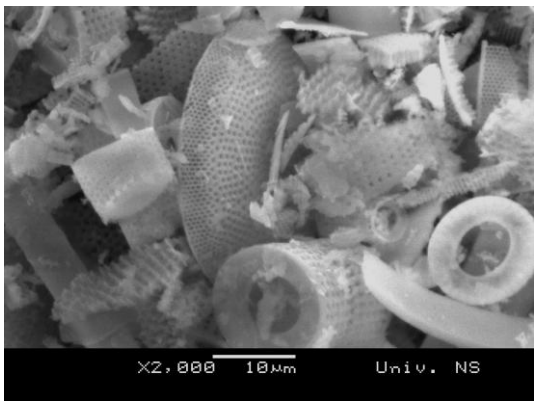

Figure: SEM images of diatomite.

***Joint Proceedings of Meeting of 9th Multinational Conference on Microscopy 2009 and Dreiländertagung 2009,* Graz 30.08-4.09.2009, Austria, pp. 545-546.**

Advanced ceramics

Kinetic study of the hydrogen oxidation reaction on sub-stoichiometric titanium oxide-supported platinum electrocatalyst acid solution

B. Babić[a], J. Gulicovski[a], Lj. Gajić-Krstajić[b], N. Elezović[c], V.R. Radmilović[d], N.V. Krstajić[e], Lj.M. Vračar[e]

[a]Vinča Institute of Nuclear Sciences, P.O. Box 522, Belgrade, Serbia
[b]Institute of Technical Sciences-SASA, Belgrade, Serbia
[c]Center of Multidisciplinary Researches, Belgrade, Serbia
[d]National Center for Electron Microscopy, LBLN University of California, Berkeley, USA
[e]Faculty of Technology and Metallurgy, University of Belgrade, Belgrade, Serbia

The kinetics and mechanism of the hydrogen oxidation reaction were studied in 0.5 moldm^{-3} $HClO_4$ solution on an electrode based on titanium oxide with Magneli phase structure-supported platinum electrocatalyst applied on rotation Au disk electrode. Pt catalyst was prepared by impregnation method from 2-propanol solution of $Pt(NH_3)_2(NO_2)^2$ and sub-stoichiometric titanium oxide powder. Substiochiometric titanium oxide support was characterized by X-ray diffraction and BET techniques. The synthesized catalyst was analyzed by TEM technique. Based on Tafel–Heyrovsky–Volmer mechanism the corresponding kinetic equations were derived to describe the hydrogen oxidation current–potential behavior on RDE over the entire potential region. The polarization RDE curves were fitted with derived polarization equations according to proposed model. The fitting shows that the HOR on Pt proceeds mostlikely via the Tafel–Volmer (TV) pathway in the lower potential region, while the Heyrovsky–Volmer (HV) pathway is operative in the higher potential region. It is pointed out that Tafel equation that has been frequently used for the kinetics analysis in the HOR, can not reproduce the polarization curves measured with high mass-transport rates. Polarization measurements on RDE revealed that the Pt catalystdeposited on titanium suboxide support showed equal specific activity for the HOR compared to conventional carbon-supported Pt fuel cell catalyst.

Keywords: Titanium sub-oxide, Hydrogen oxidation reaction, Kinetic equation, Mechanism

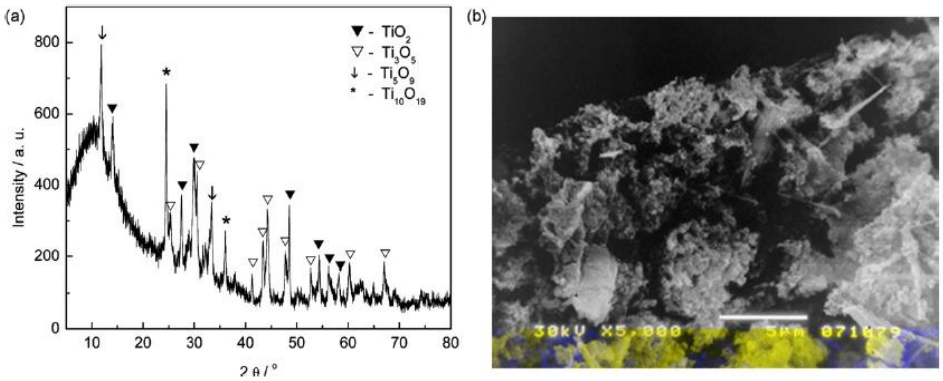

Figure: (a) XRD pattern of titanium oxide with Magneli phase structure. (b) SEM image of titanium oxide with Magneli phase structure.

***Journal of Power Sources*, 193 (2009) 99-106.**

Preparation and characterization TiO_x-Pt/C catalyst for hydrogen oxidation reaction

N.R. Elezović[a], B.M. Babić[b], Lj.M. Vračar[c], V. R. Radmilović[d], N.V. Krstajić[c]

[a]Institute for Multidisciplinary Research, Kneza Viseslava 1, Belgrade, Serbia
[b]Vinča Institute of Nuclear Sciences, Belgrade, Serbia
[c]Faculty of Technology and Metallurgy, University of Belgrade, Karnegijeva 4, Belgrade, Serbia
[d]National Center for Electron Microscopy, LBLN University of California, Berkeley, USA

The hydrogen oxidation reaction (HOR) was studied at the home made TiOx–Pt/C nanocatalysts in 0.5 mol dm^{-3} $HClO_4$ at 25 °C. Pt/C catalyst was first synthesized by modified ethylene glycol method (EG) on commercially used carbon support (Vulcan XC-72). Then TiOx–Pt/C catalyst was prepared by the polyole method followed by TiOx post-deposition. The synthesized catalyst was characterized by XRD, TEM and EDX techniques. It was found that Pt/C catalyst nanoparticles were homogenously distributed over carbon support with the mean particle size of about 2.4 nm. The quite similar, homogenous distribution and particle size were obtained for Pt/C doped by TiOx catalyst which was the confirmation that TiOx post-deposition did not lead to significant growth of the Pt nanoparticles. The electrochemically active surface area of the catalyst was determined by using the cyclic voltammetry technique. The kinetics of hydrogen oxidation was investigated by the linear sweep voltammetry technique at the rotating disc electrode (RDE). The kinetic equations used for the analysis were derived considering the reversible or irreversible nature of the kinetics of the HOR. It was found that the hydrogen oxidation reaction for an investigated catalyst proceeded as an electrochemically reversible reaction. The values determined for the kinetic parameters-Tafel slope of 28 mV dec^{-1} and exchange current density about 0.4 mA cm^{-2} Pt are in good agreement with usually reported values for a hydrogen oxidation reaction with platinum catalysts in acid solutions.

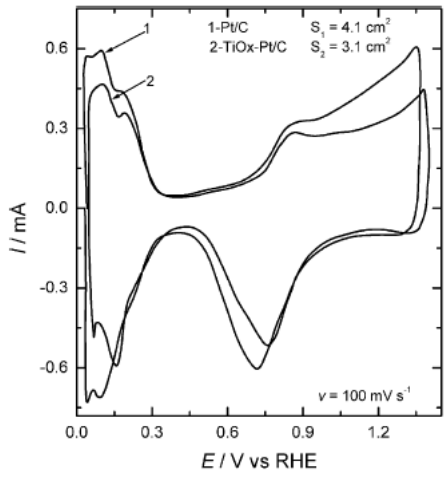

Figure: Cyclic voltammogram of Pt/C and TiOx–Pt/C electrodes (0.1 V s^{-1}) in nitrogen-purged 0.5 mol dm^{-3} $HClO_4$ solution at 25 °C.

***Physical Chemistry Chemical Physics*, 11 (2009) 5192-5197.**

Nb-doped TiO_2 as a support of Pt-Ru anode catalyst for PEMFCs

S. Lj. Gojković[a], B. M. Babić[b], V. R. Radmilović[c], N. V. Krstajić[a]

[a]Faculty of Technology and Metallurgy, University of Belgrade, Karnegijeva 4, 11120 Belgrade, Serbia
[b]Vinča Institute of Nuclear Sciences, P.O. Box 522, 11001 Belgrade, Serbia
[c]National Centre for Electron Microscopy, Lawrence Berkeley National Laboratory, Berkeley, CA 94720, USA

TiO_2 doped by 0.5% Nb was synthesized by the acid-catalyzed sol–gel method. BET surface area was determined to be 72 m^2 g^{-1}. XRD measurements showed that TiO_2 has structure of anatase with ~13 nm average crystallite size. Using Nb–TiO_2 as a support, Pt/Nb–TiO_2 and Pt–Ru/Nb–TiO_2 were prepared by borohydride reduction method. TEM imaging of Pt–Ru/Nb–TiO_2 revealed rather uniform distribution of the metallic particles on the support with a mean diameter of 3.8 nm. According to XRD analysis, Pt–Ru particles consist of the solid solution of Ru in Pt (40 at.% Ru) and a small amount of RuO2. Cyclic voltammetry of Pt/Nb–TiO_2 and Pt–Ru/Nb–TiO_2 indicated good conductivity of the supporting material. Oxidation of pre-adsorbed CO and methanol on Pt–Ru/Nb–TiO_2 was faster than on Pt/Nb–TiO_2. However, when the activities of Pt/Nb–TiO_2 and Pt–Ru/Nb–TiO_2 for methanol oxidation were compared to those of Pt/XC-72 and Pt–Ru/XC-72, no significant difference was observed. This means that Nb–TiO_2 is a promising replacement for high area carbon supports in PEMFC anodes, but without the influence on the reaction kinetics.

Keywords: Oxide support, TiO_2, Pt–Ru nanocatalyst, Methanol oxidation, Polymer electrolyte membrane fuel cell

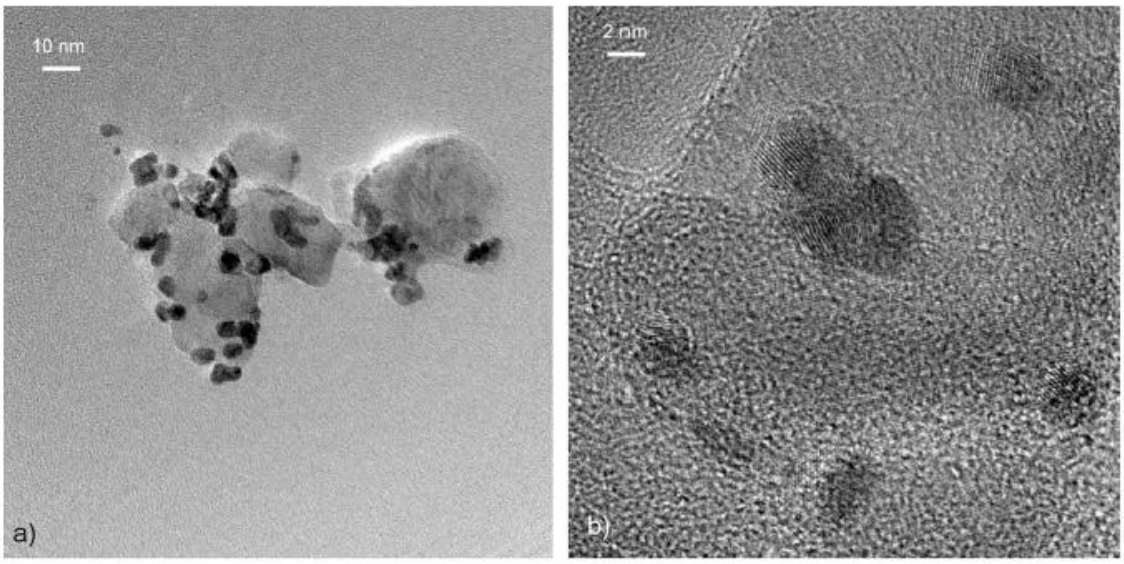

Figure: (a) TEM image of Pt–Ru nanoparticles on Nb–TiO2 support at low resolution, (b) HRTEM image of the same sample.

***Journal of Electroanalytical Chemistry*, 639 (2010) 161-166.**

Synthesis, characterization and electroanalytical behaviour of Nb-TiO_2/Pt nanocatalyst for oxygen reduction reaction

N.R. Elezović[a], B.M. Babić[b], Lj. Gajić-Krstajić[c], V. Radmilović[d], N.V. Krstajić[e], Lj. Vračar[e]

[a]Institute for Multidisciplinary Research, Belgrade, Serbia
[b]Vinča Institute of Nuclear Sciences, Belgrade, Serbia
[c]Institute of Technical Sciences-SASA, Belgrade, Serbia
[d]National Center for Electron Microscopy, LBLN University of California, Berkeley, USA
[e]Faculty of Technology and Metallurgy, University of Belgrade, Belgrade, Serbia

In order to point out the effect of the support to the catalyst for oxygen reduction reaction nano-crystalline Nb-doped TiO_2 was synthesized through a modified sol–gel route procedure. The specific surface area of the support, SBET, and pore size distribution, were calculated from the adsorption isotherms using the gravimetric McBain method. The support was characterized by X-ray diffraction (XRD) technique. The borohydride reduction method was used to prepare Nb–TiO_2 supported Pt (20 wt.%) catalyst. The synthesized catalyst was analyzed by TEM technique. Finally, the catalytic activity of this new catalyst for oxygen reduction reaction was investigated in acid solution, in the absence and the presence of methanol, and its activity was compared towards the results on C/Pt catalysts. Kinetic analysis reveals that the oxygen reduction reaction on Nb–TiO2/Pt catalyst follows four-electron process leading to water, as in the case of C/Pt electrode, but the Tafel plots normalized to the electrochemically active surface area show very remarkable enhancement in activity of Nb–TiO2/Pt expressed through the value of the current density at the constant potential. Moreover, Nb–TiO2/Pt catalyst exhibits higher methanol tolerance during the oxygen reduction reaction than the C/Pt catalyst. The enhancement in the activity of Nb–TiO2/Pt is consequence of both: the interactions of Pt nanoparticles with the support and the energy shift of the surface d-states with respect to the Fermi level what changes the surface reactivity.

Keywords: Nb–TiO_2 support, Nb–TiO_2/Pt catalyst, Oxygen reduction reaction, Methanol

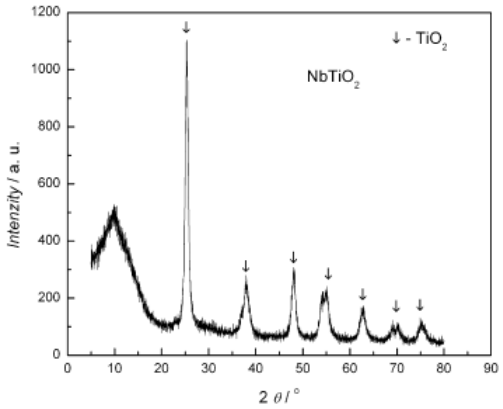

Figure: X-ray diffraction spectra of Nb–TiO2 substrate with specified composition.

***Journal of Power Sources*, 195 (2010) 3961-3968.**

Morphology and phase composition of as-deposited and recrystallized Ni–Mo–O powders

U. Lačnjevac[1], B.M. Jović[1], Z. Baščarević[1], V.M. Maksimović[2], V.D. Jović[1]

[1]Institute for Multidisciplinary Research, P.O. Box 33, 11030 Belgrade, Serbia
[2]Institute of Nuclear Sciences Vinča, P.O. Box 522, 11001 Belgrade, Serbia

The Ni–Mo–O alloy powders were electrodeposited from ammonium sulfate containing electrolytes for different Ni/Mo ions concentration ratios. Electrodeposition was investigated by the polarization measurements. The morphology, chemical composition and phase composition of these powders were investigated using SEM, EDS, AAS and XRD analysis. The EDS and AAS analysis showed that the powder composition depends on the Ni/Mo ions concentration ratio, with the Ni/Mo metals ratio in the powders being the same as the one in the solution. The as-deposited alloy powders were nanocrystalline, while after stepwise annealing at 300, 400, 500 and 600 °C for 2 h in N_2 atmosphere their crystallinity became more and more pronounced, with the dimension of crystallites increasing with the increase of the annealing temperature. Already after the annealing at 300 °C the presence of two phases, MoO_3 and $NiMoO_4$, was identified by XRD, while SEM analysis showed that the surfaces of powder particles were partially recrystallized. With the increase of the annealing temperature the amount of the $NiMoO_4$ was found to increase in all powders. For the powder electrodeposited from the solution with the highest Ni/Mo ratio (1/0.3) $NiMoO_4$ phase was detected together with a small amount of Ni_4Mo phase, indicating phase transition of MoO_3 into $NiMoO_4$ (and probably Ni_4Mo) at the temperature of 600 °C.

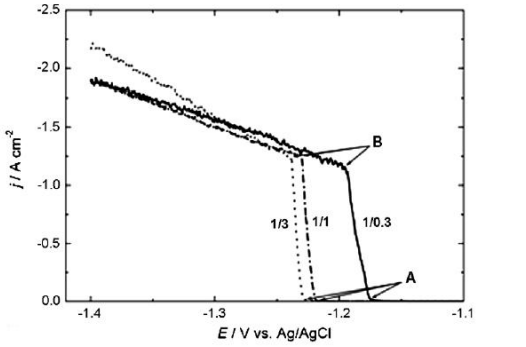

a

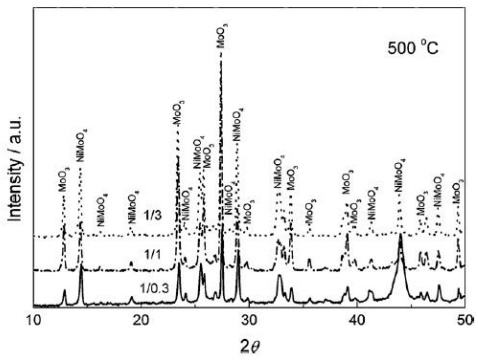

b

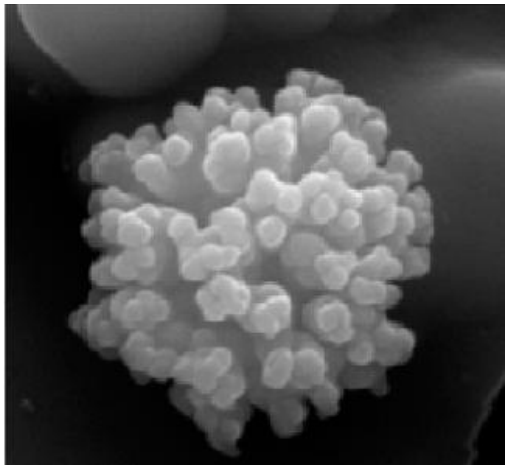

c

Figures: (a) The polarization diagrams for the Ni–Mo–O powders electrodeposition recorded at a sweep rate of $1mVs^{-1}$ (after IR drop compensation) for different Ni/Mo ions concentration ratios; (b) The diffractograms for the powders annealed at 500 °C electrodeposited at different Ni/Mo ions ratios (marked in the figure); (c) The SEM micrograph of the as-deposited powders for the Ni/Mo=1/3.

***Electrochimica Acta*, 54 (2009) 3115-3123.**

Structure and magnetic investigations of $Ca_{1-x}Y_xMnO_3$ (x=0, 0.1, 0.2, 0.3) and Mn^{4+}/Mn^{3+} relation analysis

J. Zagorac[a], S. Bošković[a], B. Matović[a], B. Babić-Stojić[b]

[a]Vinča Institute of Nuclear Sciences, Laboratory of Material Science, P. O. Box 522, 11001 Belgrade, Serbia
[b]Vinča Institute of Nuclear Sciences, Laboratory of Radiation Chemistry and Physics, Belgrade, Serbia

Structure and magnetic features of nanostructured materials with general formula $Ca_{1-x}Y_xMnO_3$ (x = 0; 0.1; 0.2; 0.3) were investigated. Goldschmidt tolerance factor, G_t and global instability index, *GII* were calculated for $Ca_{1-x}Y_xMnO_3$ (x = 0, 0.25, 0.5, 0.75, 1) using the software SPuDS (Structure Prediction Diagnostic Software). According to these two parameters possibility of forming perovskite structure type for $Ca_{1-x}Y_xMnO_3$ solid solution was analysed.

Substitution of Y^{3+} for Ca^{2+} provokes reduction of equivalent amount Mn^{4+} into Mn^{3+}, the presence of which is a reason for many interesting magnetic, transport and structural features of doped $CaMnO_3$. Crystal structure refinement was carried out using Rietveld analysis. $Ca_{1-x}Y_xMnO_3$ (x = 0; 0.1; 0.2; 0.3) has an orthorombic, *Pnma* space group that, according to Glazer´s classification belongs to $a^-b^+a^-$ tilt system. Influence of Y amount on Mn–O bond angles and distances, tilting of MnO_6 octahedra around all three axes and octahedra deformation were analysed. Bond valence calculations (BVC) were performed to determine Mn valence state. Using EPR (electron paramagnetic resonance) magnetic measurements were performed and magnetic properties of solid solutions, orthorombicity degree of unit cell, as well as Mn^{4+}/Mn^{3+} cations ratio in position *B* were analysed. Microstructure size-strain analysis was performed and these results are in nanometric range which is confirmed by TEM images.

Keywords: Nanostructured materials, Rietveld analysis, BVC calculations, Magnetic properties.

***Science of Sintering,* 42 [2] (2010) 221-232.**

Room-temperature synthesis of nanometric α-Bi_2O_3

Marija Prekajski[1], Aleksandar Kremenović[2], Biljana Babić[1], Milena Rosić[1], Branko Matović[1], Ana Radosavljević-Mihajlović[1], Jelena Zagorac[1]

[1]Institute of Nuclear Science, Vinča, University of Belgrade, 11001 Belgrade, Serbia
[2]Faculty of Mining and Geology, Laboratory for Crystallography, University of Belgrade, Đušina 7, 11000 Belgrade, Serbia

Nanometric Bi_2O_3 powder was successfully synthesized by applying the method based on self-propagating room temperature reaction (SPRT) between bismuth nitrates and sodium hydroxide. X-ray powder diffraction (XRPD) and Rietveld's structure refinement method was applied to characterize prepared powder. It revealed that synthesized material is single phase monoclinic α-Bi_2O_3 (space group $P2_1/c$ with cell parameters $a = 5.84605(4)$Å, $b = 8.16339(6)$ Å, $c = 7.50788(6)$ Å and $\beta = 112.9883(8)$). Powder particles were of nanometric size (about 50 nm). Raman spectral studies conformed that obtained powder is single phase α-Bi_2O_3. Specific surface area of obtained powder was measured by Brunauer-Emmet-Teller (BET) method.

Keywords: Bi_2O_3, nanomaterials, self-propagating reaction.

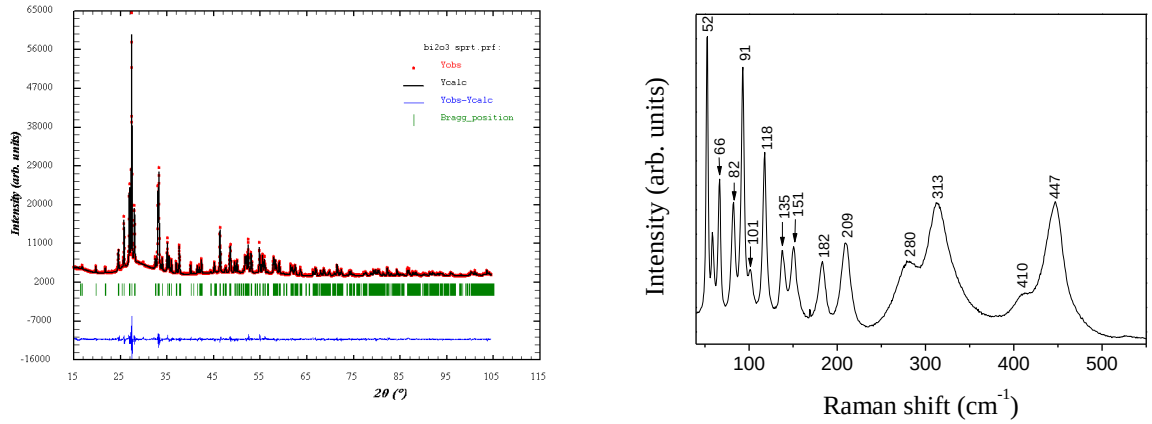

Figures: (a) XRD pattern after structural refinement procedure using Rietveld's method. A difference (observed - calculated) plot is shown beneath. Tick marks above the difference data indicate the reflection position. (b) Raman spectrum of α-Bi_2O_3

***Materials Letters*, 64 (2010) 2247–2250.**

Preparation of nanometric ceria powders by different synthesis procedure

Milena Rosić, Olivera Cvetković*, Branko Matović

Institute of Nuclear Sciences, Vinča, Belgrade, Serbia
*IHTM, Centar of Chemistry, Belgrade, Serbia

The paper presents the results concerning the preparation of ceria CeO_2 powder by self-propagating room temperature synthesis (SPRT) and combustion synthesis (CS) using different fuel mixtures. Nanometric size powder particles were obtained with a fluorite-type crystal structure. Powders properties like specific surface area, crystallite and particle size, and lattice parameters were followed by X-ray diffraction and Raman spectroscopy and BET measurements.

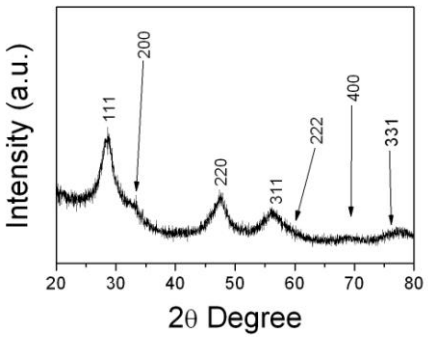

Figure: XRD patterns of CeO_2 powder sample obtained by SPRT method.

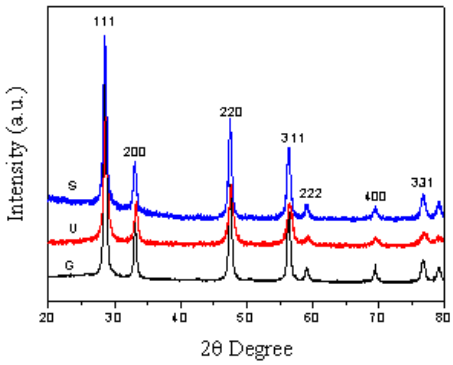

Figure: XRD patterns of CeO_2 powder sample obtained by combustion synthesis.

Some problems in modeling of laser interaction with transparent and absorptive materials

Milesa Srećković,[a] B. Kaluđerović,[b] Aleksander Kovačević[c], Višeslava Rajković [b], Slađana Pantelić [a], Zoran Latinović [a], Dragan Družijanić [a], Milovan Janićijević [d]

[a]Faculty of Electrical Engineering, University of Belgrade, Belgrade, Serbia,
[b]Laboratory for the Materials, Institute of Nuclear Sciences, Vinča, University of Belgrade, Serbia,
[c]Institute of Physics, University of Belgrade, Belgrade, Serbia
[d]"Metalac", Gornji Milanovac, Serbia,

In this work, the interaction of laser beams (of well-known lasers, like Nd^{3+}:YAG, CO_2, but also alexandrite and others) with optical materials (in broader sense of view) and accessories has been done. As an experimental part, some damages have been analyzed by optical and electron microscopies, as well as EDX, which confirm material content change or preservation. The shapes of damages depend on the laser working regime, pulse width, mono- or multi-pulse expositions. Cumulative effects are the subject of investigation of many authors. In the terminology of optical damages, there are precise defined protocols for "laser damage", but they differ in both investigation types and the "damage" term application. Obtained results on various materials could enable analyses of several types including the data on the source itself, of materials resistance to optical beams, and of research by other developed fatigue tests as well. For some approaches, calculations which represent numerical implementation for given geometries and chosen pulse shapes, have been performed. Besides them, interpretations which would be commonly deduced, based on the models of obtained record processing, has been given.

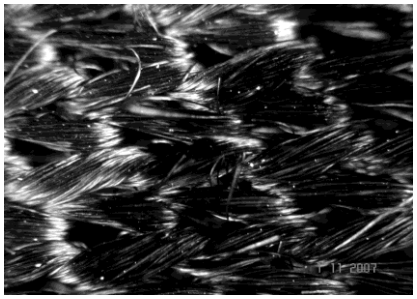

Figure: Light microscope ACC, alexandrite laser, 5 pulses, spot 10mm, 36J/cm^2 Magn.x84.

Figure: ACC, Er $^{3+}$:YAG, 15 sec (.12Hz, ,700mJ/pulse); Magn.x28.

***2nd International Conference on Physics of Optical Materials and Devices ICOM 2009,* August 26th -31st 2009, Herceg-Novi, Montenegro, Book of Abstracts, pp. 205.**

Preparation, sintering and electrical properties of nano-grained multidoped ceria

S. Bošković[a], S. Zec[a], G. Branković[b], Z. Branković[b], A. Devečerski[a], B. Matović[a], F. Aldinger[c]

[a]Institute of Nuclear Sciences, Vinča, POB 522, 11001 Belgrade, Serbia

[b]Institute for Multidisciplinary Studies, Belgrade, Serbia

[c]Max/Planck Institute fur Metallforschung, PML, 70569 Stuttgart, Heissenbergstr. 3, Germany

Multiply doped ceria nanopowders were synthesized by applying MGNP (modified glycine/nitrate procedure). The overall concentration of dopants was kept constant (x = 0.2) whereby Gd ion as the main dopant was gradually substituted by Sm and by Sm + Y. The compositions of solid solutions were calculated by applying defect model introducing anion vacancy radius. Characterization of powders involved BET, TEM, XRD and chemical analyses. Densification was performed at 1500 ^{o}C, in an oxygen atmosphere for 1 h. The results showed that with increasing number of dopants, specific surface area of powders increased, followed by decrease of crystallite and grain sizes. Densification degree was also found to rise with increasing number of dopants. According to impedance measurements it was found that ionic conductivity was the highest 1.14 x 10^{-3} S cm^{-1} at 450^{o}C in sample doped with Gd, Sm and Y simultaneously.

Keywords: Nanometric powders; Multiple doping; Densification; Electrical conductivity

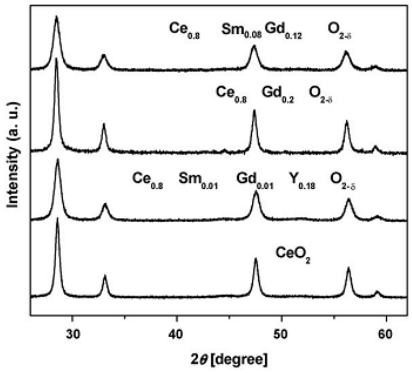

Figure: XRD patterns of nanometric doped ceria powders.

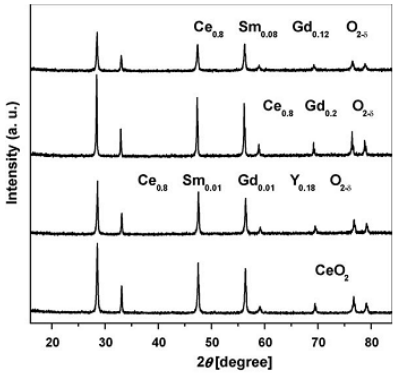

Figure: XRD pattern of sintered samples.

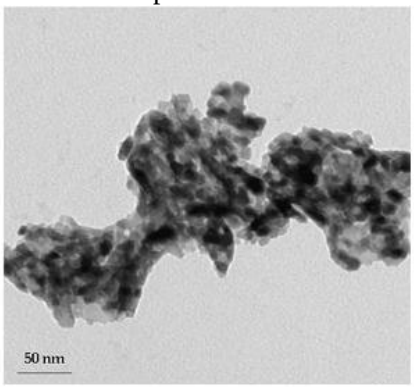

Figure: TEM of $Ce_{0.8}Sm_{0.01}Gd_{0.01}Y_{0.18}O_{2-d}$.

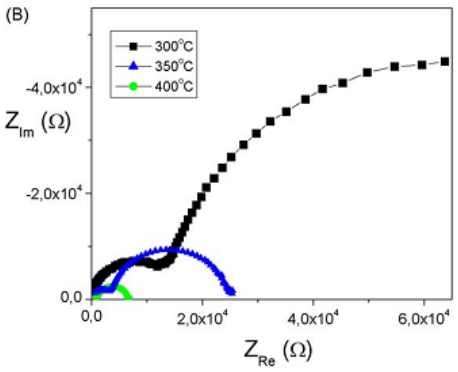

Figure: Impedance spectra for $Ce_{0.8}Sm_{0.01}Gd_{0.01}Y_{0.18}O_{2-d}$.

***Ceramics International*, 36 (2010) 121-127.**

Characterization of nanometric multidoped ceria powders

M. Stojmenović[a], S. Bošković[a], S. Zec[a], B. Babić[a], B. Matović[a], D. Bučevac[a], Z. Dohčević-Mitrović[b], F. Aldinger[c]

[a]Institute of Nuclear Sciences Vinča, University of Belgrade, Belgrade, Serbia
[b]Institute of Physics, University of Belgrade, Belgrade, Serbia
[c]Max-Planck Institute, Heisenbergstrasse 1, 70569 Stuttgart, Germany

The ceria solid solutions doped with rare earth cations were synthesized by two methods and the microstructural and morphological characterization of powders was performed. The results obtained by X-ray diffraction (XRD), transmission electron microscopy (TEM), Brunauer–Emmett–Teller (BET) method and Raman spectroscopy were studied and discussed. The results showed that finer powders have not only higher specific surface area, smaller particles and crystallite sizes, but also larger lattice parameters in the case of both single and multidoped solid solutions.

Keywords: nanostructured materials, oxide materials, solid solutions, vacancy formation, X-ray diffraction, TEM.

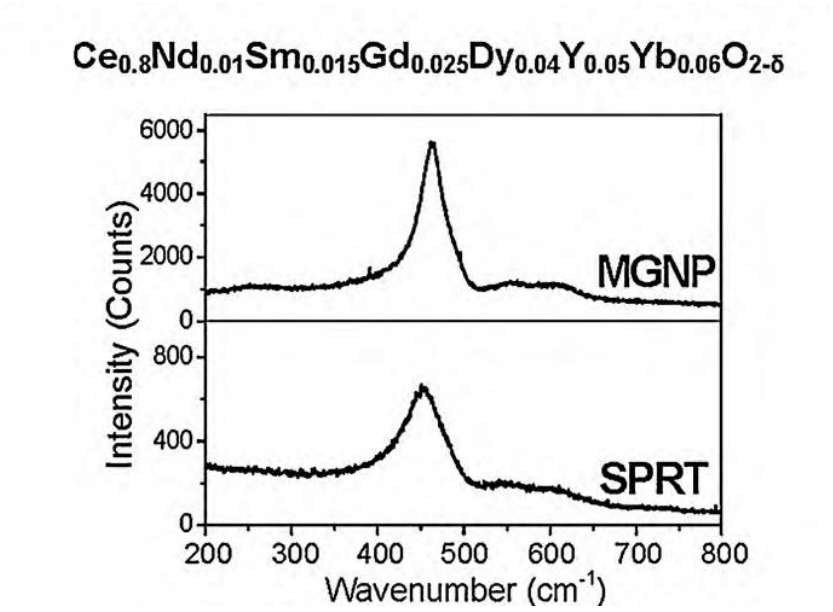

Figure: Raman spectra of nanopowders obtained by MGNP and SPRT methods.

***Journal of Alloys and Compounds*, 507 (2010) 279–285.**

Characterization of nanometric multidoped ceria powders

M. Stojmenović[a], S. Bošković[a], S. Zec[a], B. Babić[a], B. Matović[a], D. Bučevac[a], Z. Dohčević-Mitrović[b], F. Aldinger[c]

[a]Institute of Nuclear Sciences Vinča, Mihajla Petrovića-Alasa 12-14, POB 522, 11001 Belgrade, University of Belgrade, Serbia
[b]Institute of Physics, Pregrevica 118, POB 68, 11080 Belgrade, Serbia
[c]Max-Planck Institute, Heisenbergstrasse 1, 70569 Stuttgart, Germany

The ceria solid solutions doped with rare earth cations were synthesized by two methods and the microstructural and morphological characterization of powders was performed. The results obtained by X-ray diffraction (XRD), transmission electron microscopy (TEM), Brunauer–Emmett–Teller (BET) method and Raman spectroscopy were studied and discussed. The results showed that finer powders have not only higher specific surface area, smaller particles and crystallite sizes, but also larger lattice parameters in the case of both single and multidoped solid solutions.

Keywords: Nanostructured materials, Oxide materials, Solid solutions, Vacancy formation, X-ray diffraction, TEM

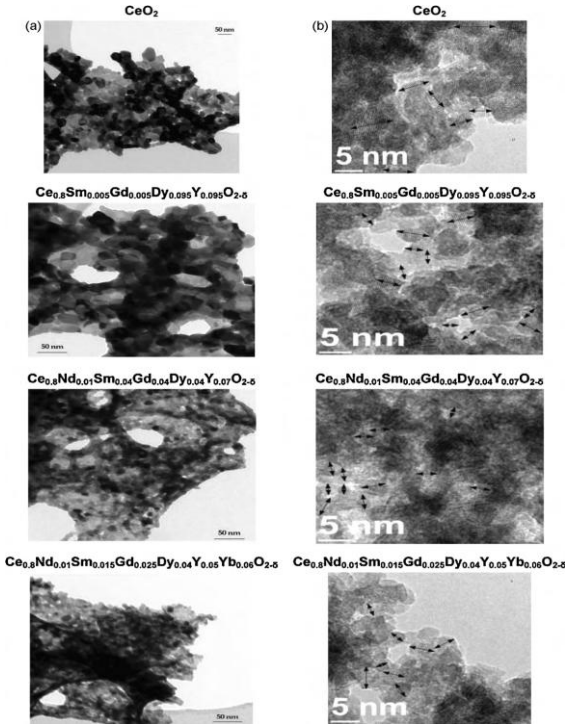

Figure: TEM micrographs: (a) MGNP powders, (b) SPRT powders.

***Journal of Alloys and Compounds*, 507 (2010) 279–285.**

Synthesis of multidoped ceria based nanopowders

M. Puševac[1], S. Bošković[1], S. Zec[1], B. Babić[1], B. Matović[1], Z. Dohčević-Mitrović[2], S. Mentus[3]

[1]Institute of Nuclear Sciences, Vinča, Belgrade, Serbia,
[2]Institute of Physics, Belgrade, Serbia,
[3]Faculty of Physical Chemistry, University of Belgrade, Belgrade, Serbia

Mulitidoped ceria nanopowders with different particle sizes were produced by two different methods. The following compositions were prepared: $Ce_{0.8}Nd_{0.01}Sm_{0.04}Gd_{0.04}Dy_{0.04}Y_{0.07}O_{2-\delta}$ and $Ce_{0.8}Sm_{0.005}Gd_{0.005}Dy_{0.095}Y_{0.095}O_{2-\delta}$, as well as pure ceria for comparison. Parameters of the MGNP synthesis process were investigated by variation of glycine to nitrate ratio from 1.00 to 1.67, which affected powders properties like specific surface area, crystallinity, as well as crystallite size. In addition, the room temperature self propagating synthesis was applied to synthesize the same compositions. Characterization of the obtained powders revealed that all the samples were single phase ceria solid solutions, while the particle size of the powders prepared by the two mentioned methods, differed by an order of magnitude. It is interesting to note that with powders obtained at room temperature inspite of very small particle size (2-4 nm) crystallinity was very high, which was proved by XRD, TEM as well as by Raman spectroscopy.

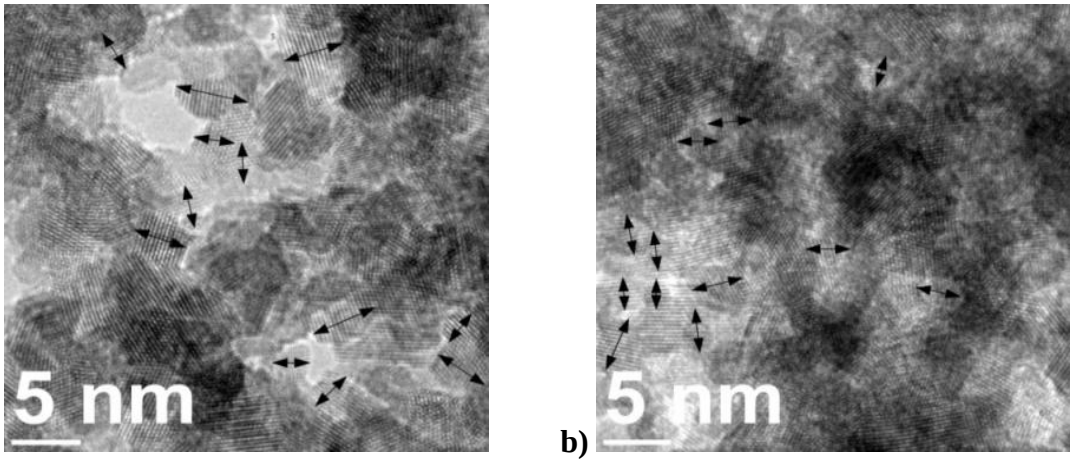

Figure: TEM images of synthetisized nanopowders obtained by MGNP method: (a) $Ce_{0.8}Nd_{0.01}Sm_{0.04}Gd_{0.04}Dy_{0.04}Y_{0.07}O_{2-\delta}$, (b) $Ce_{0.8}Sm_{0.005}Gd_{0.005}Dy_{0.095}Y_{0.095}O_{2-\delta}$.

***YUCOMAT 2009*, Herceg Novi, Montenegro, August 31-September 4 (2009), pp. 88.**

Synthesis of multidoped ceria nanopowders

M. Puševac[1], S. Bošković[1], S. Zec[1], B. Babić[1], B. Matović[1], Z. Dohčević-Mitrović[2], S. Mentus[3]

[1]Institute of Nuclear Sciences, Vinča, Belgrade, Serbia,
[2]Institute of Physics, Belgrade, Serbia,
[3]Faculty of Physical Chemistry, University of Belgrade, Belgrade, Serbia

Mulitidoped ceria nanopowders with different particle sizes were produced by two different methods. The following compositions were prepared: $Ce_{0.8}Nd_{0.01}Sm_{0.04}Gd_{0.04}Dy_{0.04}Y_{0.07}O_{2-\delta}$ and $Ce_{0.8}Sm_{0.005}Gd_{0.005}Dy_{0.095}Y_{0.095}O_{2-\delta}$, as well as pure ceria for comparison. Parameters of the MGNP synthesis process were investigated by variation of glycine to nitrate ratio from 1.00 to 1.67, which affected powders properties like specific surface area, crystallinity, as well as crystallite size. In addition, the room temperature self propagating synthesis was applied to synthesize the same compositions. Characterization of the obtained powders revealed that all the samples were single phase ceria solid solutions, while the particle size of the powders prepared by the two mentioned methods, differed by an order of magnitude. It is interesting to note that with powders obtained at room temperature in spite of very small particle size (2-4 nm) crystallinity was very high, which was proved by XRD, TEM as well as by Raman spectroscopy.

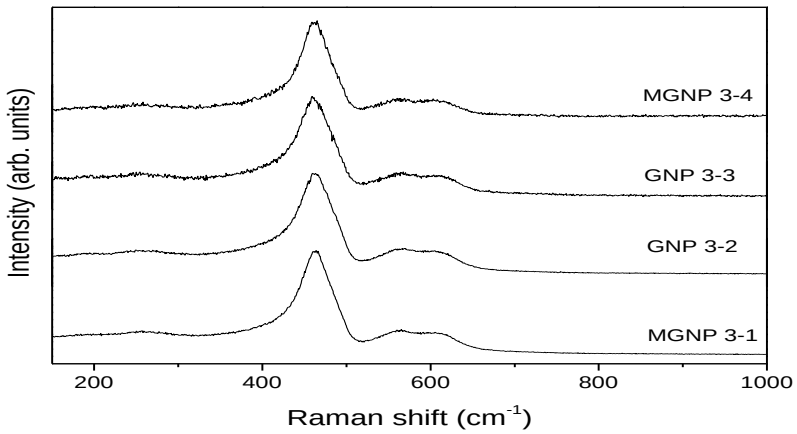

Figure: Raman spectra of nanopowders obtained by GNP and MGNP methods with different glycine/nitrate ratio.

***Second Humboldt Conference on Noncovalent Interactions*, Vršac, Serbia, October 22-25 (2009), pp. 59.**

Functional ceramics

Analysis of irregular copper deposits by the optical and scanning electron microscopy (SEM) techniques

N.D. Nikolić[1], V. M. Maksimović[2], G. Branković[3]

[1]ICTM – Institute of Electrochemistry, University of Belgrade, Njegoševa 12, P.O. Box 473, 11001 Belgrade,
[2]Institute of Nuclear Sciences, Vinča, University of Belgrade, P.O. Box 522, 11001 Belgrade, Serbia
[3]Institute for Multidisciplinary Research, University of Belgrade, P.O. Box 33, 11030 Belgrade, Serbia

The 3D foam or honeycomb-like structure is the type of irregular metal deposition which is of high both academic and technological significance. This type of deposits is formed by electrodeposition processes at high overpotential and current densities where parallel to metal electrodeposition, hydrogen evolution reaction occurs. The main characteristics of this deposit type are holes or pores formed due to attached hydrogen bubbles and agglomerates of metals grains or dendrites particles formed among them. Due to the extremely high surface area of these deposits, they are very suitable to be used as electrodes in many electrochemical devices, such as fuel cells, batteries and sensors.

For structural analysis of open and porous structures with the extremely high surface area (the honeycomb-like structures), the techniques of scanning electron (SEM) and optical microscopes are widely used. The SEM technique gives information concerning surface morphology ("top view") of deposits. For the purpose of the analysis of internal structure (cross-section analysis) of these deposits, the use of optical microscope is preferable.

In the last time, improvement of micro- and nanostructural characteristics of honeycomb-like structures related to those obtained at constant regimes of electrolysis was attained by the application of pulsating overpotential (PO) regime. Meanwhile, the application of PO regime is primarily important from academic point of view for understanding of mechanism of electrodeposition processes at periodically changing rate. For technological purposes, pulse and reverse plating techniques, such as pulsating current (PC) and reversing current (RC), are more important. The aim of this work is the examination of different parameters of the regime of pulsating current (PC) on morphology of electrodeposited copper obtained in the hydrogen co-deposition range.

***4th Serbian Congress for Microscopy*, October 11-12 2010., Belgrade, Serbia, pp. 69-72.**

Synthesis and characterization of MoOx-Pt/C nano-catalysts for oxygen reduction

N.R. Elezović[a], B.M. Babić[b], V.R. Radmilović[c], Lj.M. Vračar[d], N.V. Krstajić[d]

[a]Institute for Multidisciplinary Research, Kneza Višeslava, 1a, Belgrade, Serbia
[b]Vinča Institute of Nuclear Sciences, Belgrade, Serbia
[c]National Center for Electron Microscopy, LBLN University of California, Berkeley, USA
[d]Faculty of Technology and Metallurgy, University of Belgrade, Belgrade, Serbia

The oxygen reduction reaction (ORR) was studied at carbon supported MoO*x*-Pt/C and TiO*x*-Pt nanocatalysts in 0.5 moldm−3 HClO4 solution, at 25 °C. The MoO*x*-Pt/C and TiO*x*-Pt/C catalysts were prepared by the polyole method combined by MoO*x* or TiO*x* post-deposition. Home-made catalysts were characterized by TEM and EDX techniques. It was found that catalyst nanoparticleswere homogenously distributed over the carbon support with a mean particle size about 2.5 nm. Quite similar distribution and particle size was previously obtained for Pt/C catalyst. Results confirmed that MoO*x* and TiO*x* post-deposition did not lead to a significant growth of the Pt nanoparticles. The ORR kinetics was investigated by cyclic voltammetry and linear sweep voltammetry at the rotating disc electrode. These results showed the existence of two $E-\log j$ regions, usually observed with polycrystalline Pt in acid solution. It was proposed that the main path in the ORR mechanism on MoO*x*-Pt/C and TiO*x*-Pt/C catalysts was the direct four-electron process with the transfer of the first electron as the rate-determining step. The increase in catalytic activity for ORR on MoO*x*-Pt/C and TiO*x*-Pt/C catalysts, in comparison with Pt/C catalyst, was explained by synergetic effects due to the formation of the interface between the platinum and oxide materials and by spillover due to the surface diffusion of oxygen reaction intermediates.

Keywords: Oxygen reduction reaction, MoOx-Pt/C catalyst, TiOx-Pt/C catalyst, Nanoparticles, Acid solution

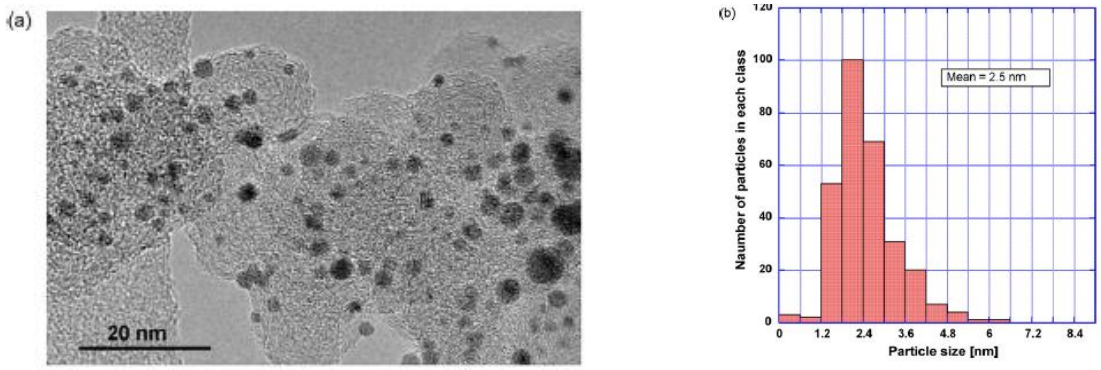

Figure: (a) HRTEM micrographs of MoO*x*-Pt nanoparticles on carbon support. (b) The corresponding histogram of particle size distribution.

***Electrochimica Acta,* 54 (2009) 2404-2409.**

Tribological Behavior of Composites Based on ZA-27 Alloy Reinforced with Graphite Particles

Miroslav Babić[1], Slobodan Mitrović[1], Dragan Džunić[1], Branislav Jeremić[1], Ilija Bobić[2]

[1]Mechanical Engineering Faculty, Tribology Center, University of Kragujevac, Sestre Janjic 6, 34000 Kragujevac, Serbia
[2]Department of Materials Science, Institute of Nuclear Sciences, Vinča, P.O. Box 522, 11001 Belgrade, Serbia

The objective of this investigation is to assess the influence of graphite reinforcement on tribological behavior of ZA-27 alloy. The composite with 2 wt% of graphite particles was produced by the compocasting procedure. Tribological properties of unreinforced alloy and composite were studied, using block-on-disk tribometer, under dry and lubricated sliding conditions at different specific loads and sliding speeds. The worn surfaces of the samples were examined by the scanning electron microscopy (SEM). The obtained results revealed that ZA-27/graphite composite specimens exhibited significantly lower wear rate and coefficient of friction than the matrix alloy specimens in all the combinations of applied loads (Fn) and sliding speeds (v) in dry and lubricated tests. The positive tribological effects of graphite reinforcement of ZA-27 in dry sliding tests were provided by the tribo-induced graphite film on the contact surface of composite. In test conditions, characterized by the small graphite content and modest sliding speeds and applied loads, nonuniform triboinduced graphite films were formed leading to the increase of the friction coefficient and wear rate, with increase of the sliding speed and applied load. In conditions of lubricated sliding, the very fine graphite particles formed in the contact interface mix with the lubricating oil forming the emulsion with improved tribological characteristics. Smeared graphite decreased the negative influence of Fn on tribological response of composites, what is manifested by the mild regime of the boundary lubrication, as well as by realization of the mixed lubrication at lower values of the v/Fn ratio, with respect to the matrix alloy.
Keywords ZA-27 alloy, Graphite particles, Composites, Tribological behavior

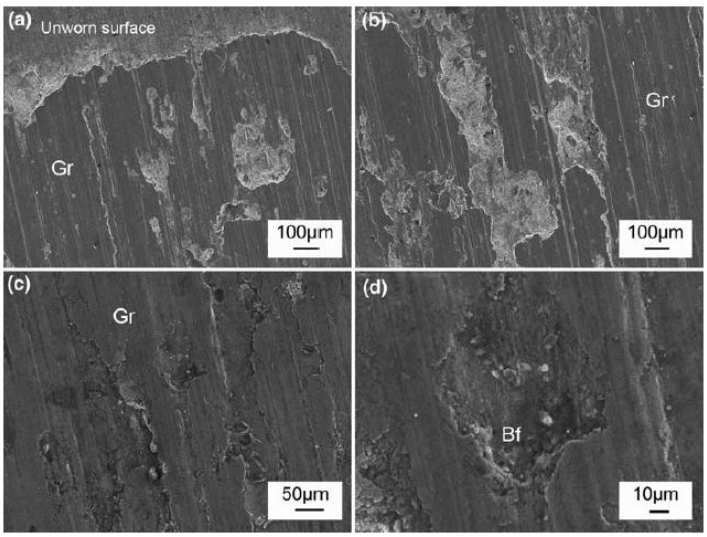

Figure: Wear surfaces of the composite in conditions of dry sliding for 50 N of applied load and 0.10 m/s of sliding speed.

***Tribology Letters,* 37 (2010) 401–410.**

Wear Behavior of Composites Based on ZA-27 Alloy Reinforced by Al_2O_3 Particles Under Dry Sliding Condition

Miroslav Babić[1], Slobodan Mitrović[1], Fatima Živić[1], Ilija Bobić[2]

[1]Mechanical Engineering Faculty, Tribology Center, University of Kragujevac, Sestre Janjic 6, 34000 Kragujevac, Serbia
[2]Department of Materials Science, Institute of Nuclear Sciences, Vinča, P.O. Box 522, 11001 Belgrade, Serbia

In present study, the effect of Al_2O_3 particle reinforcement on the sliding behavior of ZA-27 alloy composites was investigated. The composites with 3, 5, and 10 wt% of Al_2O_3 particles were produced by the compocasting procedure. Tribological properties of unreinforced alloy and composite were studied, using block-on-disk tribometer under unlubricated sliding conditions at different specific loads and sliding speeds. The worn surfaces of samples were examined by the scanning electron microscopy (SEM). The test results revealed that those composite specimens exhibited significantly lower wear rate than the ZA-27 matrix alloy specimens in all combinations of applied loads and sliding speeds. The difference in the wear resistance of composite with respect to the matrix alloy, increased with the increase of the applied load/sliding speed and Al_2O_3 particle content. The highest degree of improvement of the ZA-27 alloy tribological behavior corresponded with change of the Al_2O_3 particles content from 3 to 5 wt%. At low sliding speed, moderate lower wear rate of the composites over that of the matrix alloy was noticed. This has been attributed to micro cracking tendency of the composites. Significantly reduced wear rate, experienced by the composite over that of the matrix alloy at the higher sliding speeds and loads, could be explained due to enhanced compatibility of matrix alloy with dispersoid phase and greater thermal stability of the composite in view of the presence of the dispersoid. Level of wear rate of tested ZA-27/Al_2O_3 samples pointed to the process of mild wear, which was primarily controlled by the formation and destruction of mechanical mixed layers (MMLs).

Keywords: ZA-27 alloy, Al_2O_3 particles, Composites,Tribological behavior

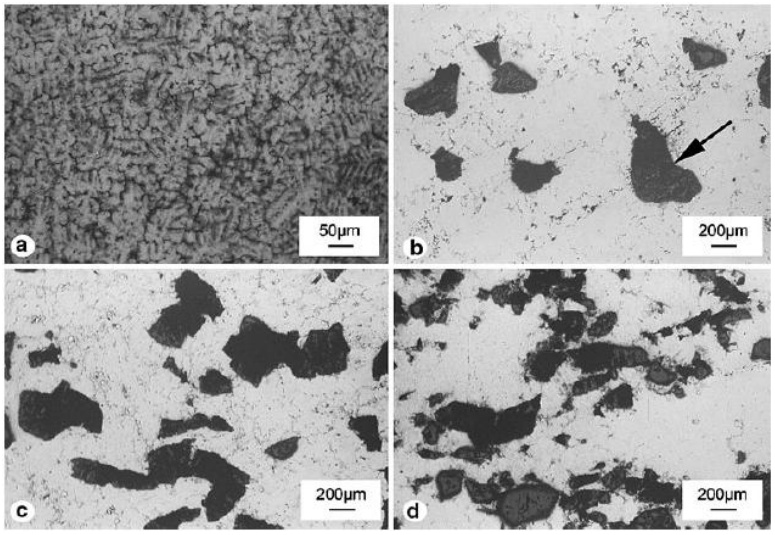

Figure: Microstructure of the tested materials: a) ZA-27 alloy, b) composite 3% Al_2O_3, c) composite 5% Al_2O_3 and d) composite 10% Al_2O_3.

***Tribology Letters,* 38 (2010) 337–346.**

Structural, mechanical and tribological properties of A356 aluminium alloy reinforced with Al_2O_3, SiC and SiC + graphite particles

Aleksandar Vencl[a], Ilija Bobić[b], Saioa Arostegui[c], Biljana Bobić[d], Aleksandar Marinković[a], Miroslav Babić[e]

[a]Tribology Laboratory, Mechanical Engineering Faculty, University of Belgrade, Kraljice Marije 16, 11120 Belgrade 35, Serbia
[b]Institute of Nuclear Science, Vinča, Mike Petrovića Alasa 12-14, 11001 Belgrade, Serbia
[c]CSM Instruments SA, Rue de la Gare 4, CH-2034 Peseux, Switzerland
[d]R&D Center IHIS Techno-Experts, Batajnič cki put 23, 11080 Belgrade, Serbia
[e]Tribology Center, Mechanical Engineering Faculty, University of Kragujevac, Sestre Janji´c 6, 34000 Kragujevac, Serbia

Particulate composites with A356 aluminium alloy as a matrix were produced by compocasting process using ceramic particles (Al_2O_3, SiC) and graphite particles. The matrix alloy and the composites were thermally processed applying the T6 heat treatment regime. Structural, mechanical and tribological properties of heat treated matrix alloy and the composites were examined and compared. It was shown that heat treatment affected microstructure of the composites matrix. The fracture of the composites matrix was ductile, while transition from ductile to brittle fracture occurred in the zone of reinforcing particles. The values of elasticity modulus of all the composites were higher in relation to the matrix alloy. It was also established that wear resistance and coefficient of friction were better at the SiC particulate composites than at the Al_2O_3 particulate composite, while the addition of graphite particles improved tribological properties further.

Keywords: A356 alloy, Metal matrix composites, Compocasting, Microstructure, Wear, Friction

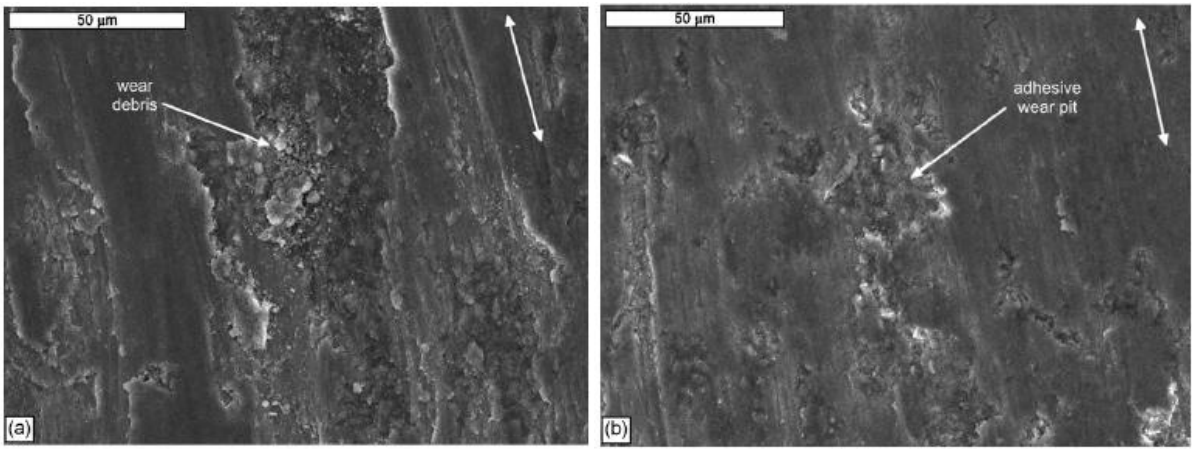

Figure: SEM micrographs of test samples worn surfaces (a) A356 aluminium alloy and (b) composite C1 (with 10 wt.% Al_2O_3 particles); sliding directions is denoted with double arrows.

***Journal of Alloys and Compounds*, 506 (2010) 631–639.**

Influence of T4 Heat Treatment on Tribological Behavior of ZA27 Alloy Under Lubricated Sliding Condition

Miroslav Babić [1], Aleksandar Vencl[2], Slobodan Mitrović[1], Ilija Bobić[3]

[1]Mechanical Engineering Faculty, Tribology Center, University of Kragujevac, Sestre Janjic 6, 34000 Kragujevac, Serbia
[2]Tribology Laboratory, Mechanical Engineering Faculty, University of Belgrade, Kraljice Marije 16, 11120 Belgrade,Serbia
[3]Department of Materials Science, Institute of Nuclear Sciences, Vinča, P.O. Box 522, 11001 Belgrade, Serbia

The effects of heat treatment on the microstructure, hardness, tensile properties, and tribological behavior of ZA27 alloy were examined. The alloys were prepared by conventional melting and casting route. The heat treatment of samples included the heating up to 370˚C for 3 or 5 h, quenching in water, and natural aging. Lubricated sliding wear test were conducted on as-cast and heat-treated ZA27 samples using block-on-disc machine. The friction and wear behavior of alloys were tested in contact with steel discs using combinations of three levels of load (10, 30, and 50 N) and three levels of linear sliding speeds (0.26, 0.50, and 1.00 m/s). To determine the wear mechanisms, the worn surfaces of the samples were examined by scanning electron microscopy (SEM). The heat treatment resulted in reduction in the hardness and tensile strength but increase in elongation. The heat-treated alloy samples attained improved tribological behavior over the as-cast ones, under all combinations of sliding speeds and contact loads. The rate of improvement increased with duration of solutionizing process before quenching in water. Obtained tribological results were related to the effects of heat treatment on microstructure changes of alloy.

Keywords: ZA27 alloy, Heat treatment, Tribological behavior

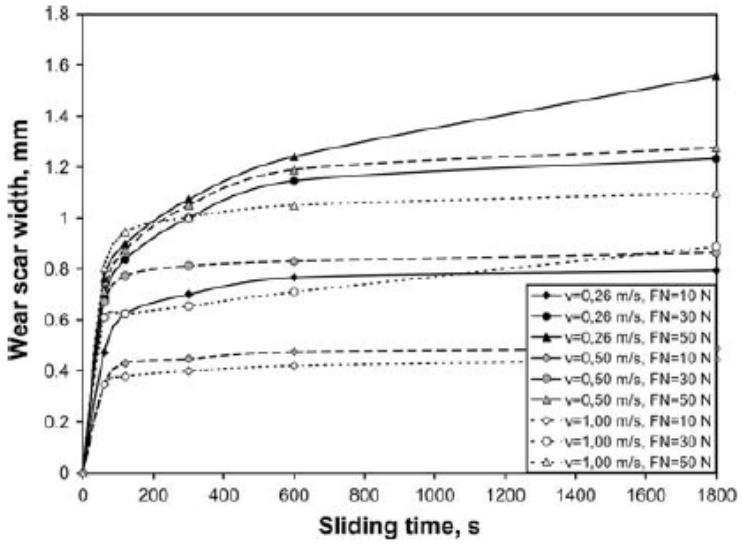

Figure: Wear curves of ZA27 HT5 alloy at different specific loads and sliding speeds.

***Tribology Letters,* 36 (2009) 125–134.**

Primena modifikovane glicin nitratne metode (MGNP) za sintezu SOFC nanoprahova

Marija D. Puševac, Snežana B. Bošković, Slavica P. Zec, Branko Z. Matović, Slavko V. Mentus*

Institut za nuklearne nauke "Vinča", Laboratorija za materijale, P. P 522, 11001 Beograd, Srbija
*Fakultet za fizičku hemiju, Univerzitet u Beogradu, Studenski trg 12-16,11000 Beograd, Srbija

Nanometarski prahovi fluoritne strukture kakav je cerijum oksid, su dopirani jonima retkih zemalja kao neodimijum, samarijum, gadolinijum, disprozijum i itrijum. Sinteza nanometarskih prahova vršena je primenom modifikovane glicin nitratne metode. Prahovi su sintetisani iz rastvora nitrata, pri čemu je modifikacijom izvršena delimična zamena nitrata acetatima, u cilju bolje kontole odvijanja hemijske reakcije, ali i niže cene koštanja procesa. Sintetisani nanoprahovi, prema XRD rezultatima, su jednofazni čvrsti rastvori CeO_2, nezavisno od broja dopanata. Takode, prema XRD rezultatima parametri rešetke čvrstih rastvora CeO_2 odgovaraju sastavima sintetisanih prahova, i veoma su slični vrednostima dobijenim računskim putem korišćenjem modela koji uključuje u jednačinu jonski radijus vakancija kiseonika. Izračunate veličine kristalita su nanometarskih dimenzija, što takođe vazi i za veličine čestica, snimljenih na TEM.

a) 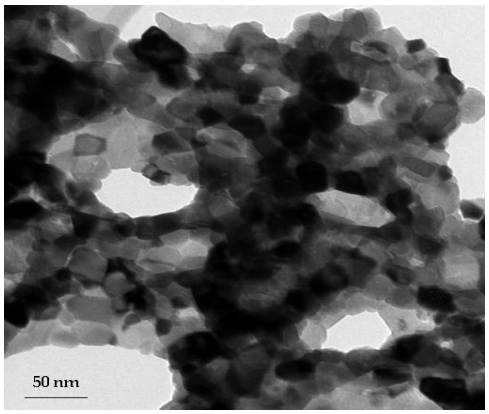

b) 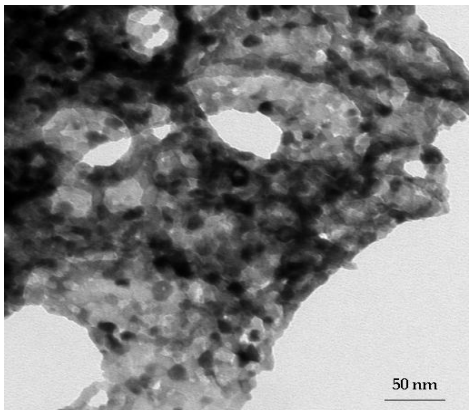

Slika: TEM snimci sintetisanih nanoprahova dobijenih SPRT metodom: (a) $Ce_{0.8}Nd_{0.01}Sm_{0.04}Gd_{0.04}Dy_{0.04}Y_{0.07}O_{2-\delta}$, (b) $Ce_{0.8}Sm_{0.005}Gd_{0.005}Dy_{0.095}Y_{0.095}O_{2-\delta}$.

***47. Savetovanje Srpskog hemijskog društva,* Beograd, Srbija, Mart 21 (2009), pp. 143.**

Chemical reduction of nanocrystalline CeO_2

Slavica Zec, Snežana Bošković, Branka Kaluđerović, Žarko Bogdanov, Nada Popović

Institute of Nuclear Sciences, Vinča, University of Belgrade, 11001 Belgrade, Serbia

The reduction of commercial and mechanochemically processed CeO_2 powders was studied. Nanostructured CeO_2, with the crystallite size of 21 nm and the lattice distortion of 0.37%, was obtained during 60 min of milling in a high-energetic vibratory mill. X-ray diffraction, scanning electron microscopy and Brunauer-Emmett-Teller method were applied to characterize the milled powders. During the thermal treatment at 1200 and 1400 °C in an argon atmosphere the nonstoichiometric CeO_{2-x} oxides with the defect fluorite structure were formed. Compositions of CeO_{2-x} oxides were determined according to its lattice parameter. The results showed that the release of oxygen, as well as the rate of reduction, was more effective in nanocrystalline then in the microcrystalline CeO_2, producing at 1200 °C $CeO_{1.80}$ and $CeO_{1.85}$ oxides, while at 1400 °C were obtained similarly, $CeO_{1.77}$ and $CeO_{1.78}$, compositions.

Keywords: milling; X-ray methods; CeO_2; nanostructure

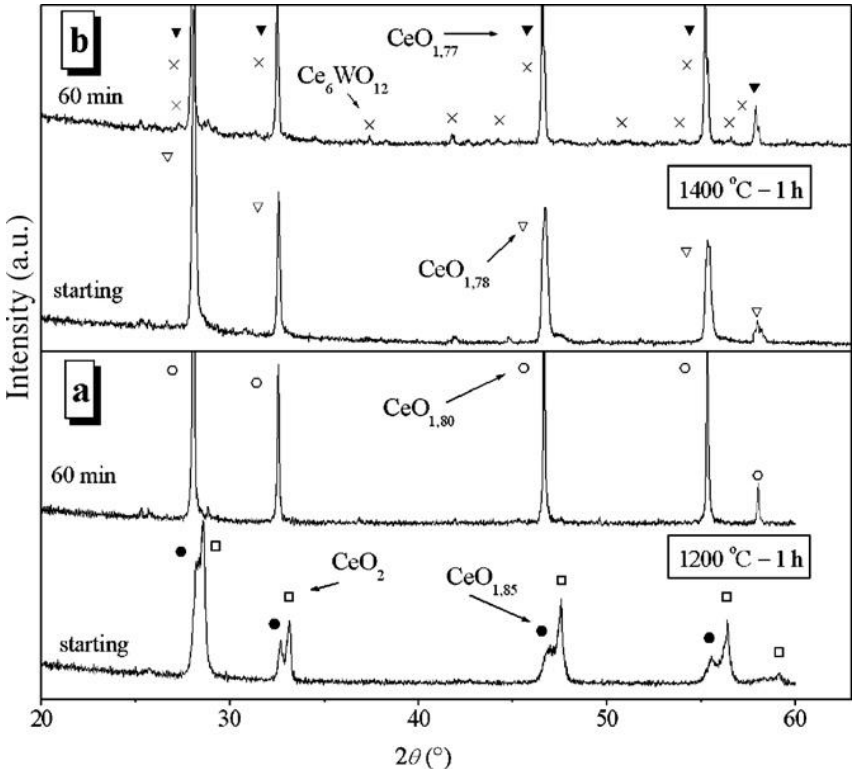

Figure: Phases identified in starting and milled CeO_2 powders fired for 1 h at (a) 1200 °C and (b) 1400 °C.

***Ceramics International*, 35 [1] (2009) 195-198.**

Structural and optical characterization of flower-like rutile nanostructures doped with Fe^{3+}

Nadica D. Abazović , Mirjana I. Čomor, Slavica Zec, Jovan M. Nedeljković, Emanuela Piscopiello[1], Amelia Montone[2], Marco Vittori Antisari[2]

Vinča Institute of Nuclear Sciences, University of Belgrade, 11001 Belgrade, Serbia
[1]ENEA, Materials and Technology Unit, 72100 Brindisi, Italy
[2]ENEA, Materials and Technology Unit, 2400 Rome, Italy

Flower-like agglomerates with sizes of 200–400 nm of pure and Fe^{3+}-doped TiO_2 with rutile crystalline structure were synthesized by the coprecipitation method. The morphology of the agglomerates was determined by electron microscopy (TEM and HRTEM). TiO_2 agglomerates consist of nanorods with clearly visible crystalline faces, parallel to the axis of elongation whose direction was along the [101] direction of pure TiO_2 and the [111] direction of doped TiO_2. Furthermore, nanorods consist of ‘‘chains’’ of spherical particles, most likely interconnected through the so-called oriented attachment or grain-rotationinduced grain coalescence (GRIGC) process. UV/Vis reflection measurements revealed that the absorption of pure TiO_2 was significantly shifted from UV toward the visible spectral region upon the incorporation of Fe^{3+} into the TiO_2 host.

Keywords: doping, rutile, nanorods, UV/Vis reflection, absorption.

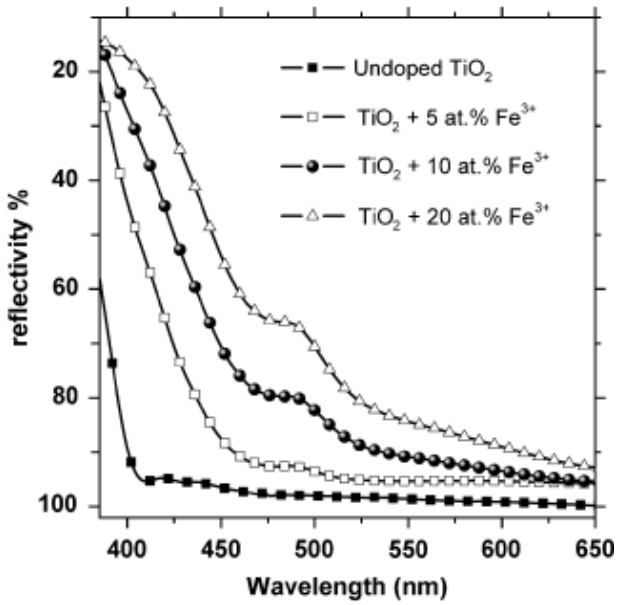

Figure: UV/Vis reflectance spectra of pure TiO_2 and TiO_2 doped with different at.% of Fe^{3+} ions, indicated in the figure.

***Journal of the American Ceramic Society*, 92(4) (2009) 894–896.**

Biomaterials

Synthesis of biomorphic SiC and SiO_2 ceramics

Adela Egelja, Biljana Babic, Aleksandar Devečerski, Milena Rosic, Branko Matovic

Institute of Nuclear Sciences ''Vinča'', Laboratory for Material Science, Belgrade, Serbia

Tillia wood was transformed by pyrolysis into carbon performs. This porous carbon perform was infiltrated with TEOS ($Si(OC_2H_5)_4$), as a source of silica, without pressure at 298K. An in situ reaction between the silica and the carbon template occurred in the cellular wall at a hight temperature. Depending of the employed atmosphere, nonoxide (SiC) or oxide (SiO_2) ceramics were obtained. Scanning electron microscopy (SEM), X-ray diffraction (XRD), infra red (IR) spectroscopy, mercury porosimetry and BET measurement were employed to characterize the phases and crystal structure of crystal structure of biomorphic ceramics. The experimental results showed that the biomorphic cellular morphology of wood maintaned in the both SiC and SiO_2 ceramics wich consisted of β- SiC with trace of α- SiC and SiO_2, respectively.

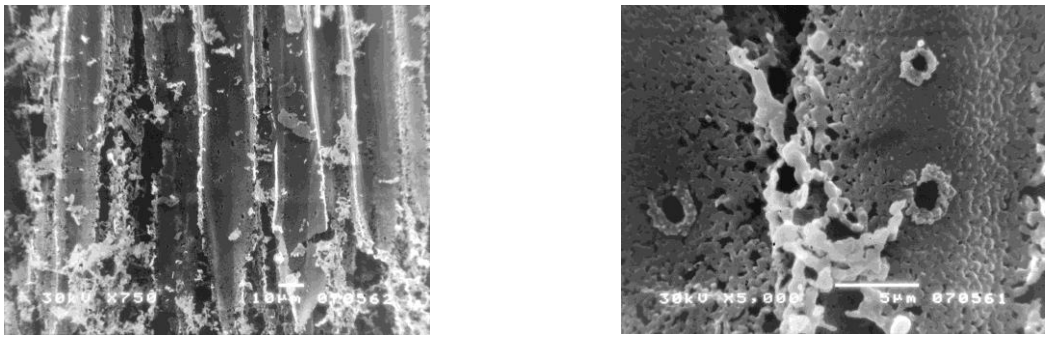

Figure: SEM micrograph of woodlike SiC ceramics.

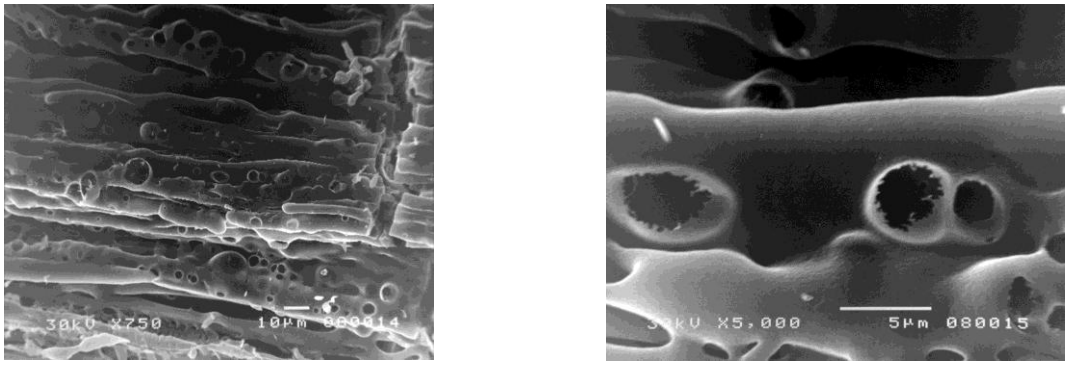

Figure: SEM mocrograph of biomorpic SiO_2 ceramics.

***VIII Students' Meeteing, Processing and Aplication of Ceramics*, Novi Sad, Serbia, December 2-5, 2009, p. 48.**

Tribological behavior of orthopedic Ti-13Nb-13Zr and Ti-6Al-4V alloys

I. Cvijović-Alagić[1], Z. Cvijović[2], S. Mitrović[3], M. Rakin[2], Đ. Veljović[2], M. Babić[3]

[1]Institute of Nuclear Sciences, Vinča, P.O.Box 522, 11001 Belgrade, Serbia
[2] Faculty of Technology and Metallurgy, University of Belgrade, Karnegijeva 4, 11120 Belgrade, Serbia
[3] Faculty of Mechanical Engineering, University of Kragujevac, Sestre Janjić 6, 34000 Kragujevac, Serbia

The aim of the present study is to compare the tribological behavior of novel orthopedic implant alloy Ti-13Nb-13Zr with that of the standard Ti-6Al-4V ELI alloy, available in four different microstructural conditions produced by variations in the heat treatments. The friction and wear tests were performed by using a block-on-disc tribometer in Ringer's solution at ambient temperature with a normal load of 20-60 N and sliding speed of 0.26-1.0 m/s. It was found that variations in microstructures produced significant variations in the wear resistance of Ti-6Al-4V ELI alloy. The wear losses of materials solution treated (ST) above the β transus temperature are significantly lower compared with those of materials ST in the (α+β) phase field and are almost insensitive to applied load and sliding speed. Wear loss of the (α+β) ST Ti-6Al-4V ELI alloy continuously increased as applied load was increased and was highest at the highest sliding speed. The Ti-6Al-4V ELI alloy in all microstructural conditions possesses a much better wear resistance than cold-rolled Ti-13Nb-13Zr alloy. Friction results and morphology of worn surfaces showed that the observed behavior is attributed to the predominant wear damage mechanism.

Keywords: Ti-13Nb-13Zr alloy; Ti-6Al-4V ELI alloy; Microstructure; Friction; Wear; Ringer's solution

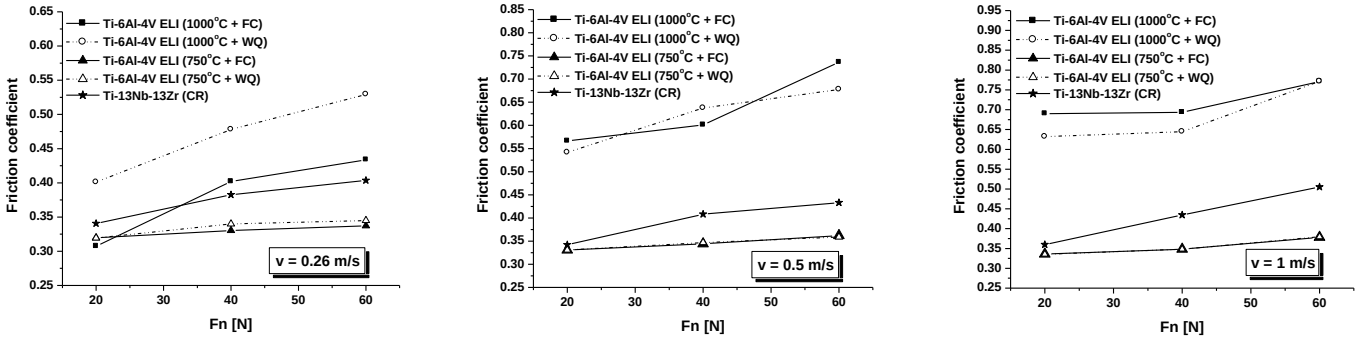

Figure: Friction coefficient of cold rolled Ti-13Nb-13Zr and heat treated Ti-6Al-4V ELI alloys as a function of applied load at the sliding speed of 0.26 (a), 0.5 (b) and 1.0 m/s (c).

***Tribology Letters*, 40 [1] (2010) 59-7.**

Influence of the Heat Treatment on the Tribological Characteristics of the Ti-based Alloy for Biomedical Applications

I. Cvijović-Alagić[1], S. Mitrović[2], Z. Cvijović[3], Đ. Veljović[3], M. Babić[2], M. Rakin[3]

[1]Institute of Nuclear Sciences, Vinča, University of Belgrade, P.O. Box 522, 11001 Belgrade, Serbia
[2]Faculty of Mechanical Engineering, University of Kragujevac, Sestre Janjić 6, 34000 Kragujevac, Serbia
[3]Faculty of Technology and Metallurgy, University of Belgrade, Karnegijeva 4, 11120 Belgrade, Serbia

The influence of diverse heat treatments on microstructural and tribological characteristics of Ti-6Al-4V ELI (mass%) alloy, which is used as implant material in biomedical engineering, was investigated on a block-on-disc tribometer. Aim of the present study was to explore the possibility of Ti-6Al-4V ELI alloy wear resistance improvement, examining the effects of different heat treatments on alloy microstructure, as well as on alloy wear characteristics in simulated body conditions using light optical microscopy (LOM) and scanning electron microscopy (SEM). Results presented in this paper show that the influence of heat treatment on microstructural and tribological characteristics of the investigated Ti-based alloy is significant and that it can be used for further wear resistance improvement of this widely used implant material.

Keywords: Ti-6Al-4V alloy; microstructural characterization; Vickers hardness; wear resistance; LOM; SEM.

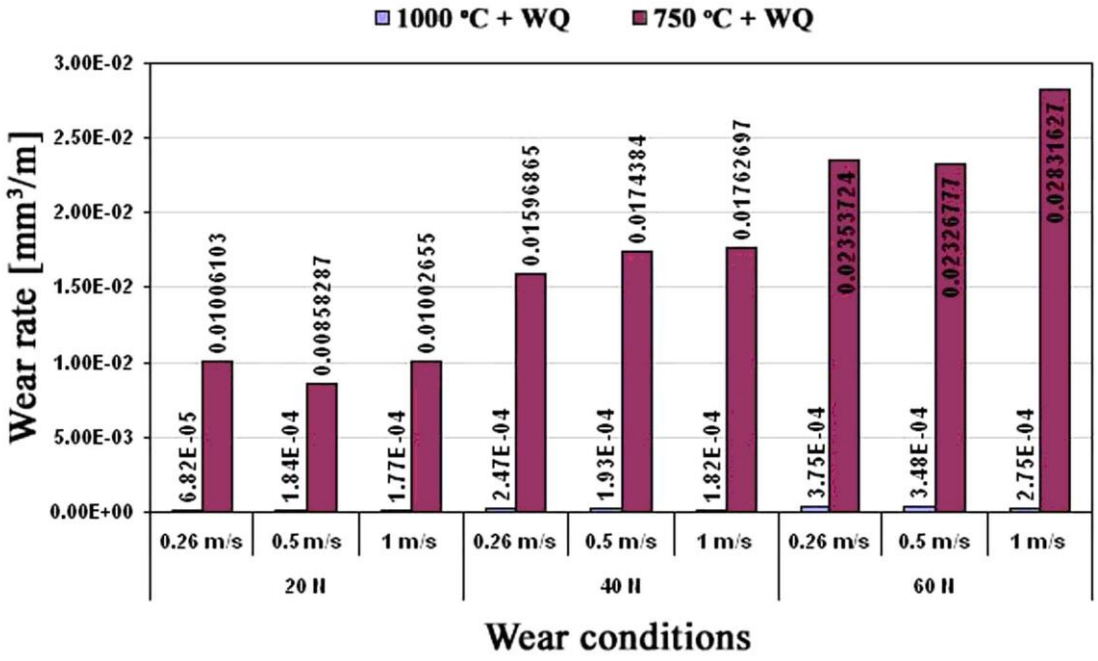

Figure: Effect of heat treatment on Ti-6Al-4V ELI alloy wear rate.

***Tribology in Industry*, 30 [3-4] (2009) 16-21.**

Application of Tribometry in Investigations of Biomaterials

F. Živić[1], S. Mitrović[1], M. Babić[1], I. Cvijović-Alagić[2]

[1]Faculty of Mechanical Engineering, University of Kragujevac, Sestre Janjić 6, 34000 Kragujevac, Serbia
[2]Institute of Nuclear Sciences, Vinča, University of Belgrade, Mike Petrovića Alasa 12-14, 11001 Belgrade, Serbia

Development of materials for manufacturing of the chirurgical implants in medicine - biomaterials (metals, polymers, ceramics and composites) is directly determined by characteristics and nature of the tissue, organs and systems that are being replaced or supplemented.
Modern material investigations at micro- and nano- level enable introspection into new aspects of material behaviour and offer possibilities to significantly improve systems in use, from different aspects of changes in material production technologies or application of surface technologies modifications or coating technologies.
Biomaterial investigations from a tribology point of view offer contribution to testing realised in this area, especially with use of novel devices for research in area of nanotribology. In this paper, some tribological characteristics of Ti-6Al-4V alloy, aimed for medicine applications, are presented. Investigation is realized at CSM nanotribometer in accordance with testing conditions significant for this type of biomaterial.

Keywords: Biomaterials, Ti alloys, Nanotribometer

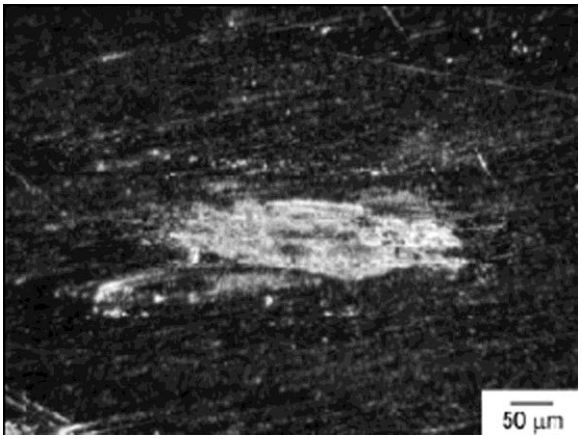

Figure: Wear track on Ti-6Al-4V alloy sample at 1000x magnification.

11th International Conference on Tribology – SERBIATRIB '09, **May 13th-15th 2009, Belgrade, Serbia, Proceedings, pp. 301-306.**

Chitosan, itaconic acid and poly(vinyl alcohol) hybrid polymer networks of high degree of swelling and good mechanical strength

Nedeljko B Milosavljević[a], Ljiljana M Kljajević[b], Ivanka G Popović[a], Jovanka M Filipović[a], Melina T Kalagasidis Krušić[a]

[a]Faculty of Technology and Metallurgy, University of Belgrade, Belgrade, Serbia
[b]Vinča Institute of Nuclear Sciences, Department of Materials, University of Belgrade, Belgrade, Serbia

Chitosan is a biodegradable, non-toxic, biocompatible polymer convenient for use in drug delivery. In this study, hybrid polymeric networks (HPNs) based on chitosan, itaconic acid and poly(vinyl alcohol) (PVA) were prepared and characterized. Chitosan was dissolved in itaconic acid in order to obtain ionic crosslinking with the dicarboxylic acid. In the second step, this chitosan/itaconic acid network wasmixed with PVA and chemically crosslinkedwith glutaraldehyde. The chitosan/itaconic acid ratio was kept constant, while the concentrations of PVA and glutaraldehydewere varied. All samples were characterized using swelling studies, dynamic mechanical analysis, Fourier transform infrared spectroscopy, differential scanning calorimetry, thermogravimetric analysis, X-ray diffraction and scanning electron microscopy. The equilibrium degrees of swelling obtained for the HPNs were higher than most of the values reported for chitosan hydrogels obtained by dissolving chitosan in acetic acid or HCl aqueous solutions. This method of synthesis also resulted in hydrogels with better mechanical properties and thermal stability. By changing the PVA content and the degree of crosslinking, it is possible to finely tune the properties of the HPNs, which could make them suitable as potentialmatrices in controlled drug delivery.

Keywords: hybrid polymer network (HPN); chitosan; poly(vinyl alcohol); itaconic acid; glutaraldehyde

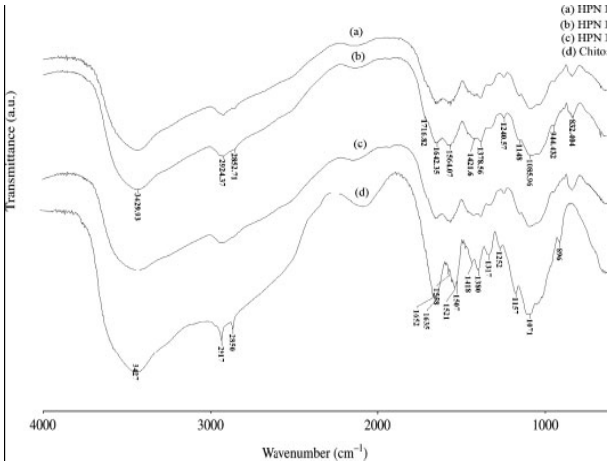

Figure: FTIR spectra of HPN I-1, HPN I-4, HPN II-5 and chitosan.

***Polymer International,* 59 (2010) 686–694.**

Sol–Gel Combustion Synthesis of $La_{9.33}(SiO_4)_6O_2$ Oxyapatite

S. Zec[1], J. Dukić[1], M. Puševac[1], S. Bošković[1], R. Petrović[2]

[1]Institute of Nuclear Sciences, Vinča, University of Belgrade, 11001 Belgrade, Serbia
[2]Faculty of Technology and Metallurgy, University of Belgrade, 11000 Belgrade, Serbia

Synthesis of $La_{9.33}(SiO_4)_6O_2$ was performed by a new method that represents the combination of sol–gel and combustion procedures using glycine as the fuel. Syntheses were performed from ethanol-water solutions of oxides precursors, lanthanum nitrate and tetraethyl orthosilicate. The optimum synthesis parameters have been established by varying molar ratio of tetraethyl orthosilicate to water as well as glycine to NO^{-3} ions. The phase identification and the structural characterization were performed by X-ray powder diffraction. The pure nanocrystalline $La_{9.33}(SiO_4)_6O_2$ with the crystallite sizes of 32nm was directly synthesized during combustion process of homogeneous gel that was generated in solution with the following molar ratios: glycine: NO^{-3} = 0.56 and tetraethyl orthosilicate: water = 1:20. Well-crystallized $La_{9\_33}(SiO_4)_6O_2$ structure was obtained after heating at 1200 °C. The lattice parameters a = 9.7156(9) and c = 7.1810(8) Å confirmed the composition $La_{9.33}(SiO_4)_6O_2$.

Keywords: apatite structure; glycine; lanthanum silicate; synthesis method derived from combustion procedure.

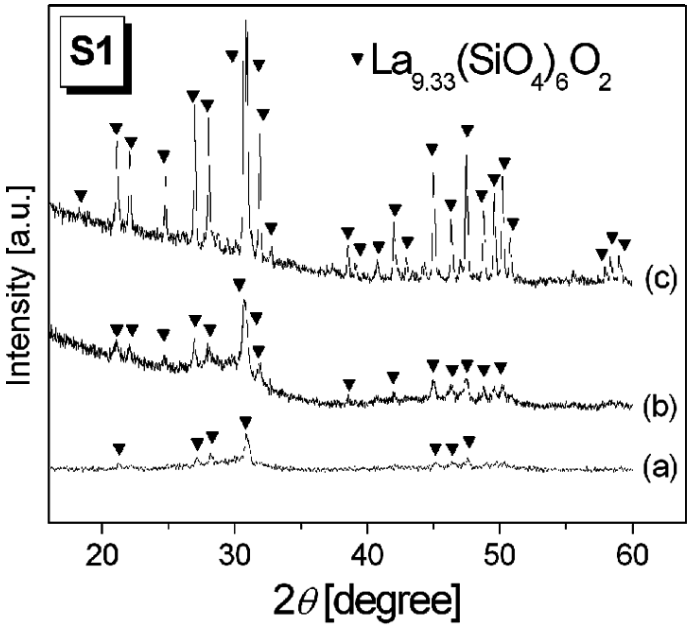

Figure: XRD patterns of directly synthesized $La_{9.33}(SiO_4)_6O_2$ during combustion process.

***Materials and Manufacturing Processes,* 24 [10-11] (2009) 1104–1108.**

Precision cast Ti-based alloys-microstructure and mechanical properties

Milan T. Jovanović, Ilija Bobić, Zoran Mišković, Slavica Zec

Institute of Nuclear Sciences, Vinča, 11001 Belgrade, Serbia

The effects of preheat and pouring temperatures as well as annealing temperatures and cooling rates on microstructure and mechanical properties of γ TiAl and Ti-6Al-4V castings have been studied performing X-ray diffraction analysis, light and scanning electron microscopy (SEM), quantitative metallography, hardness and room temperature tensile tests. Annealing of Ti-6Al-4V above and below the β phase transus temperature produces different combinations of strength and elongation, but a compromise may be achieved applying temperature just below the β phase transus of Ti-6Al-4V alloy. Higher values of tensile strength together with lower ductility than reported in the literature cannot be only ascribed to the presence of α' martensite in the microstructure of Ti-6Al-4V alloy. Yttria coating of graphite crucible must be considered as insufficient in preventing the chemical reaction between aggressive titanium melt and carbon. The processing technology of a "self-supporting" ceramic shell mold was successfully verified during precision casting of both tensile-test samples of Ti-6Al-4V and the prototype of the turbocharger wheel made of γ TiAl. According to experimental results, a processing window for precision casting of the prototype of a turbocharger wheel was established. The results of this paper also show that beside annealing treatment parameters, melting and casting practice together with ceramic mold technology strongly influence the properties Ti-6Al-4V and γ TiAl castings.

Keywords: precision casting, "self-supporting" ceramic mold, annealing, phase transformations, strength and elongation, turbocharger wheel

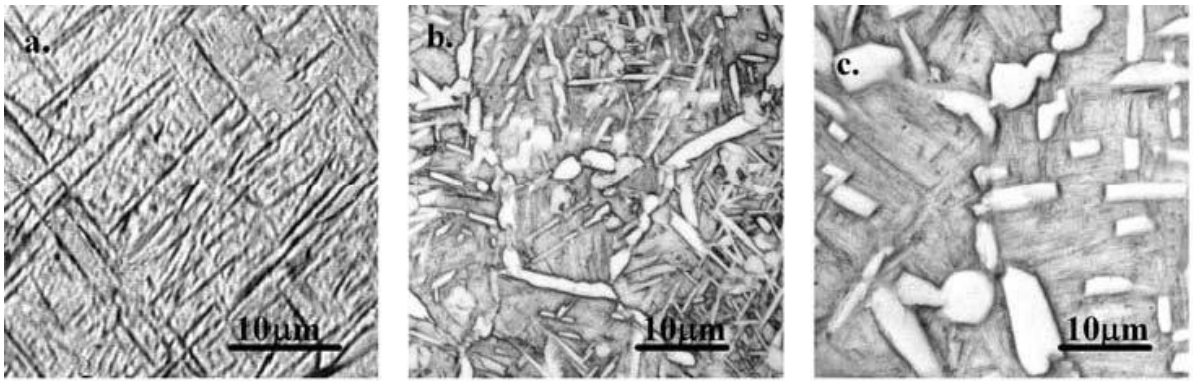

Figure: Light microscope. Microstructure of Ti-6Al-4V alloy upon water-quenching from: (a) 1100 °C; (b) 950 °C; (c) 900 °C

***Metalurgija-Journal of Metallurgy,* 15 [1] (2009) 53-69.**

Microstructure and mechanical properties of Zn25Al3Cu based composites with large Al_2O_3 particles at room and elevated temperatures

Biljana Bobić[a], Miroslav Babić[b], Slobodan Mitrović[b], Nenad Ilić[c], Ilija Bobić[d], Milan T. Jovanović[d]

[a]IHIS R&D Center, Belgrade, Serbia
[b]Faculty of Mechanical Engineering, University of Kragujevac, Kragujevac, Serbia
[c]Functional Materials, Saarland University, Saarbrücken, Germany
[d]Institute of Nuclear Sciences, Vinča, University of Belgrade, Belgrade, Serbia

Microstructure and compressive properties of Zn25Al3Cu alloy and Zn25Al3Cu/Al_2O_3 particulate composites with large reinforcing particles (250 μm) were examined. The composites were obtained by compocasting technique through infiltration of 3, 8 and 16 wt. % Al_2O_3 particles into the semi-solid metal matrix. The influence of temperature in the range from 70 to 170 °C on compressive yield strength of the matrix alloy (as-cast and thixocast Zn25Al3Cu alloy) and the composites was investigated. Above 70 °C compressive yield strength of all materials decreases, but the rate of decrease is different for the matrix alloy (as-cast and thixocast) and composites. It was found that the abrupt decrease of compressive yield strength of the matrix alloy occurred at temperatures higher than 70 °C, whereas composites retained relatively high values of compressive yield strength till the end of testing temperature range regardless of the amount of reinforcing particles.

Keywords: Metal-matrix composites; zinc-aluminum alloys; Al_2O_3 particles; compocasting; compressive yield strength

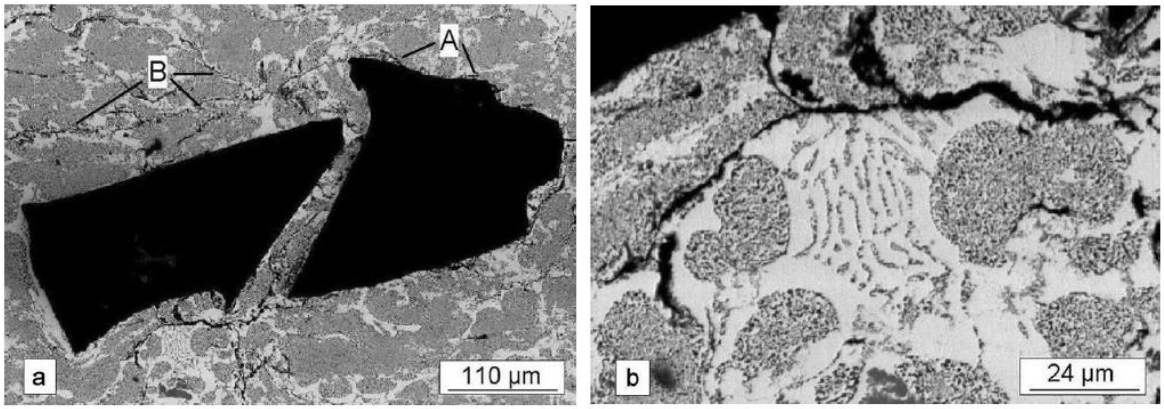

Figure: Microstructure of Zn25Al3Cu/Al_2O_3 composite (3 wt. % Al_2O_3), SEM, polished. (a) interface and microcracks; (b) microcracks development.

***International Journal of Materials Research*, 101 (2010) 1524-1531.**

Carbon materials

Adsorption characteristics of activated carbon hollow fibers

Branka V. Kaluđerović, Ljiljana M. Kljajević, Danijela Sekulić, Jelena Stašić, Žarko Bogdanov

Vinča Institute of Nuclear Sciences, University of Belgrade, Belgrade, Serbia

Carbon hollow fibers were prepared with regenerated cellulose or polysulfone hollow fibers by chemical activation using sodium phosphate dibasic followed by the carbonization process. The activation process increases the adsorption properties of fibers which is more prominent for active carbone fibers obtained from the cellulose precursor. Chemical activation with sodium phosphate dibasic produces an active carbon material with both mesopores and micropores.

Keywords: activated carbon hollow fibers; adsorption characteristics; regenerated cellulose; polysulfone.

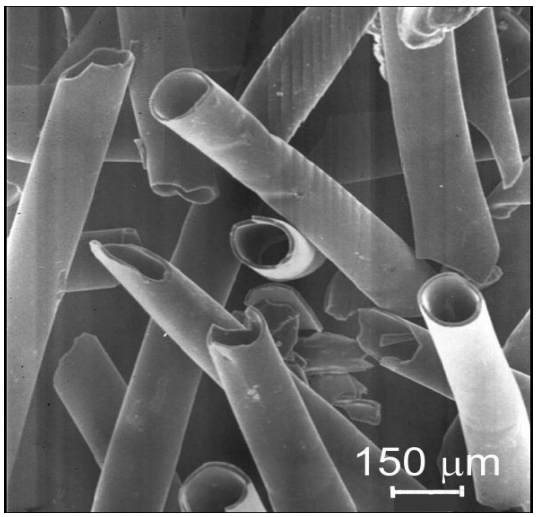

Figure: SEM micrograph of activated carbon hollow fibers obtained from polysulfone precursor.

***Chemical Industry & Chemical Engineering Quarterly,* 15 [1] (2009) 29−31.**

The effect of gamma radiation on the properties of activated carbon cloth

Danijela R Sekulić, Biljana M Babić, Ljiljana M Kljajević, Jelena M. Stašić, Branka V. Kaluđerović

Vinča Institute of Nuclear Sciences, University of Belgrade, Belgrade, Serbia

Activated carbon cloth dressing is an appropriate wound healing material due to its biocompatibility and adsorption characteristics. The influence of gamma radiation as a sterilization process on the adsorption and mechanical properties of activated carbon cloth was investigated. The specific surface area, micropore volume, pore size distribution, surface chemistry as well as the breaking load of activated carbon cloth before and after gamma radiation were examined. Characterization by nitrogen adsorption showed that the activated carbon cloth was a microporous material with a high specific surface area and micropores smaller than 1 nm. Gamma radiation decreased the specific surface area and micropore volume but increased the pore with. The sterilization process changed the surface chemistry quantititatively, but not qualitatively. In addition, the breaking load decreased but without any influence considering the futher application of this material.

Keywords: activated carbon cloth; dressing material; gamma radiation; adsorption; surface modification.

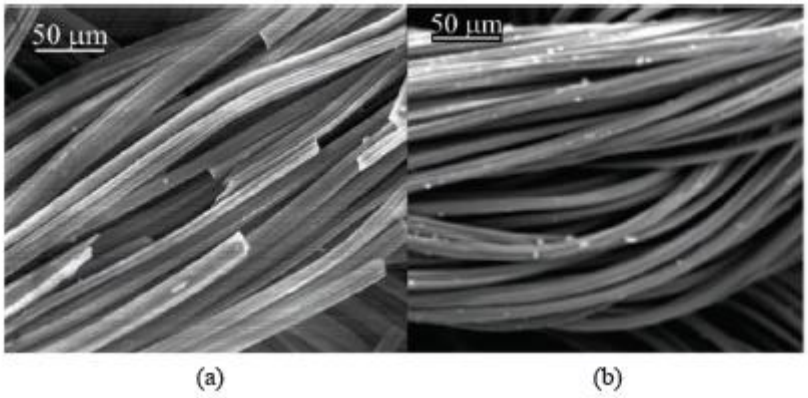

Figure: SEM Microphotographs of ACCγ from: a) side directly exposed to the γ-radiation; b) the opposite side.

***Journal of Serbian Chemical Society,* 74 [10] (2009) 1125-1132.**

New type of carbon fibrous material for supported platinum catalysts

Branka V. Kaluđerović[1], Vladislava M. Jovanović[2], Sanja I. Stevanović[2], Ljiljana Kljajević[1], Žarko D. Bogdanov[1]

[1]Vinča, Institute of Nuclear Sciences, University of Belgrade, P.O.Box 522, 11000 Belgrade (Serbia)
[2]University of Belgrade, ICTM –Institute of Electrochemistry, P.O.Box 473, 11000 Belgrade (Serbia)

High area carbon materials are usually used as supports for platinum catalysts. Physico-chemical characteristics of the support influence the properties of platinum deposited and its catalytic activity. In our studies we deposited platinum on carbon fibrous materials obtained from tree wastes. The precursor was chemically activated with different reagents prior to carbonization process. Platinum was deposited on all substrates with the aim to study an influence of the substrate properties on the activity of the catalyst. Carbon materials were characterized by nitrogen adsorption/desorption isotherms measurements, X ray diffraction and scanning electron microscopy. It was noticed that the adsorption characteristics of carbon support affected structure of platinum deposits and thus their activity.

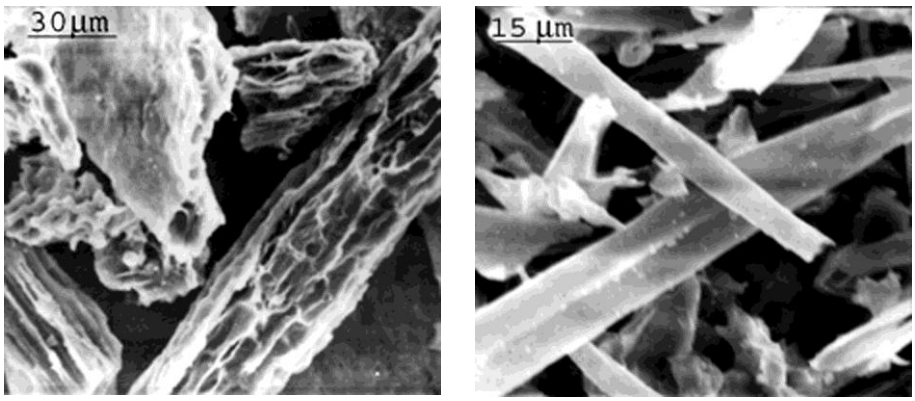

(a) (b)

Figure: SEM micrograph of carbonized achenes chemically treated with NaOH (a) and pyrogallol (b).

Carbon Conference **2009, June 14 - 19 2009, Biarritz, France, Extended Abstracts presentation CD P202.**

Modeling and experiments in the interaction of laser beam with carbon nanoporous materials

M. Janićijević[1], B. Kaluđerović[2], M. Srećković[3], A. Kovačević[4], D. Družijanić[3]

[1]Metalac, Gornji Milanovac, Serbia,
[2]Laboratory for the Materials, Institute of Nuclear Sciences, Vinča, Belgrade, Serbia,
[3]Faculty of Electrical Engineering, University of Belgrade, Belgrade, Serbia,
[4]Institute of Physics, University of Belgrade, Belgrade, Serbia

In this work, the interaction of materials with both well-known commercial lasers and rarely used lasers like alexandrite, Er^{3+}:YAG and others, are analyzed according to the dynamical regimes. Modeling through various numerical approaches and analytical approximations has been performed. The results of sample irradiation, obtained by some of microscopic techniques (optical, SEM ...), are analyzed by image processing methods. The modeling includes the processes existing up to melting point by finite differences method.
Particularly, specific critical energies have been analyzed, which lead to melting, evaporation, sublimation and so-called optimal energy. In contemporary interpretations of interaction modeling, there are developed approaches for CW and pulse (longer pulses) lasers. The interaction with ultra-short pulses demands new approaches which seem to be still in development.

Figure: Effect of 15 pulses 60J/cm2 Nd^{3+}: YAG laser, spot 2mm on carbon material P7295-2.

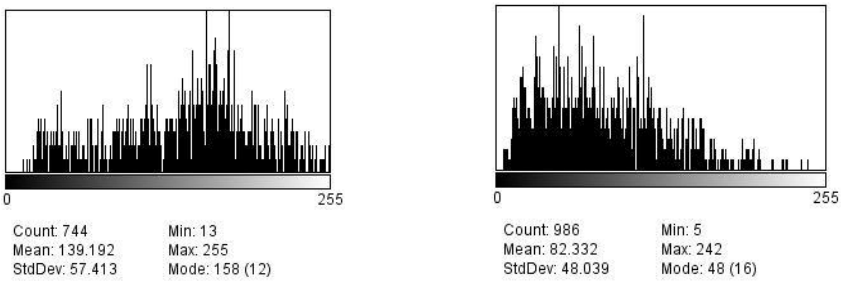

Figure: Histogram nonirradiated carbon material P7295-2(left). Histogram irradiated (with Nd^{3+}: YAG laser) carbon material P7295-2 (right).

***11th Annual Conference "YUCOMAT 2009,"* August 31-September 4, 2009, Herceg-Novi, Montenegro, Book of Abstracts, pp. 103.**

Approach to modeling interaction of carbon fiber materials and laser beam with experiment

M. Janićijević[1], B. Kaluđerović[2], M. Srećković[3], A. Kovačević[4], D. Družijanić[3]

[1]Metalac, Gornji Milanovac, Serbia,
[2]Laboratory for Materials, Institute of Nuclear Sciences, Vinča, Belgrade, Serbia,
[3]Faculty of Electrical Engineering, University of Belgrade, Belgrade, Serbia,
[4]Institute of Physics, Belgrade, Serbia

During the interaction of material, built from carbon fiber, and laser beams come to a number of processes and effects on the exposed material. Methods for characterization, qualitative and quantitative description of these effects, are numerous. In this paper the treatment of selected material using alexandrite and other lasers, and the results were analyzed by SEM microscopy. Because of the complexity of the process, the interaction can't be described with single approach. We used a thermal model and give an overview of other models (theory of fractales). Using the model can provide estimates of heat distribution in the material during the irradiation with laser beams. This is good base for prediction other processes in material, triggered by heating (e.g. photochemical processes). Surface oxidation is among the most interesting photochemical processes. Analysis of the images caused by the change deserves special discussion, which should be used for identification and interpretation induced processes.

Figure: Effect of 5 impulses 36 J/cm^2 Alexandrite laser, spot 10mm on carbon fiber material.

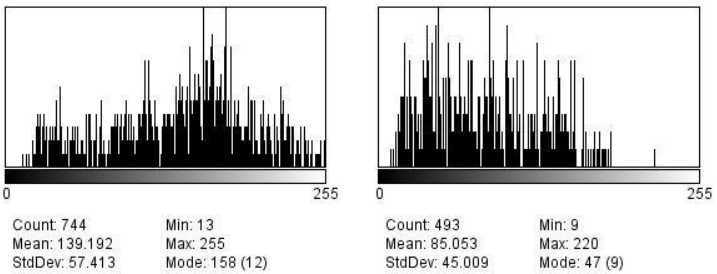

Figure: Histogram intact carbon fiber type material (left). Histogram irradiated carbon fiber type material with alexandrite laser (right).

***12th Annual Conference "YUCOMAT 2010",* September 6-10, 2010, Herceg-Novi, Montenegro, Book of Abstracts, pp. 117.**

Characterization of carbon fibrous materials obtained from tree waste

Sanja Stevanović[1], Branka V. Kaluđerović[2], Vladislava M. Jovanović[1]

[1]ICTM –Department of electrochemistry, P.O.Box 473, Belgrade, Serbia
[2]INN Vinča, Lab. For Mater. Sci. P.O.Box 522, 11001 Belgrade, Serbia

Carbon fibers can be obtained in rather wide variety of structures, compositions and properties, depending on the nature of the organic precursor and conditions of the process applied in their preparation. In order to get a high surface area, physical or/and chemical activation processes of material have usually have been employed. A challenge in the field of carbon adsorbents is to produce very specific materials with a given pore size distribution from low cost precursors.

In this study we used new type of a precursor for active carbon fibres material – achenes from the Platanus orientalis seeds. We examined the influence of different of chemical activating agents on the porous and the electrochemical properties of carbon material support. The properties of these fibers were compared with the properties of polysulfone hollow fibers treated on the similar way.

These investigations show that the waste such as fibrous seeds is very promising raw material for active carbon fibers production.

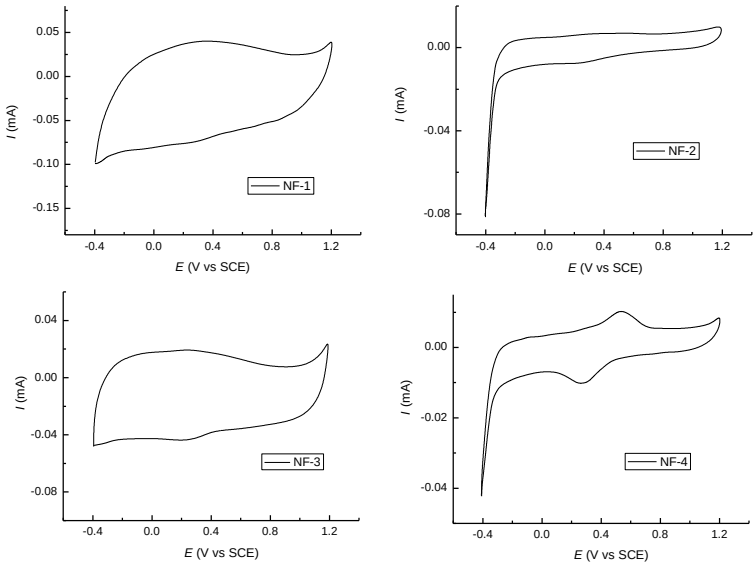

Figure: Cyclic voltammograms of natural fibers applied on glassy carbon electrode in 0.1 M $HClO_4$ solution; sweep rate 100 mV/s.

RSE SEE 2, **June 6-10., 2010, Belgrade, Serbia, Book o f Abstracts pp. 89.**

Prilaz modelovanju interakcije ugljeničnog materijala i laserskih snopova i eksperiment

Milovan Janićijević,[a,b] B. Kaluđerović,[c] Dragan Družijanić

[a]Metalac, a.d. Kneza Aleksandra 212, Gornji Milanovac
[b]Elektrotehnički fakultet u Beogradu
[c]Laboratorija za Materijale, Institut za nuklearne nauke "Vinča", Beograd

Prilikom izlaganja materijala, izgrađenih od ugljeničnih vlakana, laserskim snopovima, dolazi do brojnih procesa i efekata na izloženom materijalu. Razne su i metode za karakterizaciju, kvalitativnu i kvantitativnu ocenu ovih efekata.
U radu je tretman izabranog materijala izveden pomoću aleksandritskog i drugih lasera, a rezultati su analizirani SEM mikroskopom. Zbog složenosti procesa, interakcija se ne može opisati jednim prilazom. Korišćen je termalni model i dat je osvrt na druge modele (teorija fraktala). Korišćenje modela može da pruži procenu toplotne distribucije u materijalu prilikom dejstva laserskih snopova. Od fotohemijskih procesa mešu najinteresantnijim je oksidacija površine. Analiza slike izazvanih promena zaslužuje posebnu diskusiju, koja bi trebalo da posluži za identifikaciju i interpretaciju odigranih procesa.

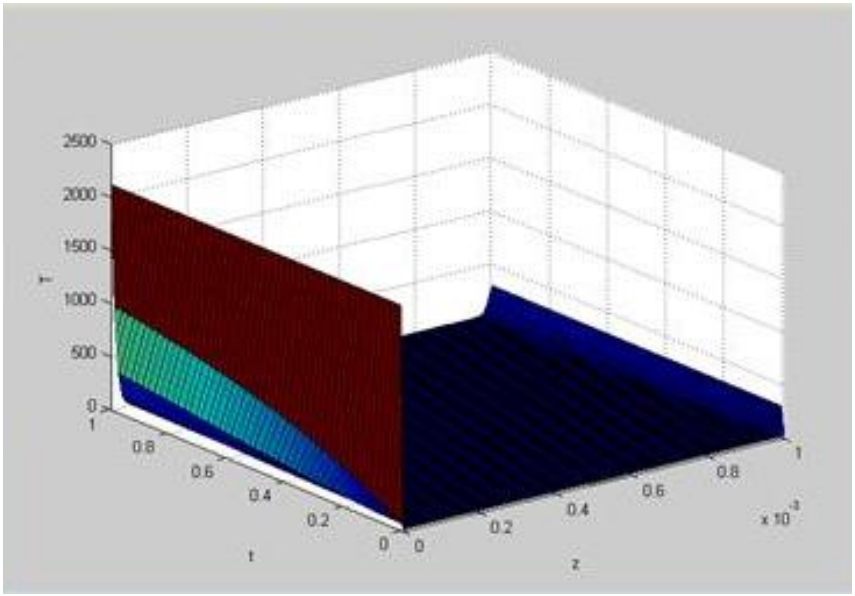

Slika: Grafički prikaz rezultata termičke jednačine.

***Fotonika 2010,* teorija i eksperiment u Srbiji, 21- 23 april, Beograd, Zbornik apstrakata str. 17-7-1.**

Ceramic composites

Effects of copper and Al_2O_3 particles on characteristics of Cu–Al_2O_3 composites

Višeslava Rajković, Dušan Božić, Milan T. Jovanović

Institute of Nuclear Sciences, Vinča, University of Belgrade, 11001 Belgrade, Serbia

High-energy milling was used for production of Cu–Al_2O_3 composites. The inert gas-atomized prealloyedcopper powder containing 2 wt.%Al and the mixture of the different sized electrolytic copper powders with 4 wt.% commercial Al_2O_3 powders served as starting materials. Milling of prealloyed copper powders promotes formation of nano-sized Al_2O_3 particles by internal oxidation with oxygen from air. Hot-pressed compacts of composites obtained from 5 and 20 h milled powders were additionally subjected to the high-temperature exposure in argon at 800 °C for 1 and 5 h. Characterization of processed material was performed by optical and scanning electron microscopy (SEM), X-ray diffraction analysis (XRD), microhardness, as well as density and electrical conductivity measurements. Due to nano-sized Al_2O_3 particles microhardness and thermal stability of composite processed from milled prealloyed powders are higher than corresponding properties of composites processed from the milled powder mixtures. The results were discussed in terms of the effects of different size of starting copper powders and Al_2O_3particles on the structure, strengthening of copper matrix, thermal stability and electrical conductivity of Cu–Al_2O_3 composites.

Keywords: composites, powder metallurgy, mechanical and physical properties, microstructure, X-ray analysis.

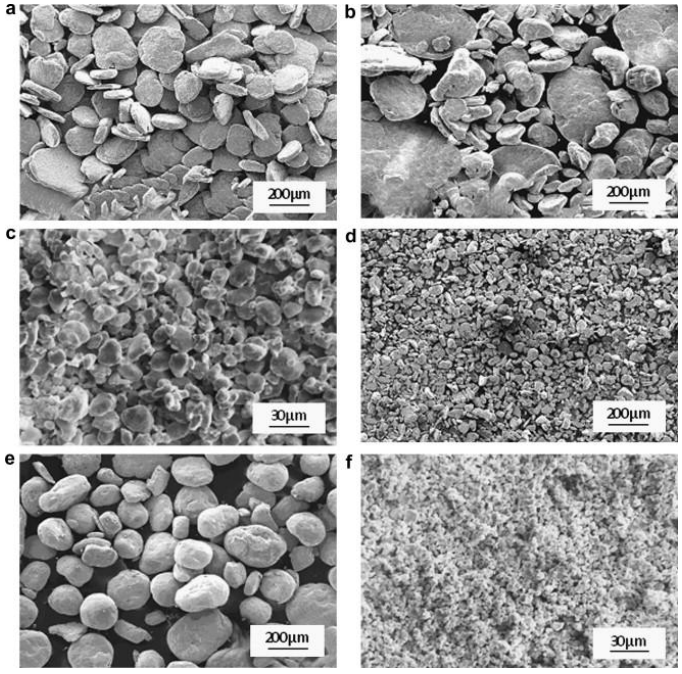

Figure: SEM. Morphology of Cu-2 wt.%Al_2O_3, Cu-4 wt.%Al_2O_3 and Cu*-4wt.%Al_2O_3 composite powders. (a–c) After 3 h and (d–f) after 20 h of milling.

***Materials & Design*, 31 (2010) 1962-1970.**

Influence of SiC particles distribution on mechanical properties and fracture of DRA alloys

D. Božić[1], B. Dimčić[1], O. Dimčić[2], J. Stašić[1], V. Rajković[1]

[1]Institute of Nuclear Sciences, Vinča, University of Belgrade, 11001 Belgrade, Serbia
[2]Technocon Filter, 11000 Belgrade, Serbia

In the last 20 years a new class of metal matrix composite material (DRA – Discontinuously Reinforced Aluminum) with aluminum alloy matrix and SiC particles as secondary phase has been developed. The most important step during composite production is the homogenization process of metal and ceramic powder particles. Quantitative analysis of a SiC particles distribution in the aluminum alloy matrix (CW67) was used to determine the optimum homogenization parameters of different powders. It was found out that the level of mixture homogeneity largely depends on the amount of mixing dish filling, homogenization time and characteristics of reinforcing particles. By introducing the concept of homogeneity index, it was shown that the lowest values of the mentioned parameter correspond to the best uniformity of SiC particles in the CW67 matrix. Composite with the lowest value of homogeneity index was the one with 5 vol.% of SiC, homogenized during 60 min and the amount of mixing dish filling of 20 vol.%. This composite displayed the best values of mechanical properties and fracture resistance.

Keywords: DRA materials, SiC-particles, quantitative microscopy, diffusion mixing, mechanical properties, fractography.

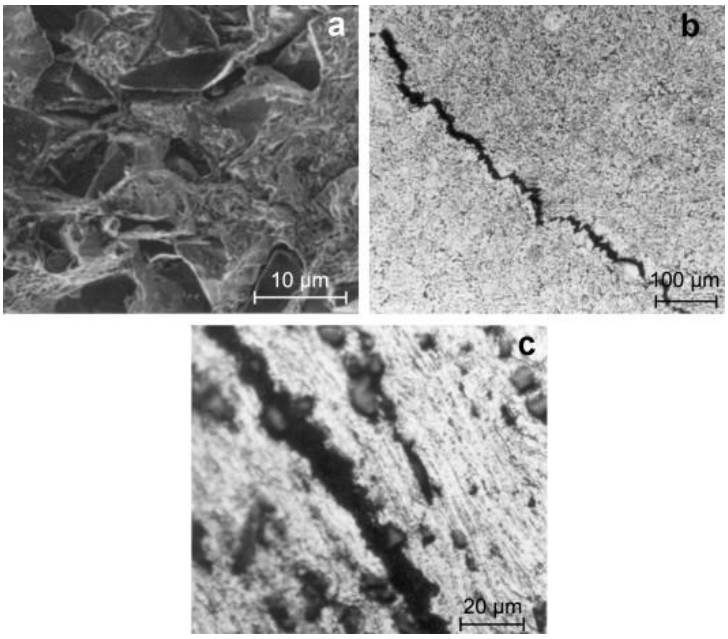

Figure: Fracture surface of DRA alloys after 60 min of homogenization. (a) SEM: CW67–10 vol.%SiC, d_{SiC} = 10 μm; (b) OM: CW67–10 vol.% SiC, d_{SiC} = 10 μm; (c) OM: CW67–10 vol.% SiC, d_{SiC} = 10 μm.

***Materials and Design*, 31 (2010) 134–141.**

Properties of copper composites strengthened by nano- and micro-sized Al_2O_3 particles

Višeslava Rajković, Dušan Božić, Milan T. Jovanović

Institute of Nuclear Sciences, Vinča, University of Belgrade, P.O.B. 522, 11001 Belgrade, Serbia

Electrolytic copper powder, inert gas atomized prealloyed copper powder containing 3.5 wt.% Al, and a mixture of copper and commercial Al_2O_3 powder particles (4 wt.% Al_2O_3) were milled separately in a high-energy planetary ball mill for up to 20 h in air. The milling was performed in order to strengthen the copper matrix by grain size refinement and Al_2O_3 particles. Milling in air of prealloyed copper powder promoted formation of fine dispersed Al_2O_3 particles by internal oxidation. Hot-pressing (800 °C for 3 h in argon at a pressure of 35 MPa) was used for compaction of milled powders. Compacts from 5 and 20 h milled powders were additionally subjected to high temperature exposure (800 °C for 1 and 5 h in argon) in order to examine their thermal stability and electrical conductivity. The effect of different size and the amount of Al_2O_3 particles on strengthening, thermal stability and electrical conductivity of the copper-based composites was studied. The results were discussed in terms of the effects of the grain size refinement along with micro- and nano-sized Al_2O_3 particles on the strengthening of the copper matrix.

Keywords: strengthened copper matrix, mechanical alloying, internal oxidation, microhardness, electrical conductivity.

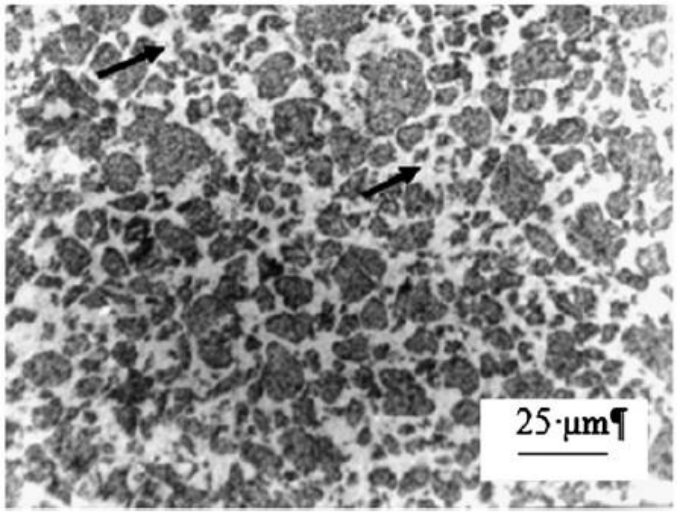

Figure: Light micrograph. Microstructure of Cu-4 wt.% Al_2O_3 compact. Arrows indicate the recrystallization areas occurred during hot pressing.

***International Journal of Materials Research*, 101 (2010) 334-339.**

Characteristics of Cu–Al_2O_3 composites of various starting particle size obtained by high-energy milling

Višeslava Rajković, Dušan Božić, Milan T. Jovanović

Institute of Nuclear Sciences, Vinča, University of Belgrade, P.O. Box 522, 11001 Belgrade, Serbia

The powder Cu–Al_2O_3 composites were produced by high-energy milling. Various combinations of particle size and mixtures and approximately constant amount of Al_2O_3 were used as the starting materials. These powders were separately milled in air for up to 20 h in a planetary ball mill. The copper matrix was reinforced by internal oxidation and mechanical alloying. During the milling, internal oxidation of pre-alloyed Cu-2 mass %-Al powder generated 3.7 mass % Al_2O_3 nano-sized particles finely dispersed in the copper matrix. The effect of different size of the starting copper and Al_2O_3 powder particles on the lattice parameter, lattice distortion and grain size, as well as on the size, morphology and microstructure of the Cu–Al_2O_3 composite powder particles was studied.

Keywords: Cu–Al_2O_3 composite powders; high-energy milling; size of the starting powder particles.

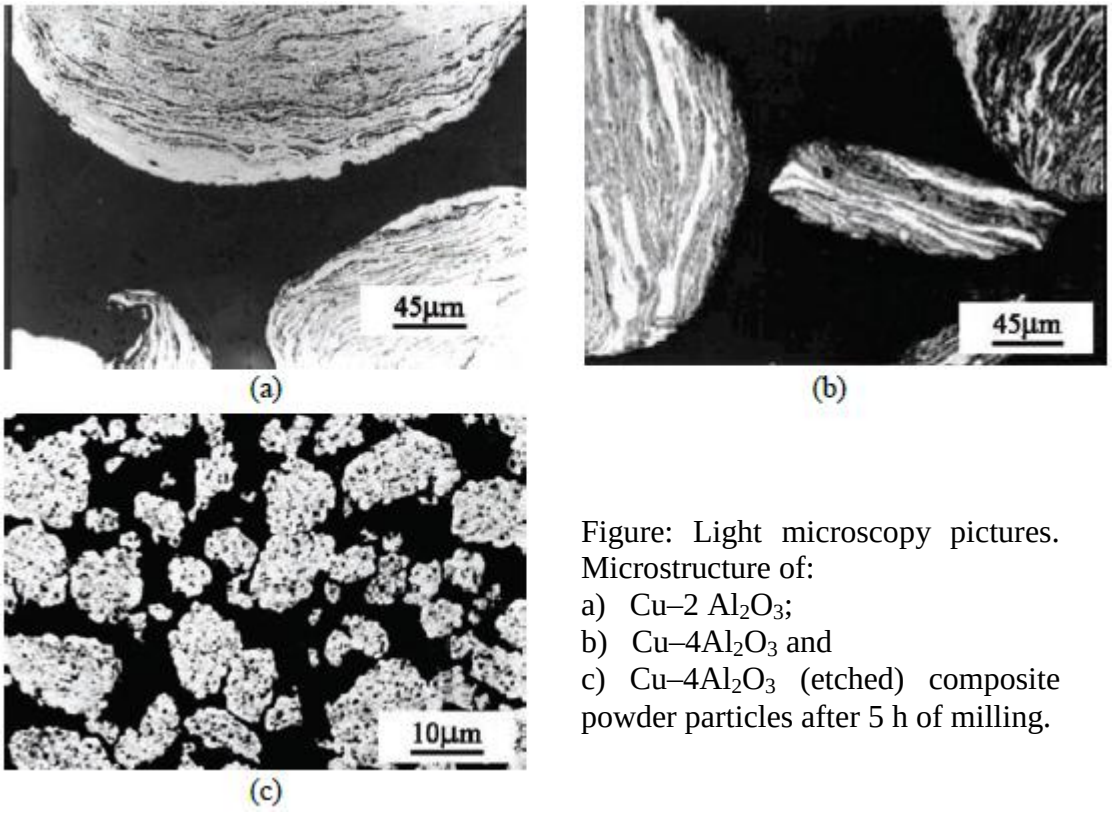

Figure: Light microscopy pictures. Microstructure of:
a) Cu–2 Al_2O_3;
b) Cu–4Al_2O_3 and
c) Cu–4Al_2O_3 (etched) composite powder particles after 5 h of milling.

***Journal of the Serbian Chemical Society*, 74 (2009) 595–605.**

Modeling of densification process for particle reinforced composites

D. Božić[1], O. Dimčić[2], B. Dimčić[1], M. Vilotijević[1], S. Riznić-Dimitrijević[1]

[1]Institute of Nuclear Sciences, Vinča, University of Belgrade, 11001 Belgrade, Serbia
[2]Technocon Filter, 11000 Belgrade, Serbia

It is a well-known fact that behavior of materials during consolidation at high temperatures is a very complex issue. Each mechanism that promotes densification depends on a large number of parameters in many different ways, making the development of the densification process very difficult to plan. For that reason, any kind of model which could encompass large number of the influencing parameters would be a great contribution for easier planning and handling of the densification process.Modeling of densification process based on the papers of well-known authors, including new appropriate modifications is presented in this work. Importance of this model is that it can be applicable to composite materials.This new model was tested on a real Al–SiC composite systems (Al–10 vol.%SiC, Al–30 vol.% SiC and Al–50 vol.% SiC). Predicted behavior of composites obtained by model calculations and the one defined through the experiments concur in the 7–30% range.

Keywords: composite material, hot pressing of two phase systems, densification mechanisms modeling, radial distribution function, partitioning factor.

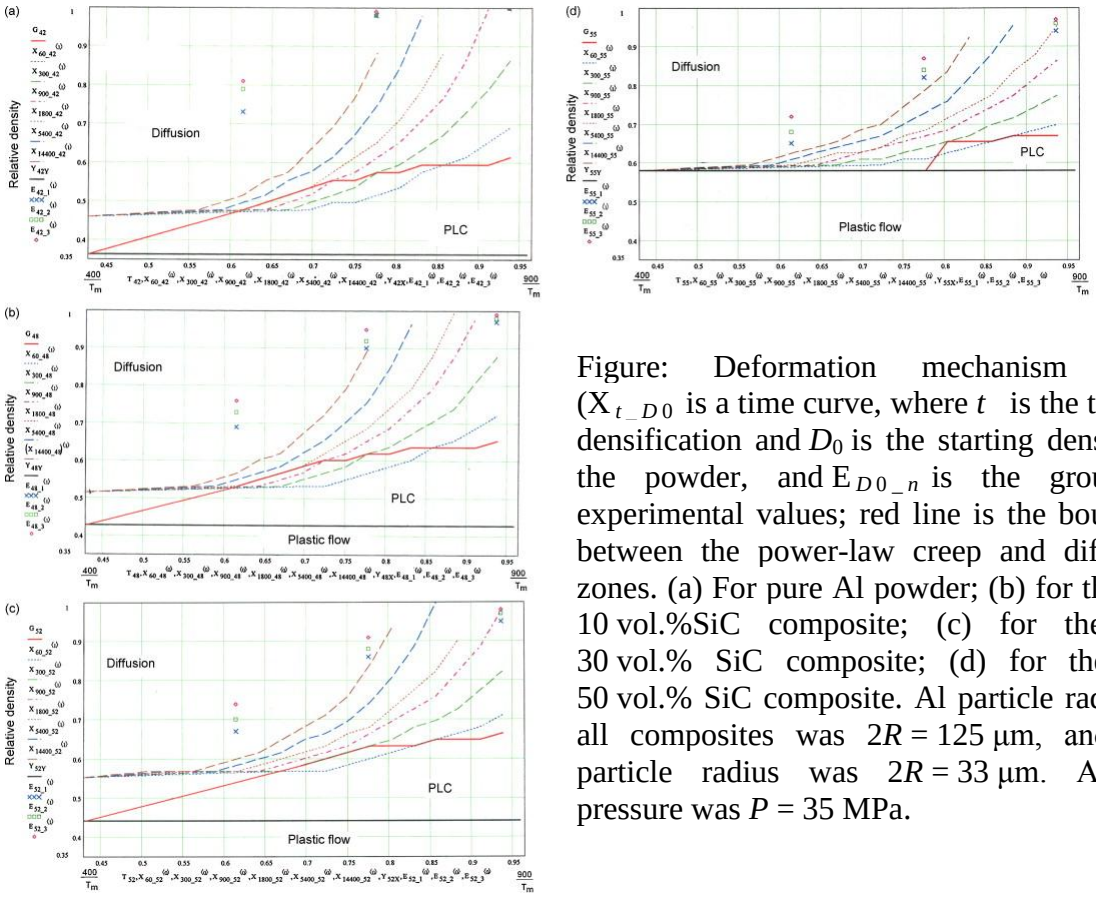

Figure: Deformation mechanism maps (X_{t_D0} is a time curve, where t is the time of densification and D_0 is the starting density of the powder, and E_{D0_n} is the group of experimental values; red line is the boundary between the power-law creep and diffusion zones. (a) For pure Al powder; (b) for the Al–10 vol.%SiC composite; (c) for the Al–30 vol.% SiC composite; (d) for the Al–50 vol.% SiC composite. Al particle radius in all composites was $2R = 125$ μm, and SiC particle radius was $2R = 33$ μm. Applied pressure was $P = 35$ MPa.

***Journal of Alloys and Compounds*, 487 (2009) 511–516.**

The influence of powder particle size on properties of Cu-Al_2O_3 composites

V. Rajković[1], D. Božić[1], M. Popović[2], M. T. Jovanović[1]

[1]Institute of Nuclear Sciences, Vinča, University of Belgrade, 11001 Belgrade, Serbia
[2]Faculty of Technology and Metallurgy, 11020 Belgrade, Serbia

Inert gas atomized prealloyed copper powder containing 2 wt.% Al (average particle size ≈ 30 μm) and a mixture consisting of copper (average particle sizes ≈ 15 μm and 30 μm) and 4 wt.% of commercial Al_2O_3 powder particles (average particle size ≈ 0.75 μm) were milled separately in a high-energy planetary ball mill up to 20 h in air. Milling was performed in order to strengthen the copper matrix by grain size refinement and Al_2O_3particles. Milling in air of prealloyed copper powder promoted formation of finely dispersed nano-sized Al_2O_3 particles by internal oxidation. On the other side, composite powders with commercial micro-sized Al_2O_3 particles were obtained by mechanical alloying. Following milling, powders were treated in hydrogen at 400 °C for 1 h in order to eliminate copper oxides formed on their surface during milling. Hot-pressing (800 °C for 3 h in argon at pressure of 35 MPa) was used for compaction of milled powders. Hot-pressed composite compacts processed from 5 and 20 h milled powders were additionally subjected to high temperature exposure (800 °C for 1 and 5 h in argon) in order to examine their thermal stability. The results were discussed in terms of the effects of different size of starting powders, the grain size refinement and different size of Al_2O_3 particles on strengthening, thermal stability and electrical conductivity of copper-based composites.

Keywords: Cu-Al_2O_3 composite, internal oxidation, mechanical alloying, different size of starting powder particles, hot-pressing, properties.

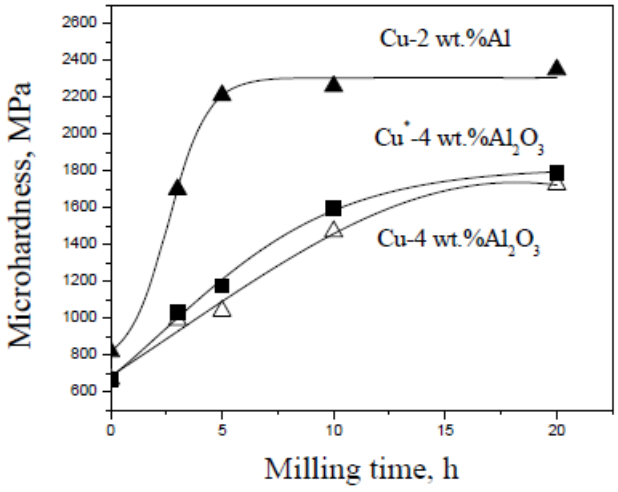

Figure: Effect of milling time on microhardness of hot-pressed composites: ▲ - based on internally oxidized Cu-2 wt.%Al prealloyed powder; ■ - based on 30 μm copper powder; Δ - based on 15 μm copper powder.

***Science of Sintering*, 41 (2009) 185-192.**

Properties of Cu-Al_2O_3 powder and compact composites of various starting particle size obtained by high energy milling

V. Rajković[1], D. Božić[1], M. Popović[2], M. Jovanović[1]

[1]Institute of Nuclear Sciences, Vinča, University of Belgrade, Belgrade, Serbia
[2]Faculty of Technology and Metallurgy, Belgrade, Serbia

Copper-based composites were obtained using high energy milling. The inert gas-atomized prealloyed copper powder (average particle size – 30 μm) containing 2 wt.% Al, and the mixture of electrolytic copper powder (average particle size – 30 and 15 μm) with 4 wt.% comertial Al_2O_3 powders (average particle size –0.75μm) served as starting materials. These powders were separately milled in air up to 20 h in the planetary ball mill. Milling of prealloyed copper powder promotes formation of nanosizedAl_2O_3 particles by internal oxidation with oxygen from air**.** It was calculated that by internal oxidation of 2 wt.% aluminum approximately 3.7 wt.% $Al_2O_3$was generated in the copper matrix. Milled powders were treated in hydrogen at 400 °C for 1 h in order to eliminate copper oxides formed at the surface during milling. Compaction executed by hot-pressing was carried out in an argon atmosphere at 800 °C for 1 h under the pressure of 35 MPa. Compacts obtained from 5 and 20 h milled powders were additionally subjected to high-temperature exposure in argon at 800 °C for 1 and 5 h. The results were discussed in terms of the effects of different size of starting powder particles on structure, strengthening of copper matrix, thermal stability and electrical conductivity of the Cu - Al_2O_3 composite.

Keywords: Cu-Al_2O_3 composite, mechanical alloying, internal oxidation, structure, microhardness, thermal stability, electrical conductivity.

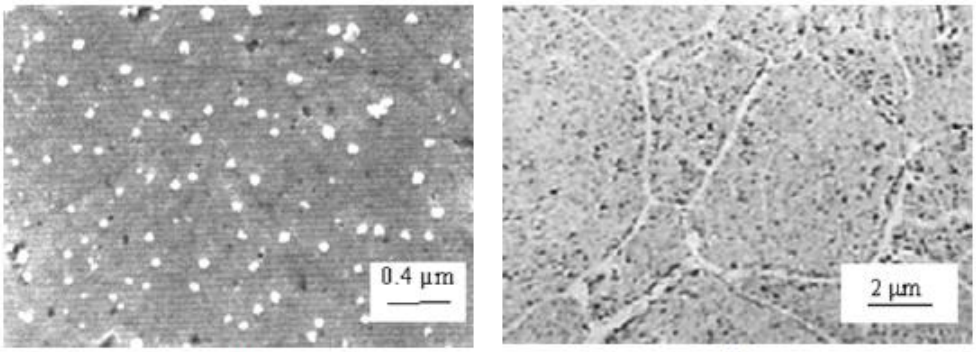

Figure: SEM and light microscopy. (a) SEM micrograph of polished Cu-2 wt.%Al and (b) light micrograph of polished Cu-4 wt.%Al_2O_3 compacts processed from 5 h milled powders.

Metallurgical & Materials Engineering, **15 (2009) 45-52.**

Properties of Cu-Al_2O_3 composites obtained by high energy milling and internal oxidation

Višeslava Rajković, Dušan Božić, Jelena Stašić, Biljana Dimčić

Institute of Nuclear Sciences, Vinča, University of Belgrade, 11001 Belgrade, Serbia

The inert gas atomized prealloyed copper powders containing 3.wt.%Al was milled up to 20 h in the planetary ball mill to oxidize aluminium*in situ* with oxygen from air. The microhardness of compacts processed from the as-received Cu-3 wt.%Alpowder was 104 HV, while in the case of composites microhardness increases up to 300 HV. The grain size of compacted Cu-3 wt.%Al powder after 5 and 20 h of milling were 55 and 30 nm, respectively. Increased microhardness and improved thermal stability of compacted composites are the result of very small grain size of compacts and alumina particles formed by internal oxidation during high-energy milling. The values of electrical conductivity of compacted Cu-3 wt.%Al powder (37 and 38 % IACS after 5 and 20 h of milling, respectively) imply that the electrical conductivity depends not only on the presence of alumina particles but also on density of composites.

Keywords: Cu-Al_2O_3 composite, high-energy milling, internal oxidation, structure, microhardness, electrical conductivity, thermal stability.

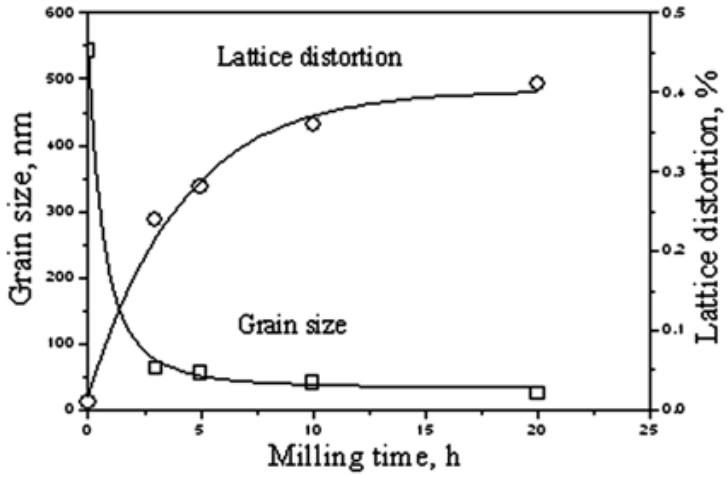

Figure: Effect of milling time on grain size and lattice distortion of Cu-3 wt.%Al.

***Metallurgical & Materials Engineering*, 15 (2009) 181-188.**

Toughening of SiC matrix with in-situ created TiB_2 particles

Dušan Bučevac[1,2], Snežana Bošković[2], Branko Matović[2], Vladimir Krstić[1]

[1]Department of Mechanical and Materials Engineering, Queen's University, Kingston, Ontario K7L 3N6 Canada
[2]Institute of Nuclear Sciences, Vinča, University of Belgrade, P.O. Box 522, Belgrade 11001, Serbia

SiC–TiB_2 composites with up to 50 vol% TiB_2 were fabricated by in-situ reaction between TiO_2, B_4C and C. The densification of the uniaxially pressed samples was done using pressureless sintering in the presence of sintering aids consisting of Al_2O_3 and Y_2O_3. The influence of the volume fraction of TiB_2 and sintering temperature on density and fracture toughness was examined. It was found that fracture toughness is strongly affected by the volume fraction of TiB_2. The presence of TiB_2 particles suppresses the grain growth of SiC and facilitates different toughening mechanisms to operate which, in turn, increases fracture toughness of the composite. The highest value for fracture toughness of 5.7 MPa·$m^{1/2}$ was measured in samples with 30 vol% TiB_2 sintered at 1940 °C.

Keywords: sintering, composites, toughness and toughening, SiC

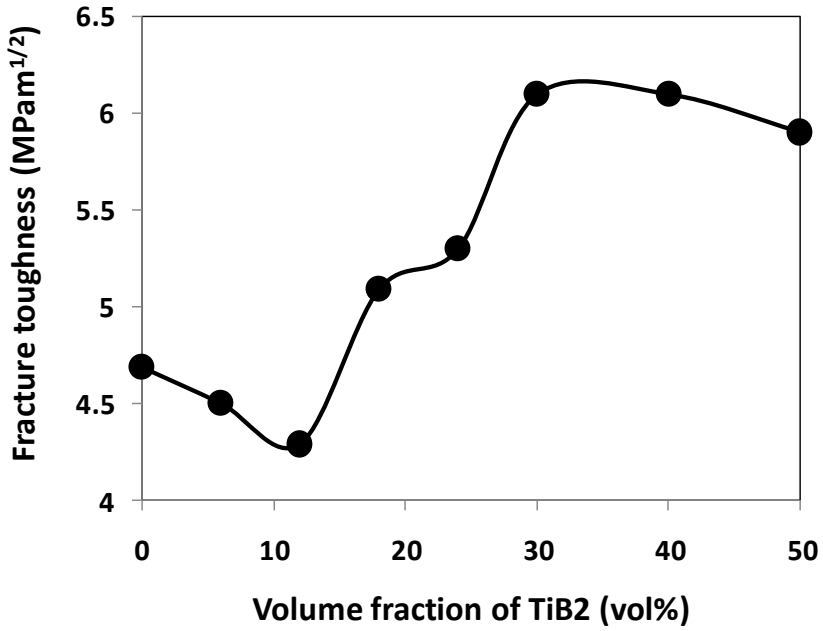

Figure: Effect of TiB_2 volume fraction on fracture toughness of SiC-TiB_2 composite sintered at 1940 °C for 1h.

***Ceramics International*, 36 (2010) 2181–2188.**

Implementation of image analysis on thermal shock and cavitation resistance testing of refractory concrete

S. Martinović[a], M. Dojčinović[b], M. Dimitrijević[b], A. Devečerski[c], B. Matović[c], T. Volkov-Husović[b]

[a] Institute for Technology of Nuclear and other Raw Mineral Materials, Franchet d'Esperey 86, Belgrade, Serbia
[b] University of Belgrade, Faculty of Technology and Metallurgy, Karnegijeva 4, POB 3503, Belgrade, Serbia
[c] Insitute of Nuclear Science, Vinča, Material Science Laboratory, Belgrade, Serbia

This paper presents monitoring of changes during thermal shock and cavitation testing for low cement concrete that was synthesized and sintered at 1600 °C for 3 h. Water quench test was applied as an experimental method for thermal stability testing. Image analysis of the samples showed some level of deterioration at the surface and inside the samples before water quench test. During the testing, the level of samples destruction was increasing. Damages inside the samples and at the surface during the water quench test were correlated to the number of quench experiments. Models based on the damage level of both the surface and inside the bulk were proposed for calculation of the strength degradation. Cavitation damages of the samples were induced by the modified vibratory cavitation set-up. Mass loss and surface erosion were determined during the experiment. The results indicated excellent thermal shock behavior and resistance to cavitation erosion.

Keywords: Refractory concrete; Thermal stability; Cavitation resistance; Image analysis

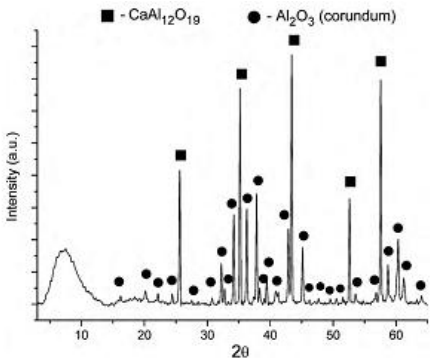

Figure: XRD pattern of the castable matrix sample sintered at 1600 °C/3 h.

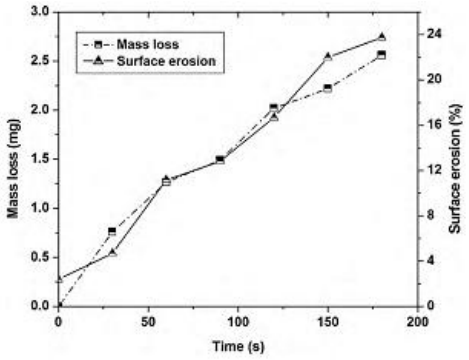

Figure: Mass loss and surface erosion during the cavitation testing.

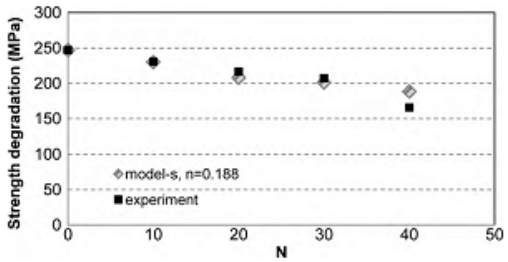

Figure: Strength degradation (model with surface damage) versus number of cycles (*N*).

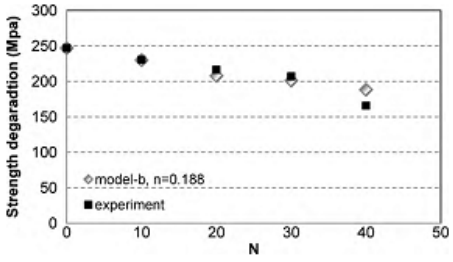

Figure: Strength degradation (model with damage inside the sample) versus number of cycles (*N*).

***Journal of the European Ceramic Society*, 30 (2010) 3303-3309.**

The Effect of Y_2O_3 Addition on Thermal Shock Behavior of Magnesium Aluminate Spinel

M. Pošarac[1], A. Devečerski[1], T. Volkov- Husović[2], B. Matović[1], D. M. Minić[3]

[1]Institute of Nuclear Science, Vinča, University of Belgrade, Belgrade, Serbia
[2]Faculty of Technology and Metallurgy, University of Belgrade, Karnegijeva 4, POB 3503, Belgrade, Serbia
[3]Faculty of Physical Chemistry, University of Belgrade, Studentski trg 16, Belgrade, Serbia

The effect of yttria additive on the thermal shock behavior of magnesium aluminate spinel has been investigated. As a starting material we used spinel ($MgAl_2O_4$) obtained by the modified glycine nitrate procedure (MGNP). Sintered products were characterized in terms of phase analysis, densities, thermal shock, monitoring the damaged surface area in the refractory specimen during thermal shock and ultrasonic determination of the Dynamic Young modulus of elasticity. It was found that a new phase between yttria and alumina is formed, which improved thermal shock properties of the spinel refractories. Also densification of samples is enhanced by yttria addition.

Keywords: Spinel, Yttria, Additive, Thermal shock

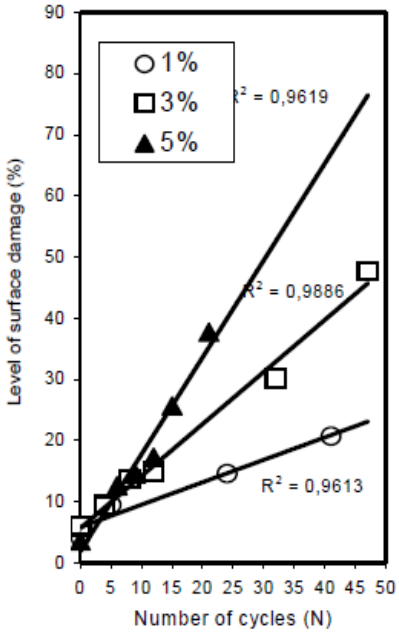

Figure: Level of surface damage.

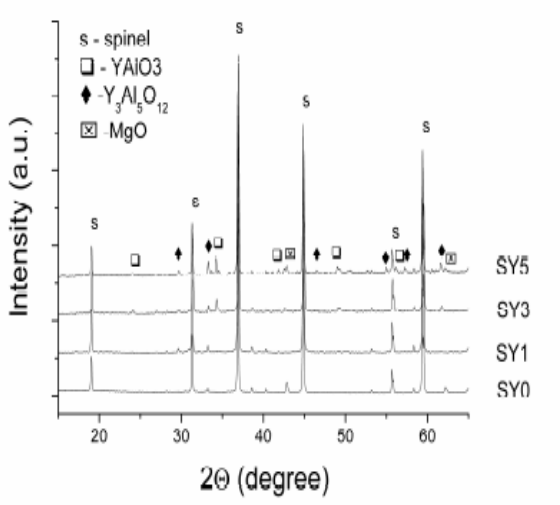

Figure: XRD paterns of samples sintered at 1500 °C.

***Science of Sintering,* 41 (2009) 75-81.**

Behavior of silicon carbide/cordierite composite material after cyclic thermal shock

M. Dimitrijević[a], M. Pošarac[b], J. Majstorović[c], T. Volkov-Husović[a], B. Matović[b]

[a]Faculty of Technology and Metallurgy, University of Belgrade, Karnegijeva 4, Belgrade, Serbia
[b]Institute of Nuclear Sciences, Vinča, University of Belgrade, 11001 Belgrade, Serbia
[c]Faculty of Mining and Geology, University of Belgrade, Djusina 4, Belgrade, Serbia

In the present work Mg-exchanged zeolite and silicon carbide were used as starting materials for obtaining cordierite/SiC composite ceramics with weight ratio 30:70. Samples were exposed to the water quench test from 950 °C, applying various number of thermal cycles (shocks). Level of surface deterioration before and during quenching was monitored by image analysis. Ultrasonic measurements were used as non-destructive quantification of thermal shock damage in refractory specimens. When refractory samples are subjected to the rapid temperature changes crack nucleation and propagation occurs resulting in loss of strength and materials degradation. The formation of cracks decreases the density and elastic properties of material. Therefore by measuring these properties one can directly monitor the development of thermal shock damage level. Dynamic Young's modulus of elasticity and strength degradation were calculated using measured values. Level of degradation of the samples was monitored before and during testing using Image Pro Plus program for image analysis. The capability of non-destructive test methods such as: ultrasonic velocity technique and image analysis for simple, and reliable non-destructive characterization are presented.

Keywords: C. Thermal shock resistance; D. Cordierite/SiC composite ceramics; E. Refractories; Ultrasonic velocity; Image analysis

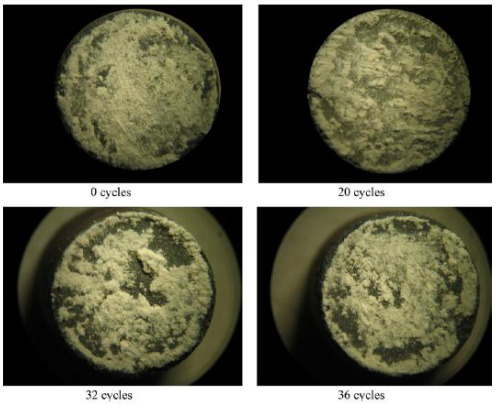

Figure: Samples KZ30 under thermal shock experiments, white area is non-damaged surface.

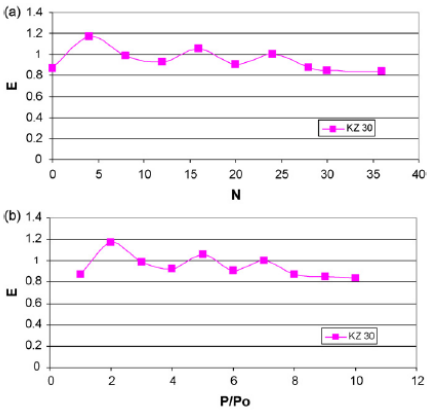

Figure: Dynamic Young modulus of elasticity versus number of
a) quench experiments N,
b) degradation P/P_0.

***Ceramics International*, 35 (2009) 1077–1081.**

The ultrasonic and image analysis method for non-destructive quantification of the thermal shock damage in refractory specimens

Milica Pošarac[a], Marija Dimitrijević[b], Tatjana Volkov-Husović[b], Jelena Majstorović[c], Branko Matović[a]

[a]Institute of Nuclear Sciences, Vinča, University of Belgrade, 11001 Belgrade Serbia
[b]Faculty of Technology and Metallurgy, University of Belgrade, Karnegijeva 4, 11120 Belgrade, Serbia
[c]Faculty of Mining and Geology, University of Belgrade, Djusina 4, Belgrade, Serbia

In the present work, Mg-exchanged zeolit and silicon carbide were used as starting materials for obtaining cordierite/SiC composite ceramics with weight ratio 50:50. Samples were exposed to the water quench test from 950 °C, applying various number of thermal cycles (shocks). Level of surface deterioration before and during quenching was monitored by image analysis. Ultrasonic measurements were used as non-destructive quantification of thermal shock damage in refractory specimens. When refractory samples are subjected to the rapid temperature changes crack nucleation and propagation occurs resulting in loss of strength and materials degradation. The formation of cracks decreases the density and elastic properties of material. Therefore measuring these properties can directly monitor the development of thermal shock damage level. Dynamic Young modulus of elasticity and strength degradation were calculated using measured values of ultrasonic velocities obtained by ultrasonic measurements. Level of degradation of the samples was monitored using Image Pro Plus program for image analysis. The capability of non-destructive test methods such are: ultrasonic velocity technique and image analysis for simple, and reliable non-destructive methods of characterization were presented in this paper.

Keywords: A. Engineering ceramics; G. Nondestructive testing; G. Image analysis;

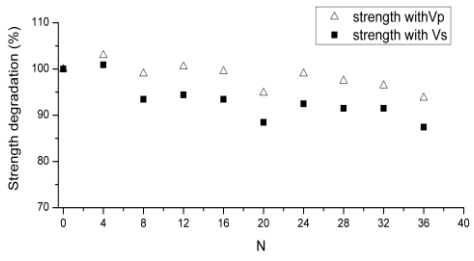

Figure: Strength degradation of material versus number of quench experiment.

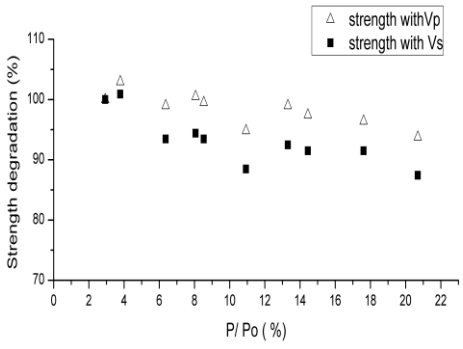

Figure: Strength degradation of material versus degradation (P/Po).

***Materials & Design,* 30 [8] (2009) 3338-3343.**

Nondestructive Testing of Thermal Shock Resistance of Cordierite/Silicon Carbide Composite Materials after Cyclic Thermal Shock

M.Pošarac[1], M.Dimitrijević[2], J.Majstorović[3], T.Volkov–Husović[2], B.Matović[1]

[1]Institute of Nuclear Sciences, Vinča, University of Belgrade, 11001 Belgrade, Serbia
[2]Faculty of Technology and Metallurgy, University of Belgrade, Karnegijeva 4, Belgrade, Serbia
[3]Faculty of Mining and Geology, University of Belgrade, Djusina 7, 1100 Belgrade, Serbia

Two different types cordierite/silicon carbide composite ceramic materials (KS 50 and KZ 50) were used for this investigation. Both materials were exposed to the water quench test from 950 °C, applying various numbers of thermal cycles. When refractory samples are subjected to the rapid temperature changes crack nucleation and propagation occurs resulting in loss of strength and materials degradation. The formation of cracks decreases the density and elastic properties of material. Therefore measuring these properties can directly monitor the development of thermal shock damage level. Dynamic Young modulus of elasticity and strength degradation were calculated using measured values of ultrasonic velocities obtained by ultrasonic measurements. Level of degradation of the samples was monitored before and during testing using Image Pro Plus program for image analysis. The capability of ultrasonic velocity technique and image analysis for simple, and reliable non-destructive methods of characterization was presented in this investigation.

Keywords: Ultrasonic velocity; Image analysis; Refractories; Cordierite/SiC composite ceramics; Thermal shock resistance

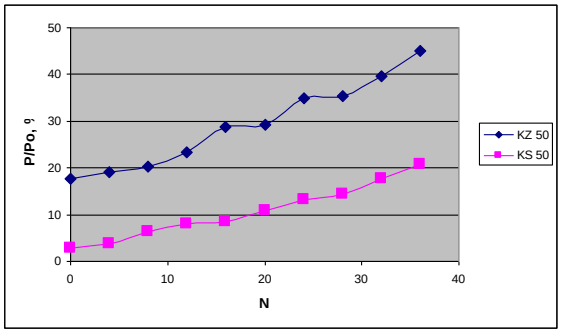

Figure:Damaged surface level (P/P_o) versus number quench experiments (N).

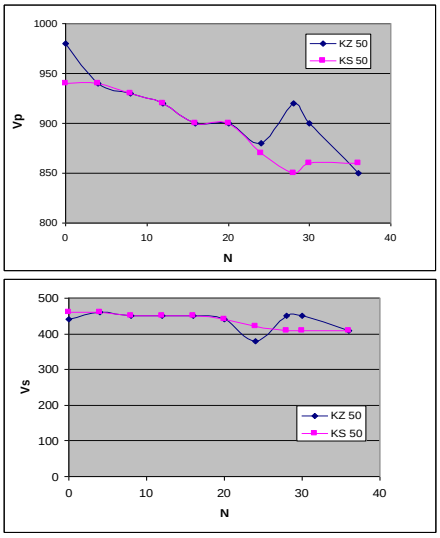

Figures: Values of longitudinal (Vp) and transversal (Vs) ultrasonic velocity during testing.

Influence of Microstructure on Mechanical Properties of Porous SiC/Cordierite Composite Materials

M.Pošarac[1], T.Volkov-Husović[2], B.Matović[1]

[1]Institute of Nuclear Sciences, Vinča, University of Belgrade, P.O. Box 522, 11001 Belgrade, Serbia
[2]Faculty of Technology and Metallurgy, University of Belgrade, Karnegijeva 4, POB 3503, Belgrade, Serbia

SiC/cordierite porous composite ceramics with weight ratio of 70:30 were prepared by a mechanical mixing of commercial SiC and cordierite from two different sources. In the one case mixture of commercially available spinel, quartz (SiO2) and alumina (Al2O3) corresponding to a cordierite stoichiometry was attrition milled using Al2O3 balls and ethyl alcohol as media for four hours. The second source of cordierite was Mg-exchanged zeolit, quartz (SiO_2) and alumina (Al_2O_3) mixed according to the chemical composition of cordierite, attrition milled using Al_2O_3 balls and ethyl alcohol as media for five hours. Graphite powder was used as the pore former to change the porosity of the specimens. The mixture was heated in air so that graphite was burned out. The weight fraction of graphite had a strong influence on porosity and strength so we used 10, 20 and 30 wt% of graphite powder. Microstructure was investigated with SEM. Pore size and pore distributions were determined by Image Pro Plus program for image analysis. Vickers hardness test was performed and influence of porosity on hardness of composite materials was investigated. Young's modulus of samples was calculated using measured values of ultrasonic velocities obtained by ultrasonic pulse velocity technique.

XXV Panhellenic Conference on Solid State Physics and Materials Science, **Thessaloniki 2009., Extended abstracts, pp. 42.**

Synthesis and crystal structure of $Ca_{(1-x)}Gd_xMnO_3$

Milena Rosić, Branko Matović, Biljana Babić, Adela Egelja, Aleksandar Devečerski, Ana Radosavljević-Mihajlović

Institute of Nuclear Sciences, Vinča', Laboratory for Material Science, P.O. Box 522, 11001 Belgrade, Serbia

This paper deals with $Ca_{(1-x)}Gd_xMnO_3$ (x = 0,1; 0,2; 0,3) synthesized by sucrose-nitrate procedure (SNP). SNP is combustion method in which sucrose $C_{12}H_{22}O_{11}$ was used as fuel while calcium nitrate tetrahydrate $Ca(NO_3)4H_2O$, manganese (II) nitrate hydrate $Mn(NO_3)2H_2O$, gadolinijum (III) nitrate hexahydrate $Gd(NO_3)_36H_2O$ were used as oxidants. Obtained powders $CaMnO_3$, $Ca_{0,9}Gd_{0,1}Mn$ and $Ca_{0,8}Gd_{0,2}Mn$ were calcinated at temperature between 600 – 800 ºC. The structural parameters of the synthesized samples and structural changes were investigated by X-ray analysis and Raman spectroscopy. Williamson - Hall plots were used to separate the effects of size and strain in the nano powders. Specific area was measured by BET method.

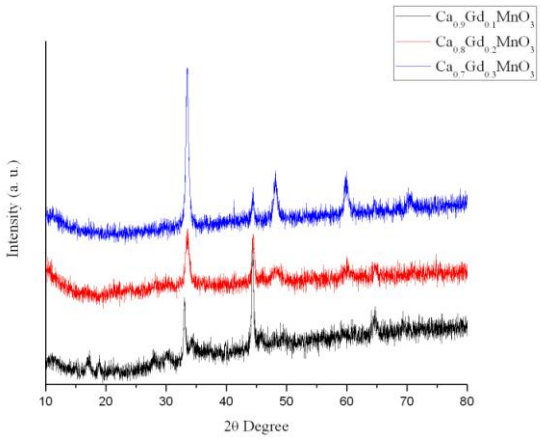

Figure: XRD patterns of $Ca_{(1-x)}Gd_xMnO_3$ (x = 0,1; 0,2; 0,3) powder sample synthesized by sucrose-nitrate procedure (SNP).

***VIII Students' Meeteing, Processing and Aplication of Ceramics*, Novi Sad, Serbia, December 2-5, 2009, p. 46.**

Synthesis and characterization of ordered mesoporous silica

M. Kokunešoski, J. Gulicovski, B. Matović, B. Babić

Institute of Nuclear Sciences, Vinča, P. O. Box 522, 11000 Belgrade, Serbia

Ordered mesoporous silica SBA-15 materials were synthesized by using Pluronic P123 (non-ionic triblock copolymer, $EO_{20}PO_{70}EO_{20}$) as a template, under acidic condition. These materials were characterized by nitrogen adsorption-desorption measurements, scanning electron microscopy (SEM), X-ray diffraction (XRD) and thermo-gravimetric analysis (TGA). It was found that structural properties can be adjusted by the different temperatures and times in the reaction solutions. Obtained samples have high specific surface area (>600 m^2g^{-1}) and developed mesoporous structure. Also, our measurements have shown that these materials have a certain amount of micropores.

Keywords: Mesoporous silica, Specific surface, Microporosity

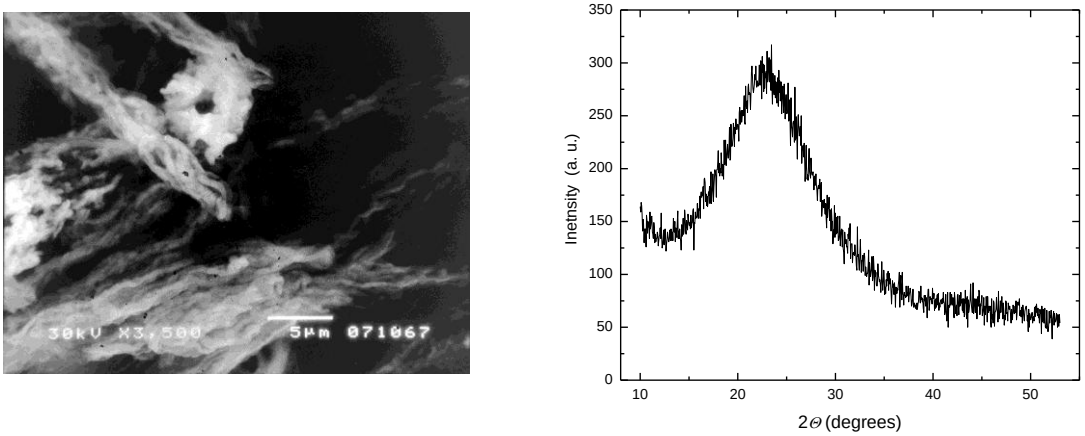

(a) (b)

Figure: Scanning electron microscopy (SEM) image (a), and X-ray diffraction (XRD) pattern (b) of silica material SBA-15.

***Journal of Optoelectronics and Advanced Materials,* 11 (2009) 1656–1659.**

Synthesis and surface characterization of ordered mesoporous silica SBA-15

M. Kokunešoski[1], J. Gulicovski[1], B. Matović[1], M. Logar[2], S.K. Milonjić[1], B. Babić[1]

[1]Institute of Nuclear Sciences, Vinča, P.O. Box 522, 11000 Belgrade, Serbia
[2]Faculty of Mining and Geology, Đušina 7, 11000 Belgrade, Serbia

Ordered mesoporous silica SBA-15 materials were synthesized using Pluronic P123 (non-ionic triblock copolymer, $EO_{20}PO_{70}O_{20}$) as a template, under acidic conditions and different heating temperatures and time of the reaction solution. These materials were characterized by nitrogen adsorption–desorption measurements, Fourier-transformed infrared spectroscopy (FT-IR), and determination of points of zero charge and izoelectric points as well as particle diameters. Synthesis at lower temperature (80 °C) and longer time of reaction (48 h) gives samples with higher specific surface area (S_{BET} = 710 m^2 g^{-1}), mesoporose surface (S_{meso} = 481 m^2 g^{-1}) and narrower pore size distribution. Material synthesized at higher temperature (100 °C) and shorter time of reaction (24 h) has lower specific surface and mesoporosity (S_{BET} = 641 m^2 g^{-1} and S_{meso} = 367 m^2 g^{-1}). At both samples, the presence of micropores was confirmed. The point of zero charge, $pH_{PZC} = 5.2 \pm 0.2$, and the isoelectric point, $pH_{IEP} = 2.3 \pm 0.1$, were not affected by synthesis conditions. Washing of silica samples in a dilute solution of nitric acid shifts the isoelectric point to a higher value ($pH_{IEP} = 3.0 \pm 0.2$) while the point of zero charge remains constant.

Keywords: amorphous materials, nanostructures, surface properties

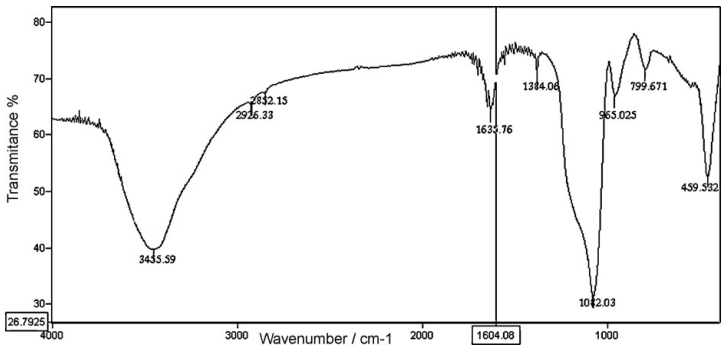

Figure: FT-IR spectra of SBA-15 sample.

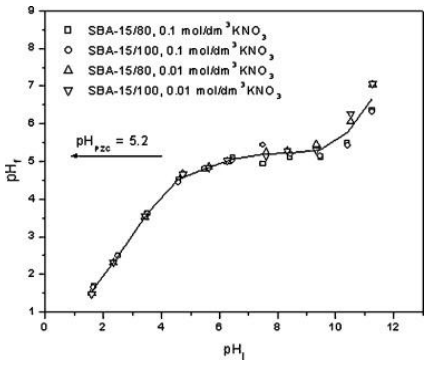

Figure: Determination of pH_{PZC} of SBA-15 samples in KNO_3 solutions (pH_i, initial value; pH_f, final value).

***Materials Chemistry and Physics,* 124 (2010) 1248–1252.**

Synthesis and characterization of nanosized Bi_2O_3

Marija Prekajski[1], Aleksandar Kremenović[2], Milena Rosić[1], Biljana Babić[1], Branko Matović[1]

[1]Institute of Nuclear Science, Vinča, University of Belgrade, 11001 Belgrade, Serbia
[2]Faculty of Mining and Geology, Laboratory for Crystallography, University of Belgrade, Djusina 7, 11000 Belgrade, Serbia

Nanometric Bi_2O_3 powder was successfully synthesized by applying the method based on self-propagating room temperature reaction (SPRT) between bismuth nitrates ($Bi(NO_3)_3 \cdot 5H_2O$) and sodium hydroxide (NaOH). X-ray powder diffraction (XRPD) and Rietveld's structure refinement method was applied to characterize prepared powder (Fig. 1). It revealed that synthesized material is single phase monoclinic α-Bi_2O_3 (space group $P2_1/c$ with cell parameters a = 5.84605(4), b = 8.16339(6), c = 7.50788(6) Å and β = 112.9883(8) º). Powder particles were of nanometric size (about 50 nm). Raman spectral studies conformed that obtained powder is single phase α-Bi_2O_3. Specific surface area of obtained powder was measured by Brunauer-Emmet-Teller (BET) method.

Keywords: Bi_2O_3, nanomaterials, self-propagating reaction

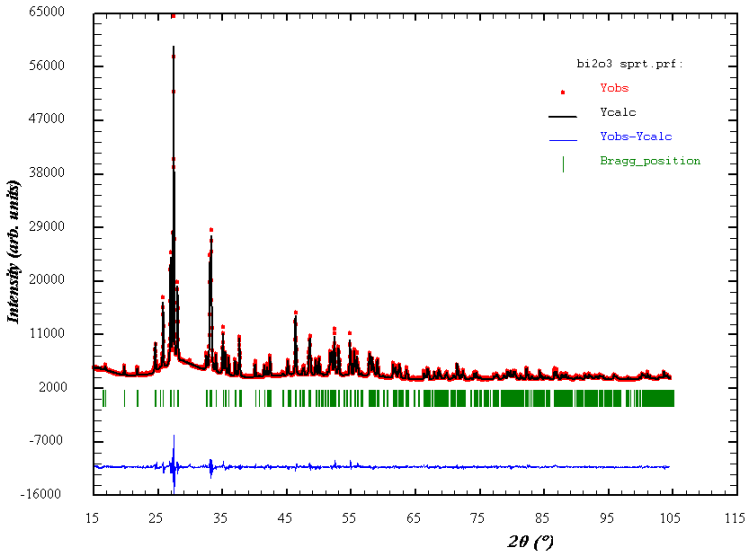

Figure: XRPD pattern after refinement procedure using Rietveld's method.

***XVII Conference of the Serbian Crystallographic society*, Ivanjica 2010 Serbia. The Book of Abstracts, pp. 50-51.**

In-situ processing of TiB_2 nanoparticle-reinforced copper matrix composites

Dušan Božić, Ivana Cvijović-Alagić, Biljana Dimčić, Jelena Stašić, Višeslava Rajković

Institute of Nuclear Sciences, Vinča, Mike Petrovića Alasa 12-14, 11001 Belgrade, Serbia

In order to produce the composite powder analyzed in this paper, two prealloys have been melted and afterwards gas atomized. Thus obtained the TiB_2-reinforced copper powder was consolidated by hot isostatic pressing (HIP). Since it is known that a decrease in size of the reinforcing phase can cause an increase in hardness of composites, the main aim of the experimental work was to obtain as small particles of the dispersed phase as possible by using standard powder metallurgy techniques. Microstructure and microhardness of the as-cast prealloys, as-atomized powder and HIP-ed compacts were examined. The results of these examinations revealed that TiB_2 particles about 10 nm in size were *in-situ* formed and homogenously dispersed in the copper matrix. As a consequence of the TiB_2 formation, the microhardness of Cu-TiB_2 composite was significantly improved.

Keywords: Cu-TiB_2 composite; powder metallurgy; hot isostatic pressing; TEM; XRD

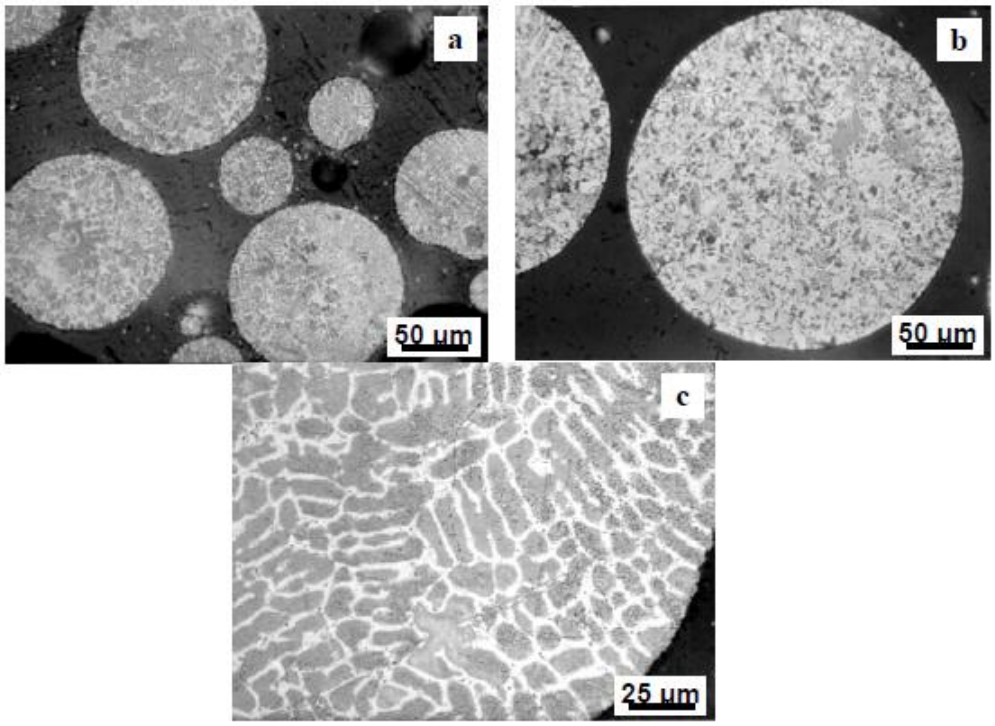

Figure: LOM micrographs showing the microstructure of different as-atomized Cu-0.6Ti-0.02B-2.5TiB_2 (wt.%) alloy powder sieved to fractions: (a) d < 80 μm, (b) 80 μm< d < 150 μm and (c) 200 μm< d < 315 μm.

***Science of Sintering*, 41 [2] (2009) 143-150.**

The influences of multiscale-sized second-phase particles on fracture behaviour of overaged 7000 alloys

Z.Cvijović[1], M. Vratnica[2], I. Cvijović-Alagić[3]

[1]Faculty of Technology and Metallurgy, University of Belgrade, Karnegijeva 4, 11120 Belgrade, Serbia
[2]Faculty of Metallurgy and Technology, University of Montenegro,Cetinjski put b.b., 81000 Podgorica, Montenegro
[3]Institute of Nuclear Sciences, Vinča, University of Belgrade, P.O. Box 522, 11001 Belgrade, Serbia

To identify the most important parameters of multiscale microstructural features influencing the fracture modes and resistance to damage, detailed microstructural and fractographic analysis of overaged 7000 alloy plates are performed using the broken plane-strain fracture toughness, K_{Ic}, test specimens. The geometric characteristics of differently sized second-phase particles are changed by the compositional variations. It was found that the fracture process involves three main micromechanisms. The dominant fracture mode changes with alloy purity, leading to fracture toughness degradation. Quantitative description of fractures by profilometry confirmed that crack initiation and propagation is fostered by the coarse Fe- and Si-rich particles.

Keywords: 7000 alloys; alloy purity; second-phase particles; fracture modes; fracture toughness; fractography; image analysis

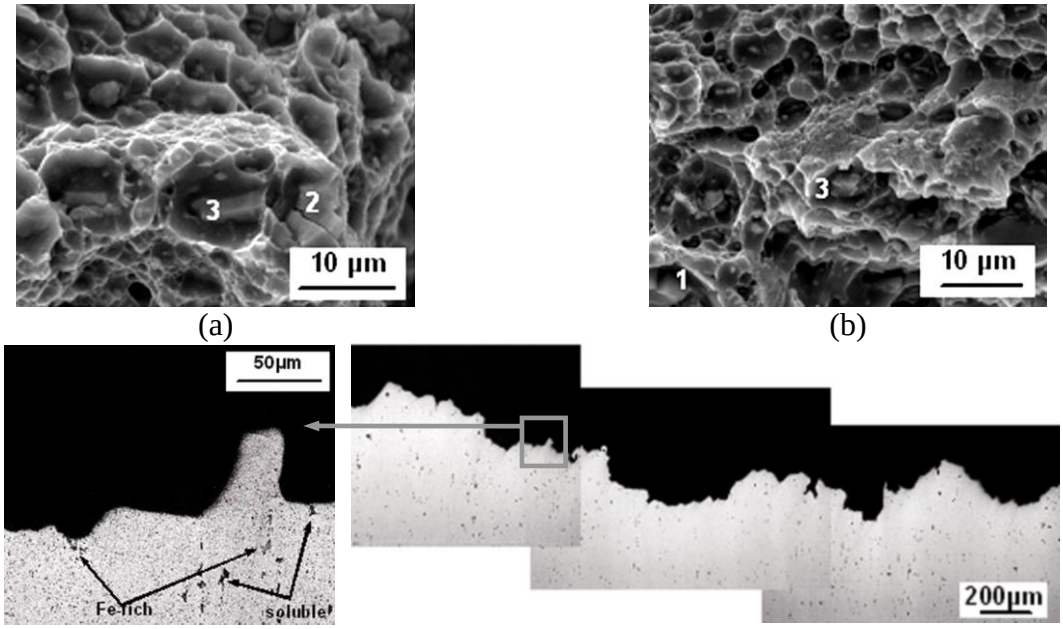

Figure: SEM micrographs showing fracture surfaces (a, b) and characteristic fragment of fracture surfaces of alloy 1 observed by OM (c). Phases: 1- Mg_2Si, 2-$(Cu,Fe,Mn)Al_3$, 3-Al_7Cu_2Fe.

***Procedia Engineering, Special Issue: Mesomechanics 2009,* 1 [1] (2009) 35-38.**

Chapter 10: Microstructure and Mechanical Properties of Investment Cast Ti-6Al-4V and γ-TiAl Alloys

Milan T. Jovanović, Ivana Cvijović-Alagić

Department of Materials Science, Institute of Nuclear Sciences, Vinča, Mike Petrovića Alasa 12-14, 11001 Belgrade Serbia

The effects of preheat and pouring temperatures, as well as annealing temperatures and cooling rates, on microstructure and mechanical properties of γ-TiAl and Ti-6Al-4V (wt.%) investment castings have been studied performing X-ray diffraction (XRD) analysis, light microscopy (LM) and scanning electron microscopy (SEM), quantitative metallography, hardness and room temperature tensile tests. Annealing of Ti-6Al-4V above and below the β phase transus temperature produces different combinations of strength and elongation, but a compromise may be achieved applying temperature just below the β phase transus of Ti-6Al-4V alloy. Higher values of tensile strength together with lower ductility than reported in the literature cannot be only ascribed to the presence of α' martensite in the microstructure of Ti-6Al-4V alloy. Yttria coating of graphite crucible must be considered as insufficient in preventing the chemical reaction between aggressive titanium melt and carbon. The processing technology of a "self-supporting" ceramic shell mold was successfully verified during precision casting of both tensile-test samples of Ti-6Al-4V and the prototype of the turbocharger wheel made of γ-TiAl. According to experimental results, a processing window for investment casting of the prototype of a turbocharger wheel was established. The results of this paper also show that besides annealing treatment parameters, melting and casting practice together with ceramic mold technology strongly influence the properties Ti-6Al-4V and γ-TiAl castings.

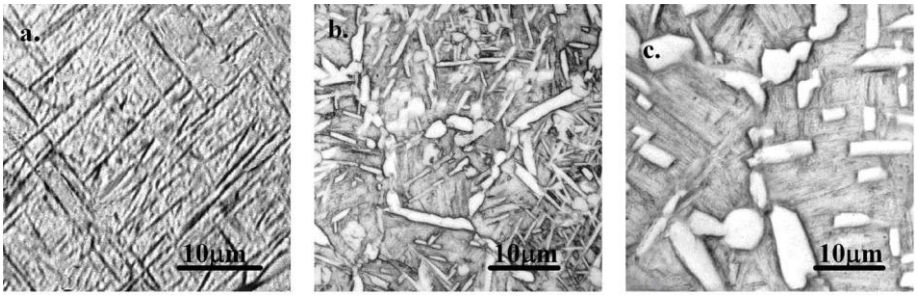

Figure: LM micrographs of Ti-6Al-4V alloy microstructure upon water-quenching from: (a) 1100 °C; (b) 950 °C; (c) 900 °C.

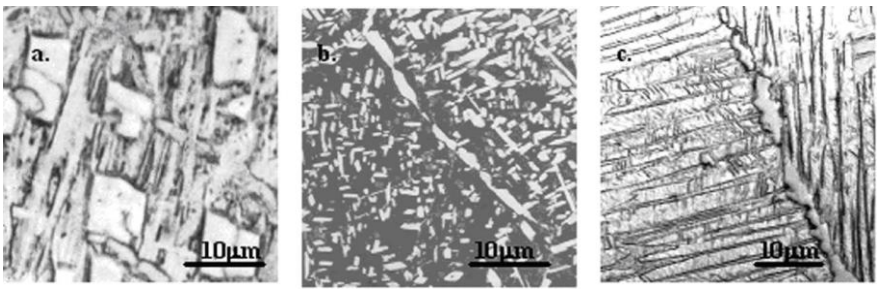

Figure: LM micrographs of Ti-6Al-4V alloy. Microstructure upon air-cooling from: (a) 1100 °C; (b) 1050 °C; (c) 950 °C.

Titanium Alloys: Preparation, Properties and Applications; ***editor:*** **Pedro N. Sanchez; Nova Science Publishers Inc., NY; 2010; p. 405-422.**

Raw materials and heritage

The role of microscopy in the evaluation of the authenticity of the material of cultural heritage

S. Polić Radovanović[1], M. Srećković[2], B. Timotijević[2], M. Timotijević[3], V. Rajković[4], R. Radovanović[5], B. Bokić[2]

[1]Central Institute for Conservation, Belgrade , Serbia;
[2]Faculty of Electrical Engineering, University of Belgrade, Serbia;
[3]Department of Art History, Faculty of Philosophy, University of Belgrade, Serbia;
[4]Department of Material Science, INN Vinca, Serbia;
[5]Academy of Criminalistic and Police Studies, Zemun, Serbia

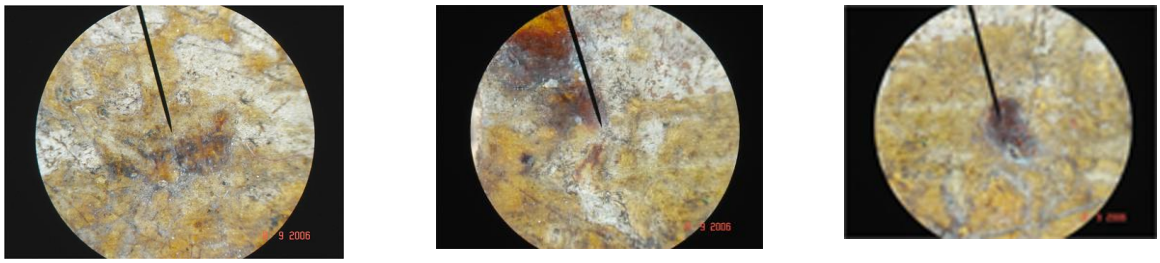

Figure: Micrographs of colored layers of material from the icon of the Virgin with Christ in the monastery Holly Prohor Pcinjski, 40x.

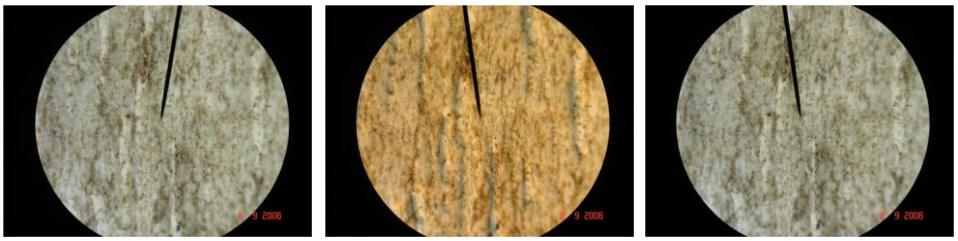

Figure: Micrographs of basic layers of material from the icon of the Virgin with Christ in the monastery Holly Prohor Pcinjski, 40x .

***4th Serbian Congress of Microscopy*, Belgrade, 11-12 October 2010. pp.83-84.**

Preparation of porous silica ceramics using the wood template

B. Matović[1], B. Babić[1], A. Egelja[1], A. Radosavljević-Mihajlović[1], V. Logar[2], A. Vučković[1], S. Bosković[1]

[1]Institute of Nuclear Sciences, Vinča, Material Science Department, Belgrade, Serbia
[2]Faculty for Mining and Geology, Belgrade 11000, Serbia

Porous silica (SiO_2) ceramic with a wood-like structure was prepared by wet impregnation tetraethyl orthosilicate (TEOS) into biological template that was derived from linden wood (tilia amurensis). After repeated pressure impregnation the subsequent annealing in air atmosphere at 800°C resulted in burn out of the template and consolidation of the oxide layers. The products exhibit structures corresponding to negative replication of biological templates. X-ray diffraction (XRD), scanning electron microscopy (SEM), infra red (IR), and Brunauer Emmett Teller (BET) measurements were employed to characterize the phases and crystal structure of biomorphic ceramics. It was found that the bio-organic structure was converted into oxide ceramics (SiO_2). At low temperature (800°C), pore radius varied between 2 and 10 nm indicating that the samples were mostly mesoporous. Samples treated at higher temperature (1300°C) lost the mesoporous character; however, they were still porous having the microstructural features of the biological perform.

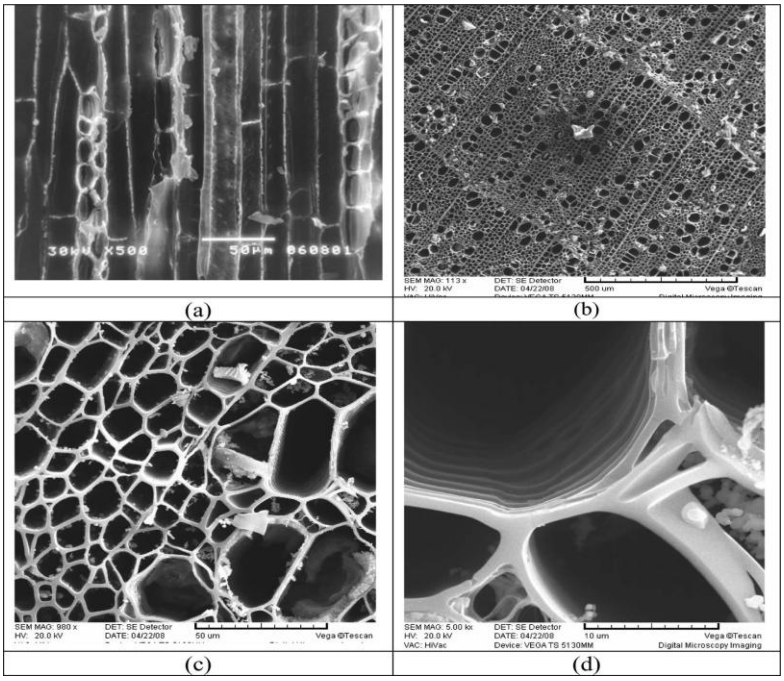

Figure: SEM microphotographs of porous silica ceramics obtained at 1300_C for 4 h: (a) cross-section parallel to axial direction, (b–d) cross-sections perpendicular to axial direction.

***Materials and Manufacturing processes,* 24 (2009) 1109-1113.**

Doctoral dissertations

Aleksandar Devečerski

STUDY OF PHYSICO-CHEMICAL PROCESSES IN SIC SYNTHESIS FROM NATURAL PRECURSORS

We demonstrate the possibility of using domestic mineral resources (Mg-silicates: two types of sepiolite; leather-like chrysotil asbestos), as SiO_2 source for synthesis of fine β-SiC powders at relatively low temperatures (1673-1873 K). Carbothermal reduction process is greatly influenced by structure and chemical composition of Mg-silicates used, and also by type of carbon used. Catalytical influence of Fe is attributed to formation of iron-silicide and its important role in reduction of Mg_2SiO_4 (and/or MgO) into $Mg_{(g)}$. Carbothermal reduction of chrysotil asbestos into the SiC, offers possibility for recycling carcinogenic waste asbestos products in an environmental-friendly manner.

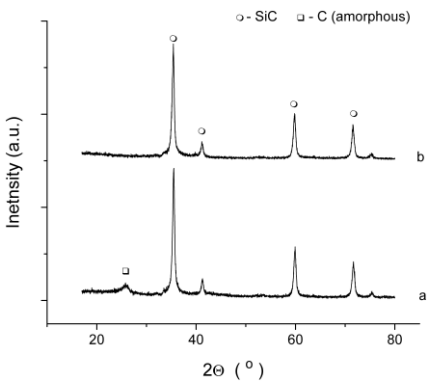

XRD patterns of SiC powders obtained from asbestos after 1873 K treatment: (a) washed with HF, (b) washed with HF and oxidized at 873K

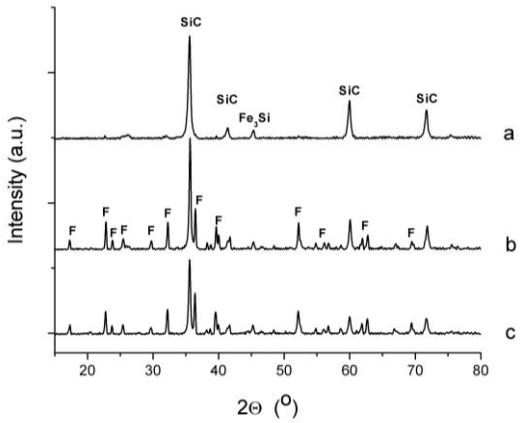

XRD patterns of novolac/sepiolite samples heat treated at 1673K: a) C/SiO_2=8, b) C/SiO_2=4, c) C/SiO_2=2; (F-forsterite)

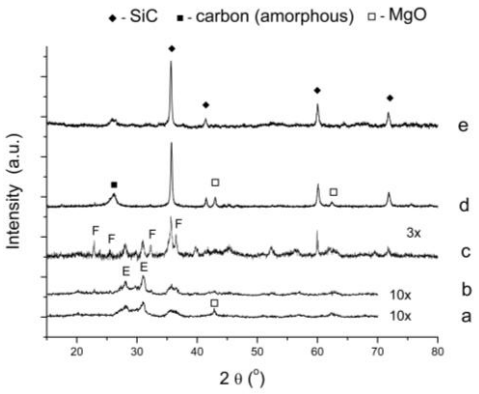

XRD patterns of Sepiolite B/novolac samples heat treated at:
a) 1473 K; b) 1573 K; c) 1673 K; d) 1773 K; e) 1873 K.

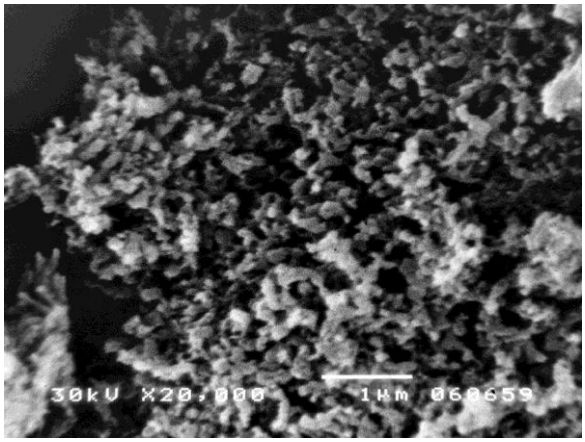

SEM micrographs of SiC obtained from novolac/sepiolite mixture (C/SiO_2=8)

Snežana Nenadović

GEOSPATIAL FACTORS AND DISPERZION CHANGES IN SOIL POLLUTANTS

The main goal of this PhD thesis was to investigate the optimal methodology in order to explain geo-space factors of dispersion and changes of pollutants in the soils. This kind of investigations was not conducted in our country yet, but it is still left many open questions. The references overview point out that the dispersion of pollutants through soils is a consequence of structure but not only the morphology of soil samples. Main concept of this paperwork is based on detailed investigation of microstructure of soils and relation of physical and chemical properties with dispersion of pollutants through soils. The mineralogical investigations were also conducted on soils profiles. Special accent was given on physical and chemical properties of profiles and on migrations of pollutants through soils for one hydrological year. Interesting was a to investigate the morphology of soils agglomerates and find the answer to the question what is the pollutants mobility through different horizons of the same profile and to investigate what is the agglomerate porosity.

The goal was to obtain dependence of vertical dispersion of pollutants through soils based on physical and chemical properties of profiles and pollutants and to predict the movement of these variables through soils. Also the investigation was focused on identification of issues caused by diffusion pollution of soils.

The focus of investigations and type of soil determine methodology and procedure for sampling the soils. To obtain quantitative index for soils properties, the samples were taken from determined profiles. Correct sampling was condition for exact results, so it was a very serious procedure, without changing soil characteristics.

Three profiles were examined and physical and chemical analysis was done before contamination. Soils were contaminated with NaCl and $CuSO_4$. The migration of anions (SO_4^{2-} i Cl^-) and cations (Cu^{2+} i Na^+) were followed.

In the theoretical part of this paperwork the theoretical foundations of geo-space factors and its influences on soils were given. Processes which cause soil-genesis were described. In the experimental part many of methods were presented and procedure of sampling was detailed described. In the chapter results and discussion all obtained results were given and explained. In the conclusion are summarized all results and investigations.

Jelena Stašić

SURFACE MODIFICATION OF CARBON STEEL AND NICKEL-BASED SUPERALLOY BY PICOSECOND AND FEMTOSECOND LASERS

This doctoral dissertation represents the investigation of the interaction of lasers, emitting radiation in ultrashort time domain, with metal materials. Ultrashort laser pulses include pico- and femtosecond time domain (pulse duration less than few tens of picoseconds). In this work, surface modification of the targets was mainly considered. The application of ultrashort pulsed lasers for a precise processing of solid targets has become increasingly interesting in the last ten years. This is due to the expected and approved physical advantages of the short pulsed lasers and a very fast development of these laser systems. When a short laser pulse interacts with a solid target, hydrodynamic motion of the ablated material during laser pulse is negligible, and the absorption is conducted directly on the target surface (surface depth). The absence (or considerably lower presence) of hydrodynamic motion is one of the short laser pulse advantages which allows precise and controlled energy deposition inside the solid target.

Material science laboratory – Domestic collaborations

IHIS Research and Development Center, Belgrade, Serbia

-Bobić, B

ICTM - Institute of Electrochemistry, University of Belgrade, Belgrade

-Jovanović, V.M
-Nikolić, N.D
-Pavlović, Lj.J
-Pavlović, M.G
-Stevanović, S.I

Faculty of Technology and Metallurgy, University of Belgrade, Belgrade

-Cvijović, Z
-Dimitrijević, M
-Gojković, S.Lj
-Kalagasidis Krušić, M.T
-Krstajić, N.V
-Milosavljević, N.B
-Popov, K.I
-Rakin, M.B
-Veljović, Đ
-Volkov-Husović, T
-Vračar, Lj.M
-Petrović, R.
-Popović, I.G
-Filipović, J.M

Faculty of Mining and Geology, University of Belgrade, Belgrade

-Kremenović, A
-Majstorovic, J
-Logar, M

Institute of Technical Sciences of SASA (Serbian Academy of Sciences and Arts), Belgrade

-Marković, S
-Gajić-Krstajić, Lj

Faculty of Physical Chemistry, University of Belgrade, Belgrade

-Mentus, S
-Minić, D.M
-Cvjetićanin, N

Institute for Multidisciplinary Research, University of Belgrade, Belgrade

-Baščarević, Z
-Branković, G
-Branković, Z
-Elezović, N.R
-Jović, B.M
-Jović, V.D
-Jovanić, P
-Lačnjevac, U.Č.

Institute of Physics, University of Belgrade, Belgrade

-Dohčević-Mitrović, Z
-Krmpot, A
-Jelenković, B
-Kovačević, A
-Romčević, N

Tribology Center, Faculty of Engineering, University of Kragujevac, Kragujevac

-Babić, M.
-Mitrović, S
-Živić, F
-Džunić, D
-Jeremić, B

Kirilo Savić Institute, Belgrade

-Brdarić, T
-Erić, O
-Stojsavljević, N
-Tonić, M

The Institut of Mining, Zemun

-Đuričić, R

Faculty of Electrical Engineering, University of Belgrade, Belgrade, Serbia,

-Bokić, B
-Družijanić
-Latinović, Z
-Srećković, M
-Pantelić, S
-Timotijević, B

Central Institute for Conservation, Belgrade

-Radovanović, S

Department of Art History, Faculty of Philosophy, University of Belgrade, Belgrade

-Timotijević, T

Academy of Criminalistic and Police Studies, Zemun, Serbia

-Radovanović, R

IRITEL AD, Belgrade

-Tomić,Ž

Nuclear Facilities of Serbia, Belgrade

-Kićević, D

Faculty of Occupational Safety, University of Nis, Nis

-Stanisavljević, M
-Krstić, I

IHTM, Centar of Chemistry, Belgrade

-Cvetković, O

Metalac, Gornji Milanovac

-Janićijević, M

Tribology Laboratory, Faculty of Mechanical Engineering, University of Belgrade, Belgrade

-Marinković, A
-Vencl, A

Technocon Filter, Belgrade

-Dimčić, O

Institute for Technology of Nuclear and Other Mineral Raw Materials, Belgrade

-Martinović, S

Institute of Nuclear Sciences, Vinča, University of Belgrade, Serbia

Laboratory of Physics (010)

-Jovanović, Z
-Šiljegović, M

Laboratory for Nuclear and Plasma Physics (011)

-Ivanović, N
-Novaković, N
-Paškaš Mamula, B
-Radisavljević, I
-Manasijević, M

Laboratory GAMMA (030)

-Jokanović, V
-Abazović, N
-Babić-Stojić, B
-Nedeljković, J.M
- Čomor, M.I
-Kačarević-Popović, Z

Laboratory for Atomic Physics (040)

-Bogdanov, Ž.D
-Nenadović, M.T
-Popović, N

Laboratory of Physical Chemistry (050)

-Trtica, M.S
-Dimčić, B
-Gaković, B
-Ilić, N
-Mišković, Z
- Pavlović, M

Laboratory for Chemical Dynamics and Permanent Education (060)

-Milonjić, S.K

Center for serification (300/300)

-Popović, P

Material science laboratory – International collaborations

National Center for Electron Microscopy, LBNL University of California, Berkely, USA

-Radmilović, V.R

Department of Mechanical and Materials Engineering, Queen's University, Kingston, Ontario, Canada

-Krstić, V

Faculty of Technology Zvornik, University of Eastern Sarajevo, Zvornik, Republic of Srpska

-Tomić, M

Plasma Jet Co, Auckland, New Zealand

-Dačić, B

North Carolina Central University, Durham, USA

-Dukić, M

Telecom of Serbian Republic, Bijeljina, Republic of Srpska

-Bugarinović, S

Max/Planck Institute fur Metallforschung, Stuttgart, Germany

-Aldinger, F

CSM Instruments SA, Peseux, Switzerland

-Arostegui, S

R&D Center IHIS Techno-Experts, Batajnič cki put 23, 11080 Belgrade, Serbia

-Bobić, B

ENEA, Materials and Technology Unit, 72100 Brindisi, Italy

-Piscopiello, E

ENEA, Materials and Technology Unit, Rome, Italy

-Montone, A
-Vittori Antisari, M

Functional Materials, Saarland University, Saarbrücken, Germany

-Ilić, N

Faculty of Metallurgy and Technology, University of Montenegro, Podgorica, Montenegro

-Vratnica, M